

Ecole Evry Schatzman 2017 du PNP8

Imagerie à Haute Résolution Angulaire des Surfaces Stellaires et de leur Environnement Proche

Roscoff, 24-29 Septembre 2017

Interférométrie optique: les instruments et leurs spécificités

Denis Mourard - UCA/OCA/CNRS Lagrange

Summary

1. Introduction on the principles
2. Back to the Object-Image relationship
3. The reality of Interferometry
4. The practice of interferometry
5. The instruments in operation
6. The future?

Introduction

Usual stellar physics

astrometry

spectroscopy

photometry

polarimetry



Star are (almost) always considered as point-like source

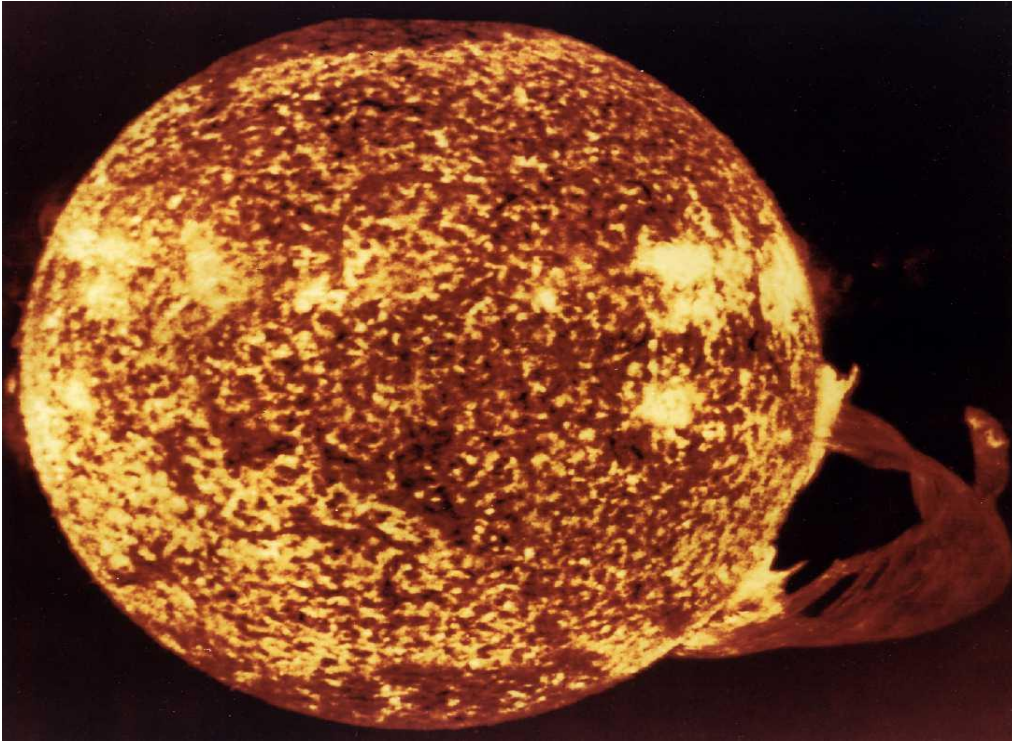


No information on the brightness distribution



Scientific niche for the High Angular Resolution

Imaging stellar surfaces and environments



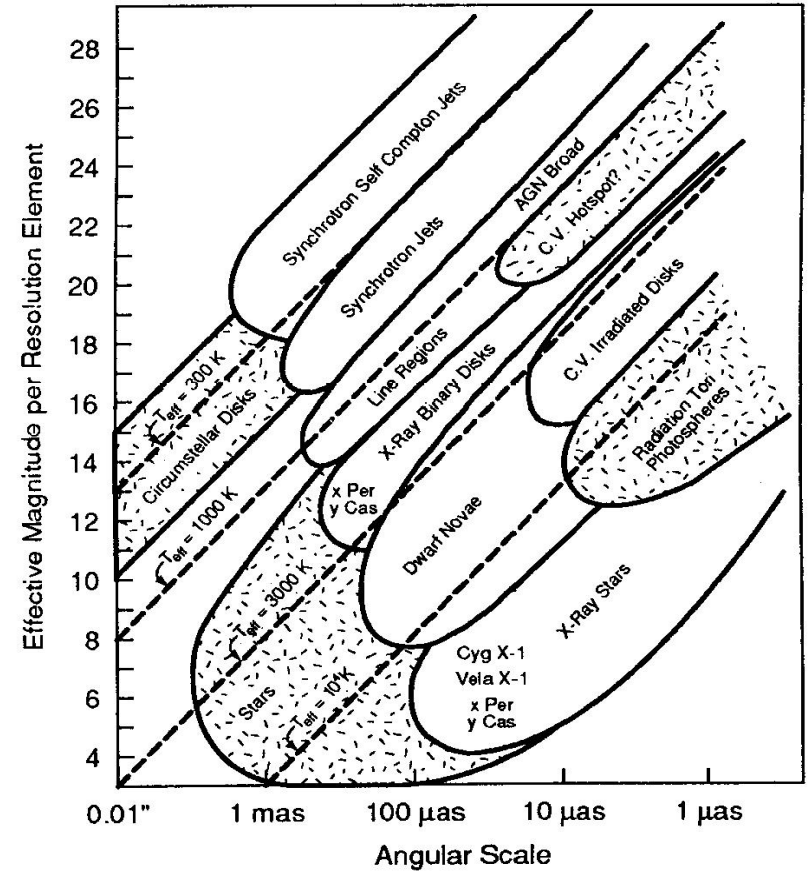
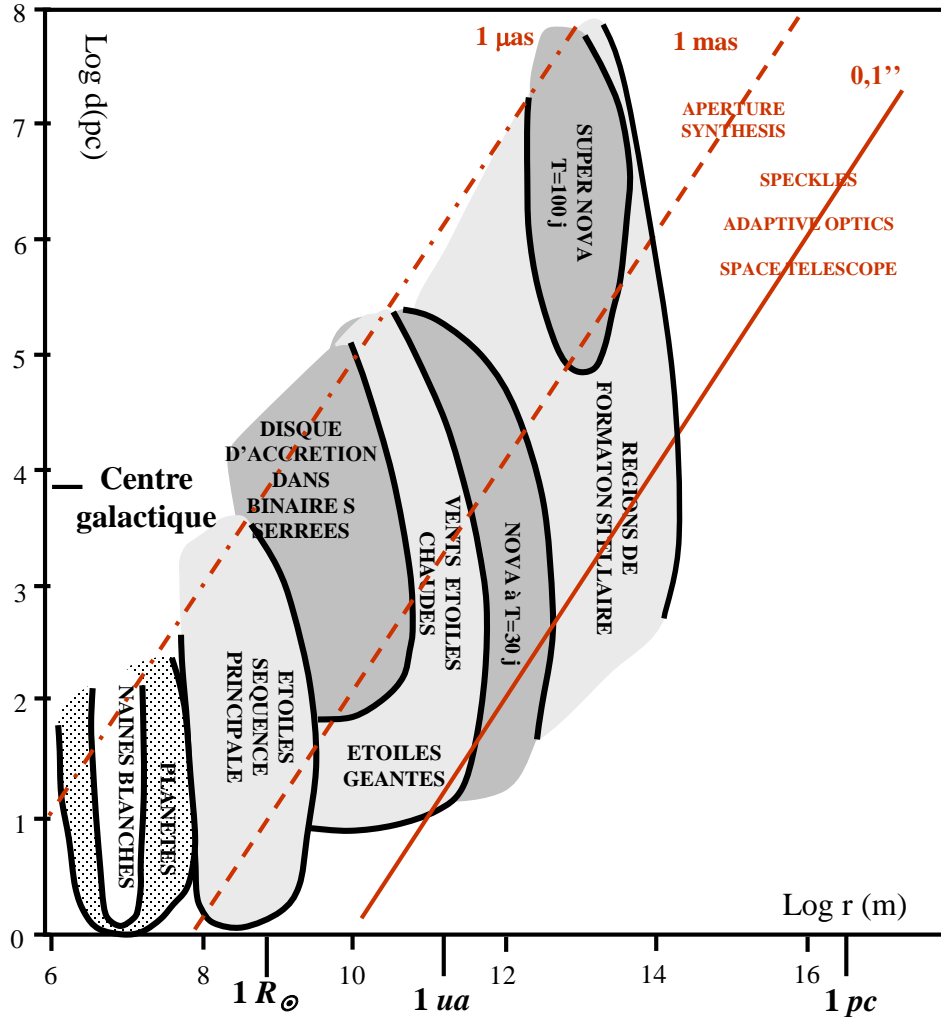
High resolution

- spatial
- temporal
- spectral

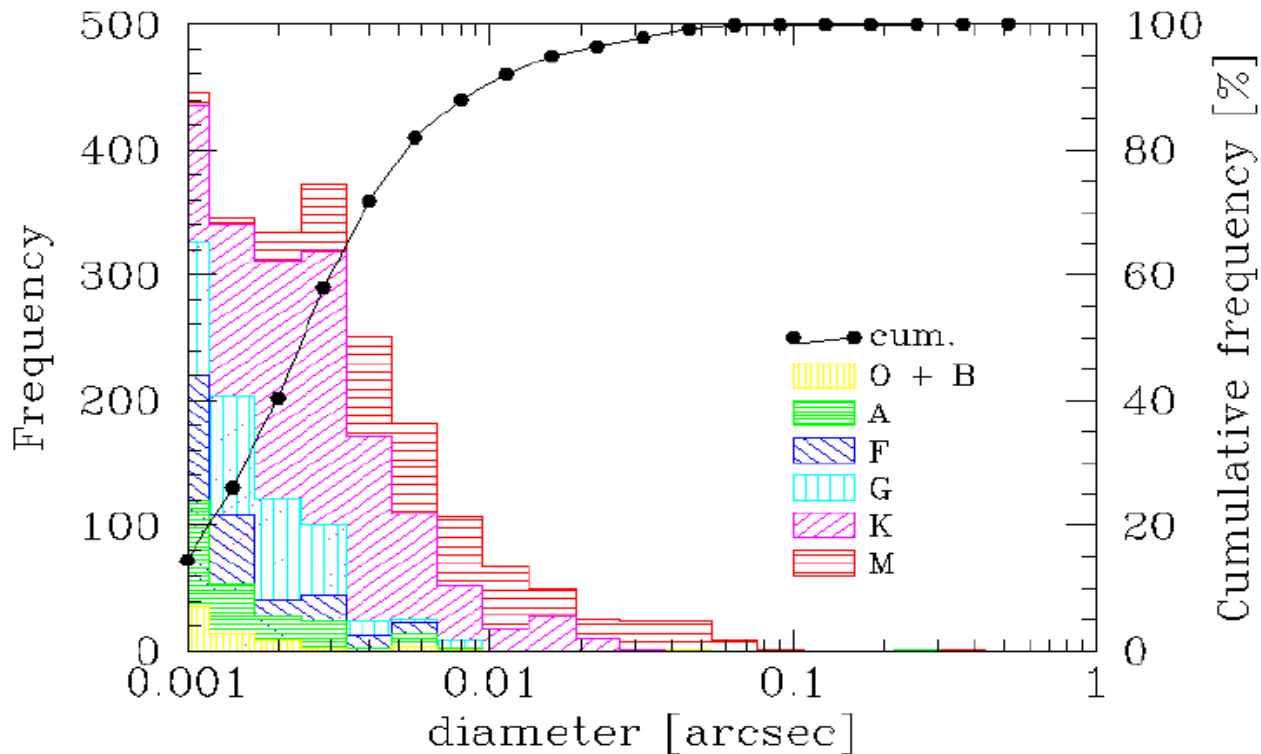
Needs for

- field of view
- transfer function

Astrophysics sources and High Angular Resolution



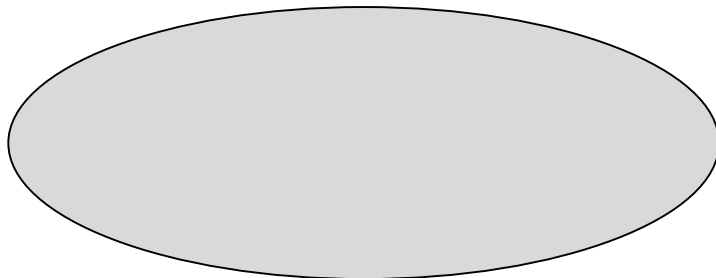
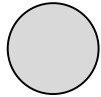
Distribution of stellar diameters



1309 sources
50 % < 2.5 mas
20 % > 5 mas
7% > 10 mas -> UT

How to measure a so small angular diameter?

Star at infinity
Angular diameter θ



Screen of radius r

Angular diameter $\theta \rightarrow$ solid angle $\Omega = \pi(\theta/2)^2$

Radius $r \rightarrow$ Surface $S = \pi r^2$

Etendue of the beam

$$\varepsilon = S\Omega = \pi^2 r^2 (\theta/2)^2$$

Definition of coherence (Goodman)

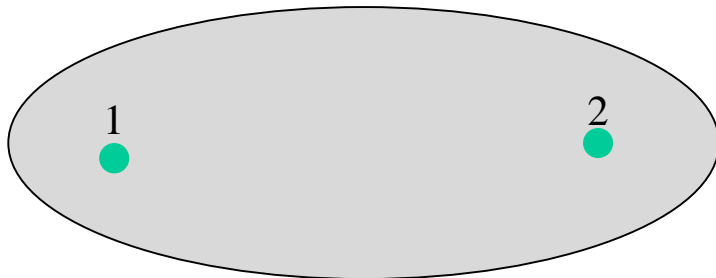
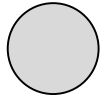
$$\varepsilon < \lambda^2$$

$$\rightarrow r_c = \frac{\lambda}{\pi(\frac{\theta}{2})}$$

N.A.: $\theta = 10 \text{ mas}$, $\lambda = 1 \mu\text{m}$ $\rightarrow r_c = 13 \text{ m}$

Coherence & Van-Cittert Zernike Theorem

Star at infinity
Angular diameter θ



Screen of radius r

The coherence of the electromagnetic wave could be determined by the computation of the complex degree of mutual coherence between points 1 & 2 of the collecting area:

$$\Gamma_{12} = \frac{|\psi_1 \psi_2^*|}{\sqrt{|\psi_1|^2 |\psi_2|^2}}$$

V-CZ \rightarrow
$$\Gamma_{12} = \frac{|\tilde{O}(B/\lambda)|}{|\tilde{O}(0)|}$$

Uniform Disk:
$$\Gamma_{12} = \left| \frac{2J_1(\pi\theta B / \lambda)}{\pi\theta B / \lambda} \right|$$

Note: The definition of r_c (Goodman) corresponds at B where $\Gamma_{12}=0.5$
i.e. $\pi\theta B/\lambda=2 \rightarrow r_c=B=2\lambda/\pi\theta \rightarrow \varepsilon=\lambda^2$.

How to measure a so small angular diameter (2)?

$$r_c = \frac{\lambda}{\pi\left(\frac{\theta}{2}\right)} \quad \Gamma_{12} = \frac{|\psi_1\psi_2^*|}{\sqrt{|\psi_1|^2|\psi_2|^2}}$$

$$\begin{aligned} \text{N.A.: } \theta=10\text{mas, } \lambda=1\mu\text{m} &\rightarrow r_c=13\text{m} \\ \Delta\lambda=0.1\mu\text{m and } t_c\cdot\Delta f=1 &\rightarrow t_c=3\cdot 10^{-14}\text{s} \end{aligned}$$

With larger λ and fast detectors, it is possible to record the electromagnetic wave at two different locations and correlate them in a computer:

- Radio Interferometry (mm, cm wavelengths)
- Very Long Baseline Interferometry

With intermediate λ , small $\Delta\lambda$ and fast detectors, one can create beating waves, record them and correlate them in a computer:

- Heterodyne Interferometry

Other cases: direct interferometry because (almost) no ways to record complex optical waves...

It could also be shown that the coherence between the two waves leads to a correlation between the fluctuation of intensities:

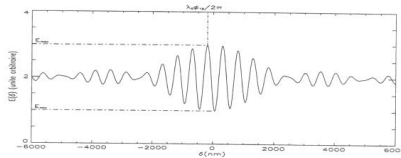
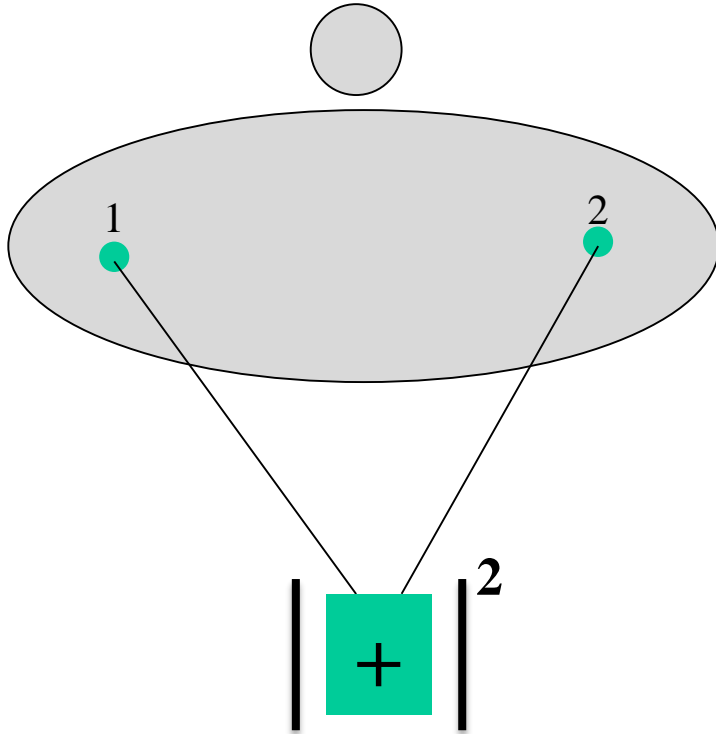
$$|\Gamma_{12}|^2 = \frac{\Delta I_1 \Delta I_2}{I_1 I_2}$$

- Narrabri Intensity Interferometer but strong limitation in magnitude

The ideal interferometer

Young experiment with a star

Star at infinity
Angular diameter θ



$$I = |\Psi_1 + \Psi_2 e^{i\theta}|^2$$

$$I = |\Psi_1|^2 + |\Psi_2|^2 + 2\Psi_1\Psi_2^* \cos(\theta)$$

$$I = (I_1 + I_2) * \left(1 + \frac{2\sqrt{I_1 I_2}}{I_1 + I_2} * \frac{\Psi_1 \Psi_2^*}{\sqrt{|\Psi_1|^2 |\Psi_2|^2}} * \cos(\theta) \right)$$

Photometric term: $\frac{2\sqrt{I_1 I_2}}{I_1 + I_2}$

Modulation term: $\frac{|\Psi_1 \Psi_2^*| e^{i\phi}}{\sqrt{|\Psi_1|^2 |\Psi_2|^2}}$

$$\gamma_{12} = \frac{|\Psi_1 \Psi_2^*|}{\sqrt{|\Psi_1|^2 |\Psi_2|^2}} = \frac{\left| \tilde{O}\left(\frac{B}{\lambda}\right) \right|}{\left| \tilde{O}(0) \right|}$$

Where are we?

- Notions
 - Coherence of a stellar wavefront
 - Fourier transform of the brightness distribution
 - Spatial frequencies of the source
- Method
 - Complex degree of mutual coherence
- This is really complicated...
- An other point of view: object-image relationship

Object-Image relationship

Brightness distribution in the image

$$I(\vec{\beta}) = H(\vec{\beta}) * O(\vec{\beta})$$

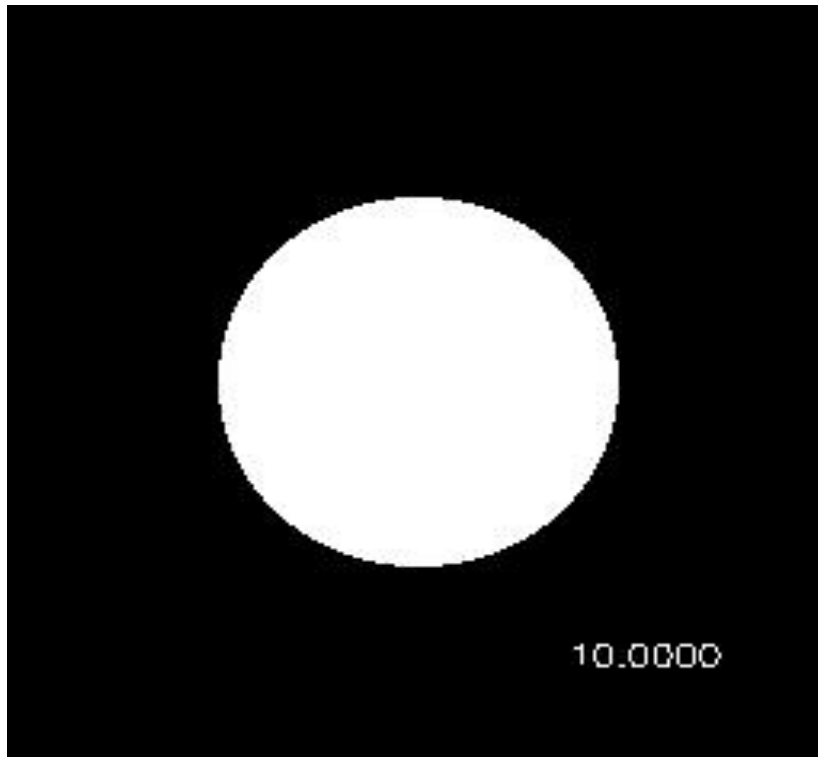
Spatial frequencies spectrum of the image

$$\tilde{I}(\vec{f}) = \tilde{H}(\vec{f}) \times \tilde{O}(\vec{f})$$

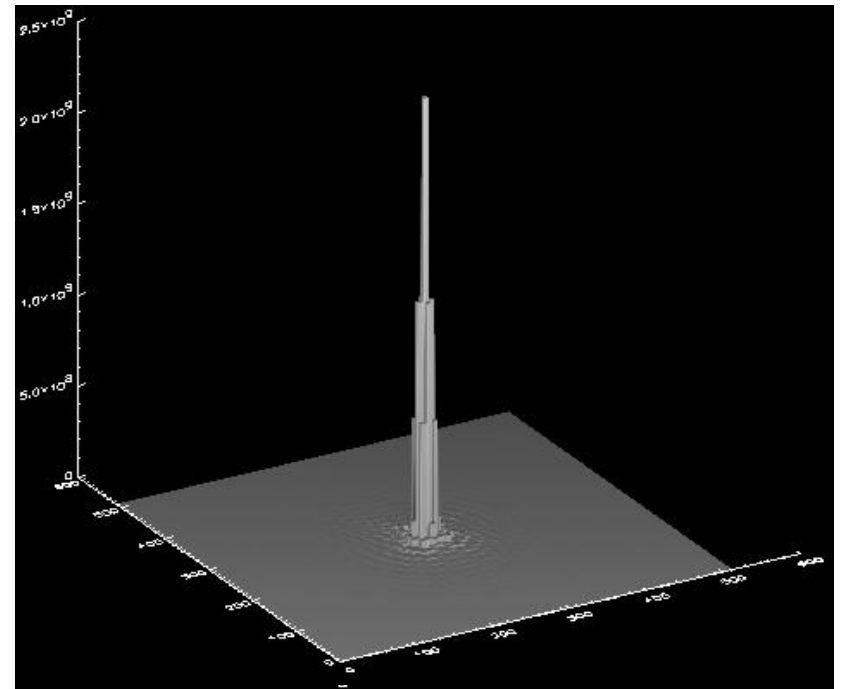
Modulation Transfer Function (MTF)

$$|\tilde{H}(\vec{f})| = AC[P(\lambda\vec{f})]$$

Telescope

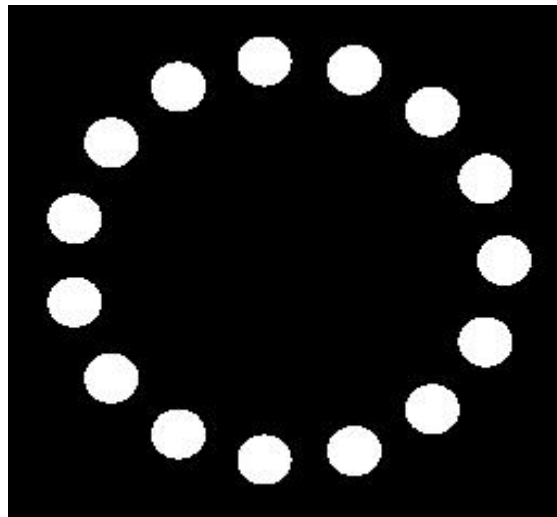
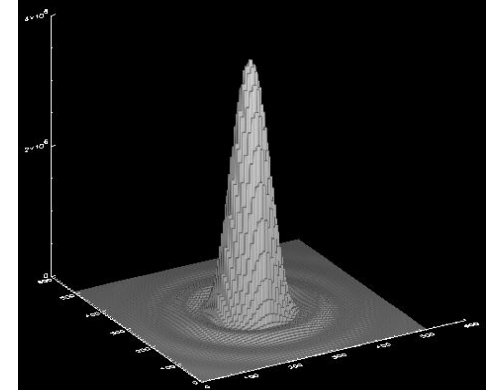


Pupil

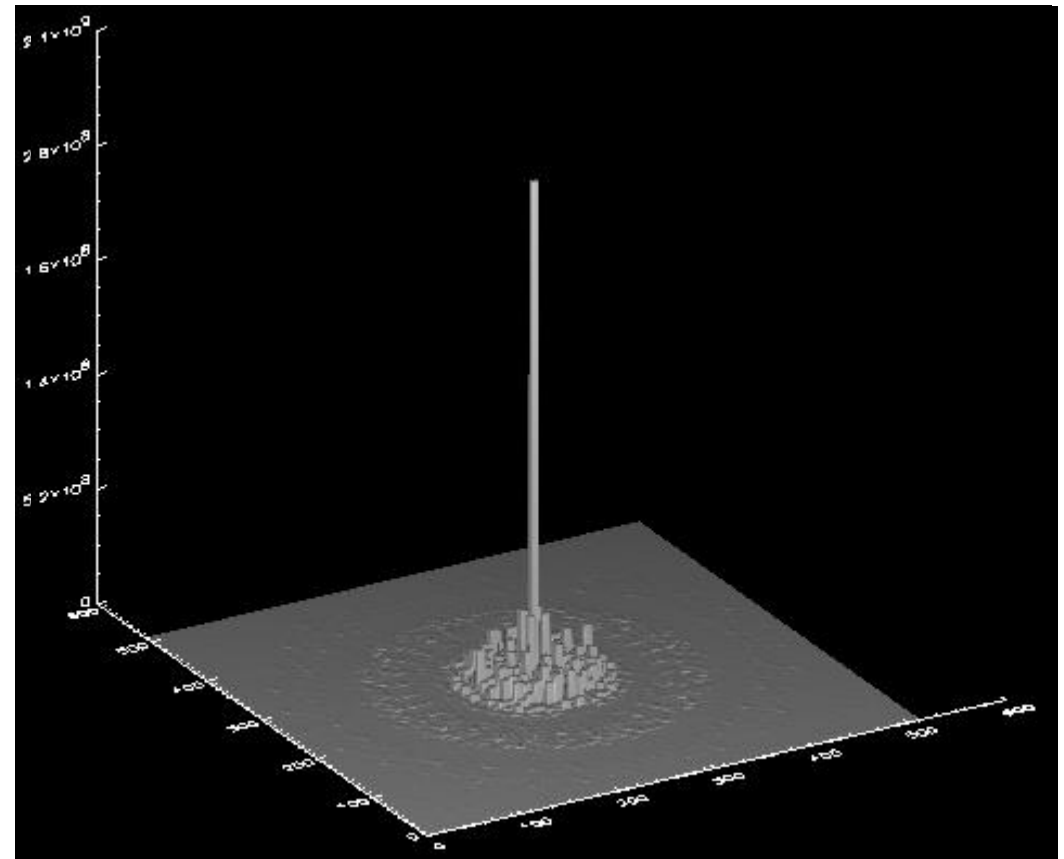


Point Spread Function

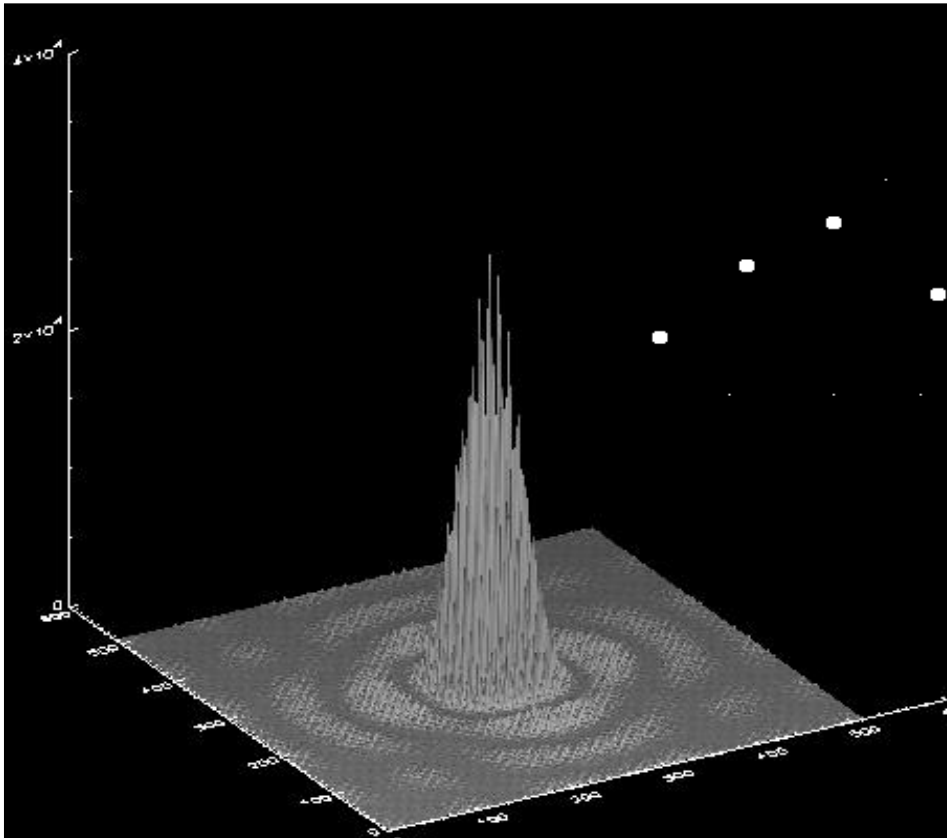
Interferometer



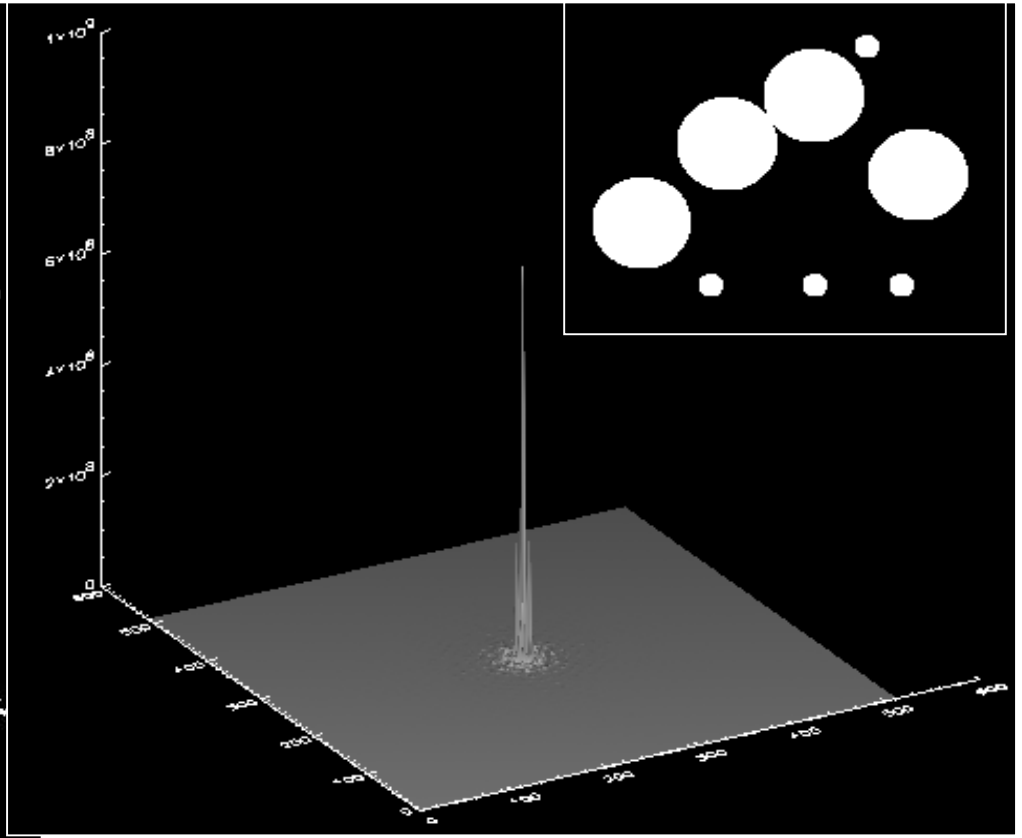
15 Pupil



PSF: Importance of the combining scheme



4 UTs + 4 ATs Fizeau



4 UTs + 4 ATs densified

The (u,v) plane

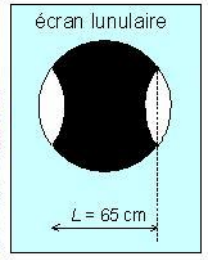
$$|\tilde{H}(\vec{f})| = AC[P(\lambda\vec{f})]$$

- The support of the MTF in the frequency plane is called the (u,v) plane.
- This is a function of
 - the input baseline
 - the latitude of the observatory
 - the target coordinates
 - the wavelength
 - the time

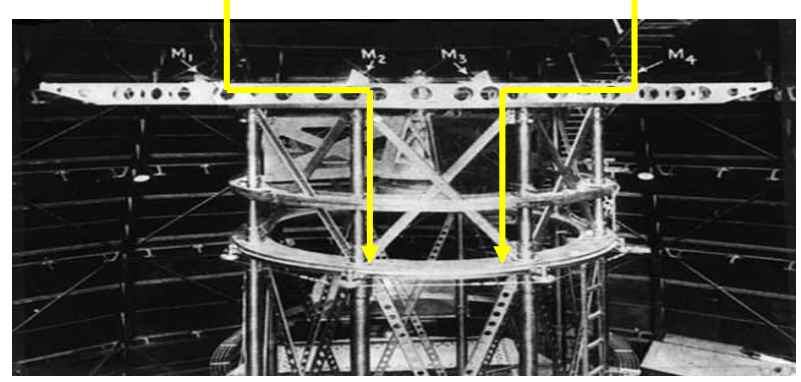
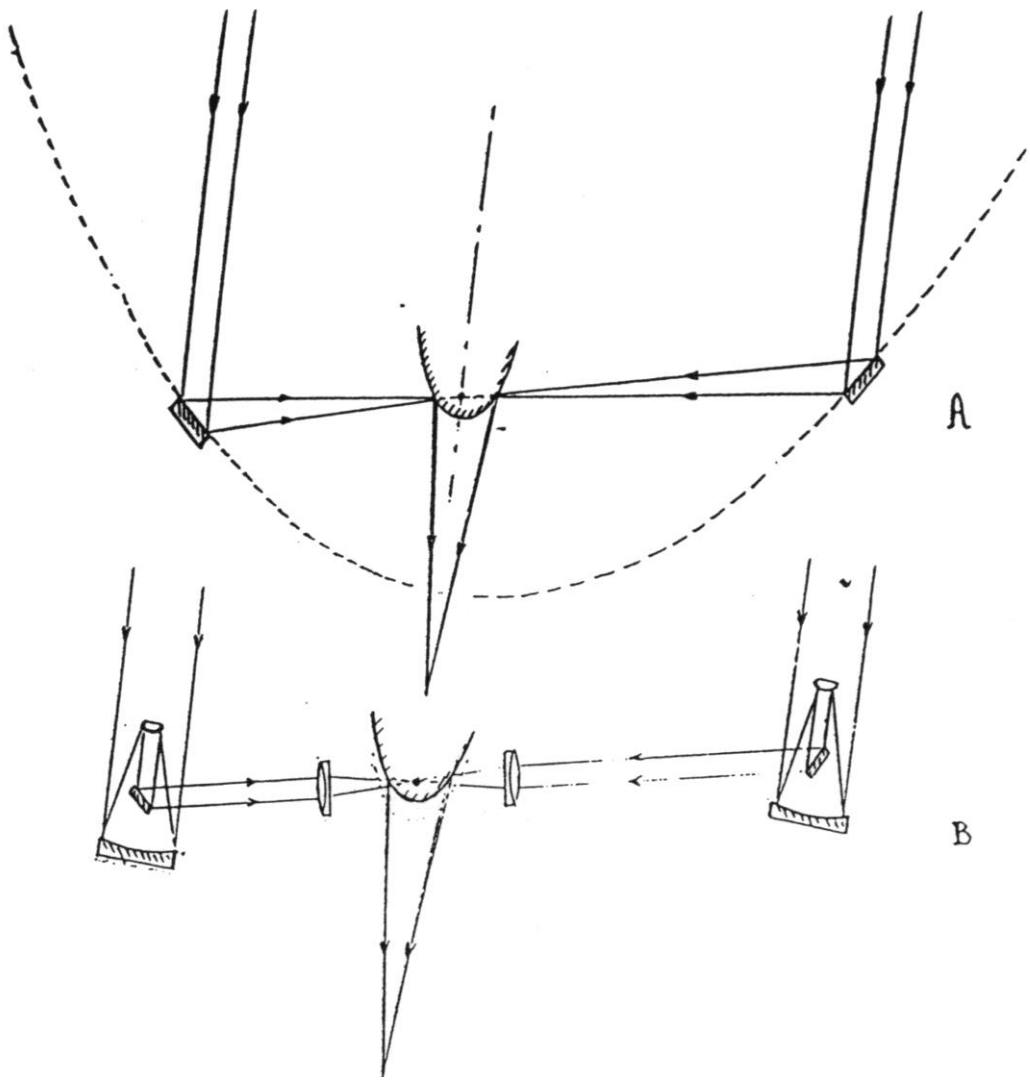
[Some examples with a simulation tool: ASPRO2](#)

Stephan, Michelson, Labeyrie

télescope de Foucault de l'observatoire de Marseille



1874



1919



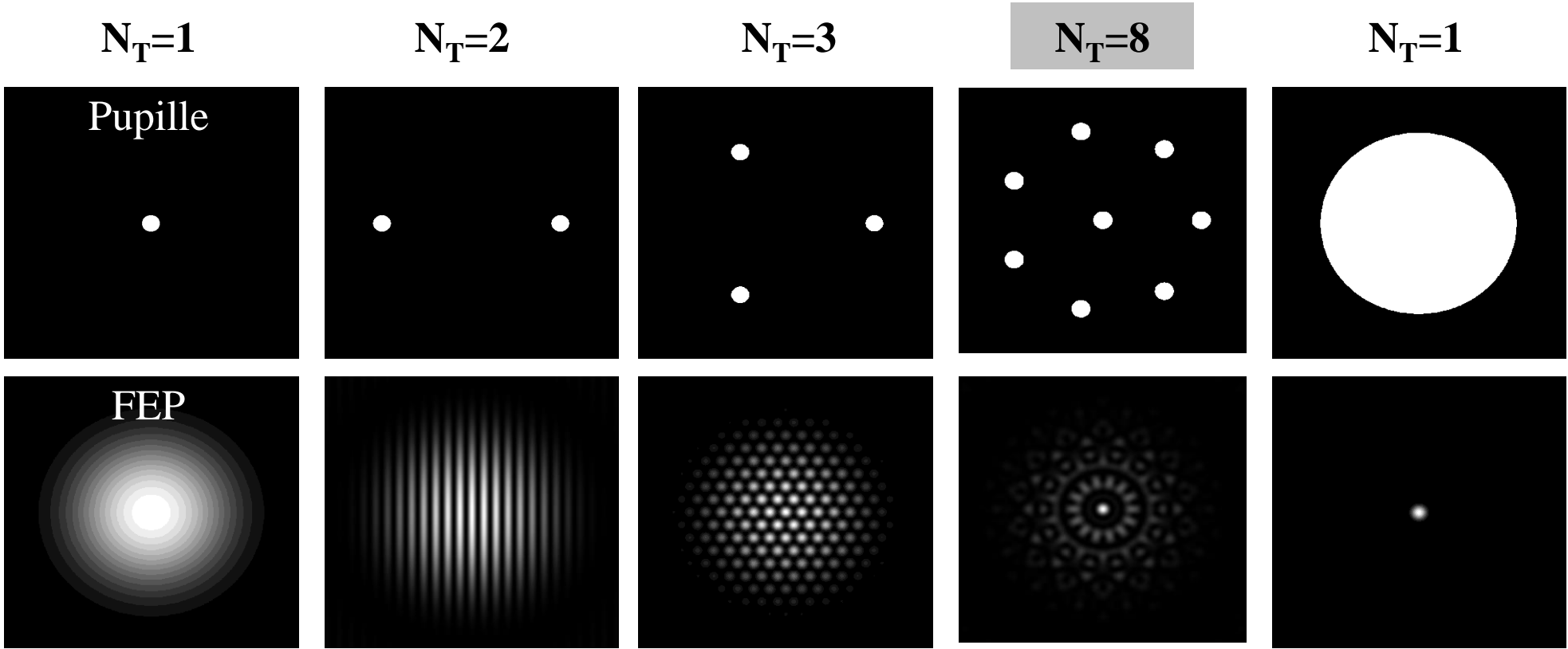
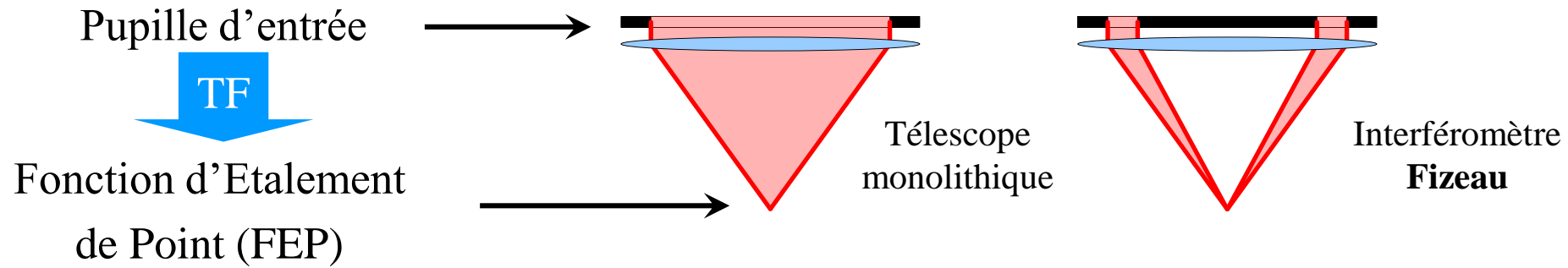
1974

Where are we (2) ?

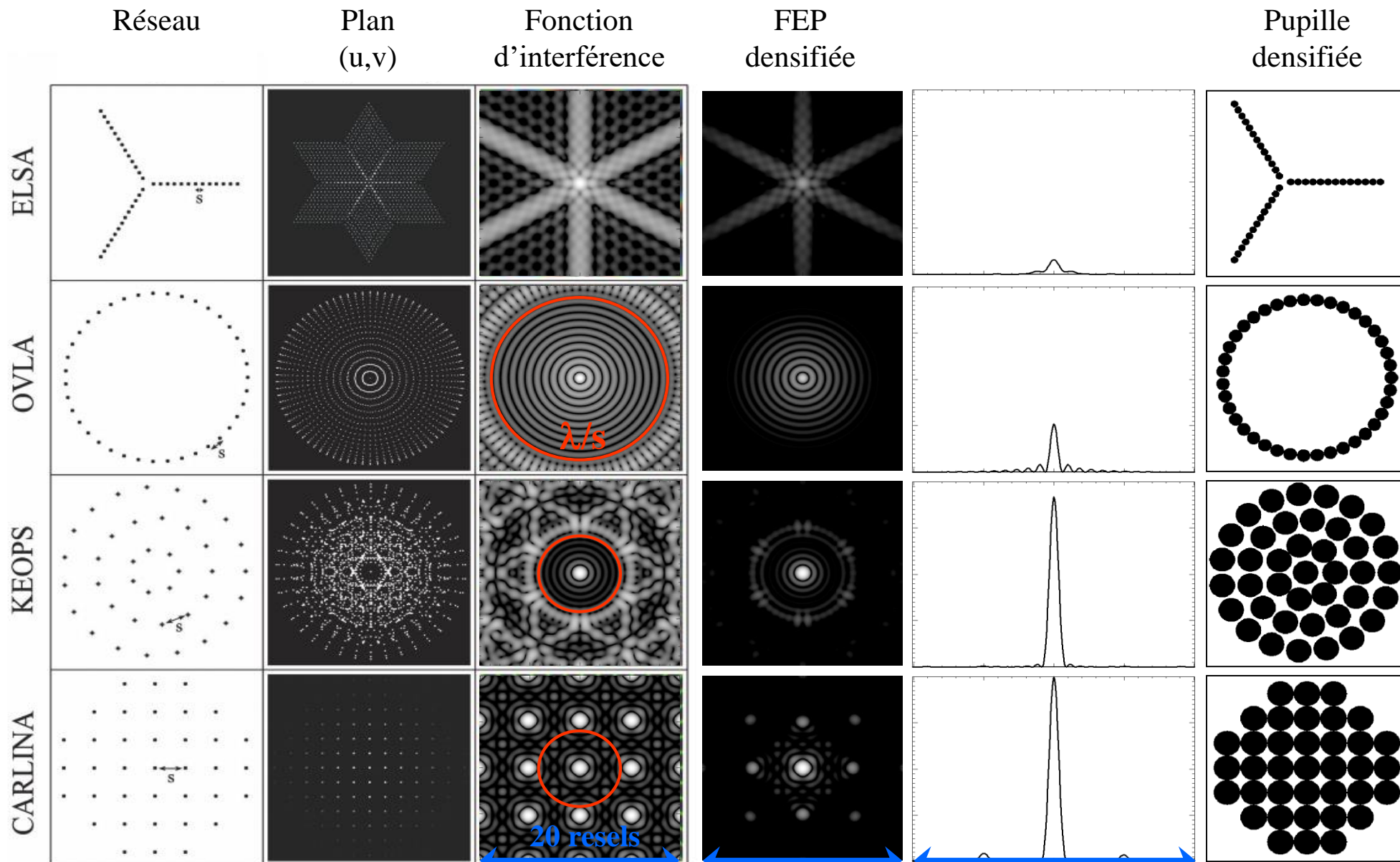
Conceptually speaking, Interferometry is really simple in fact, it's just an imaging technique!

And yes, direct imaging is possible!

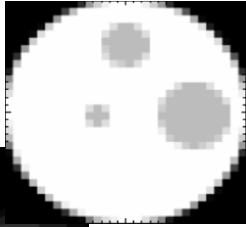
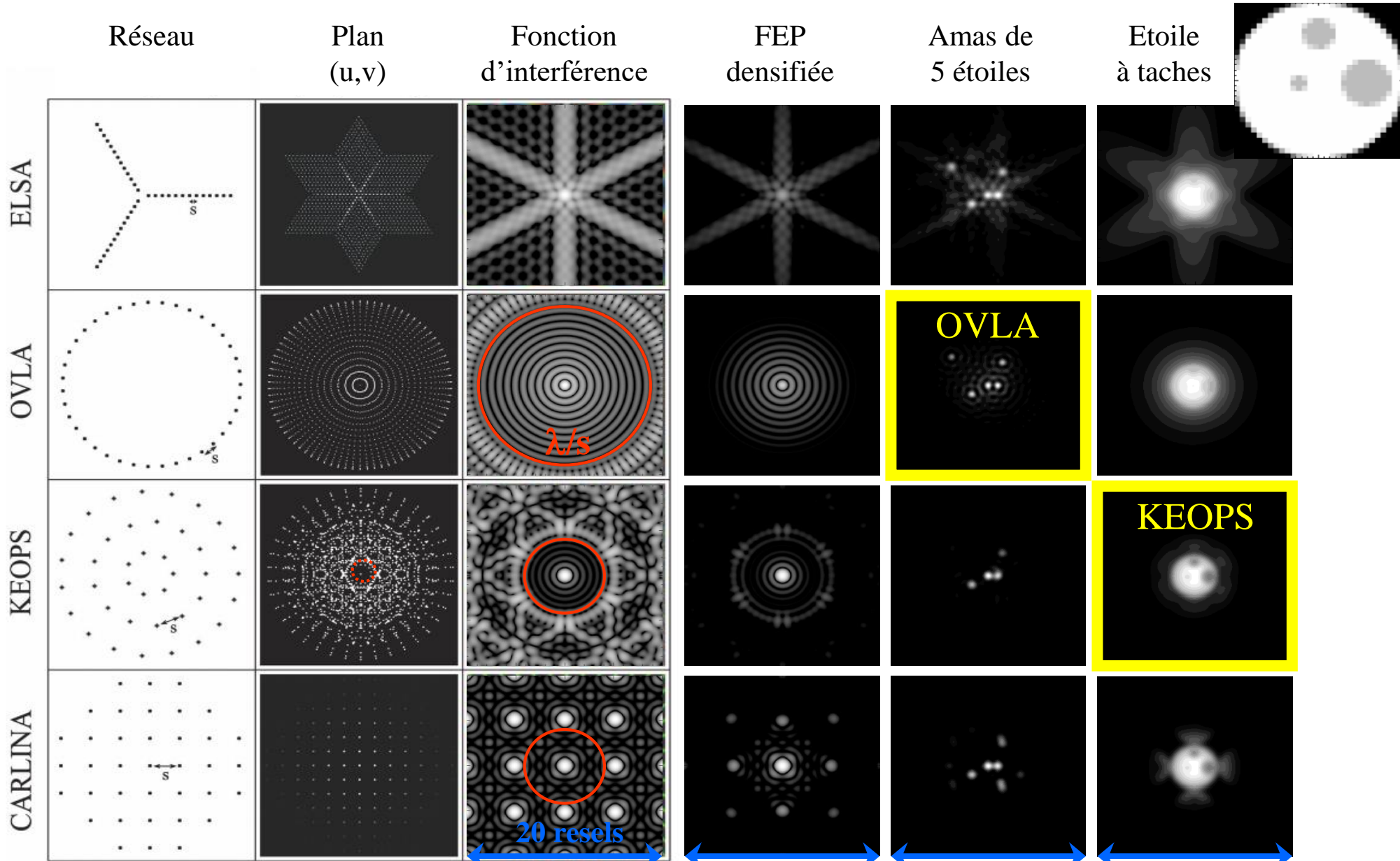
Pupil-Image relation



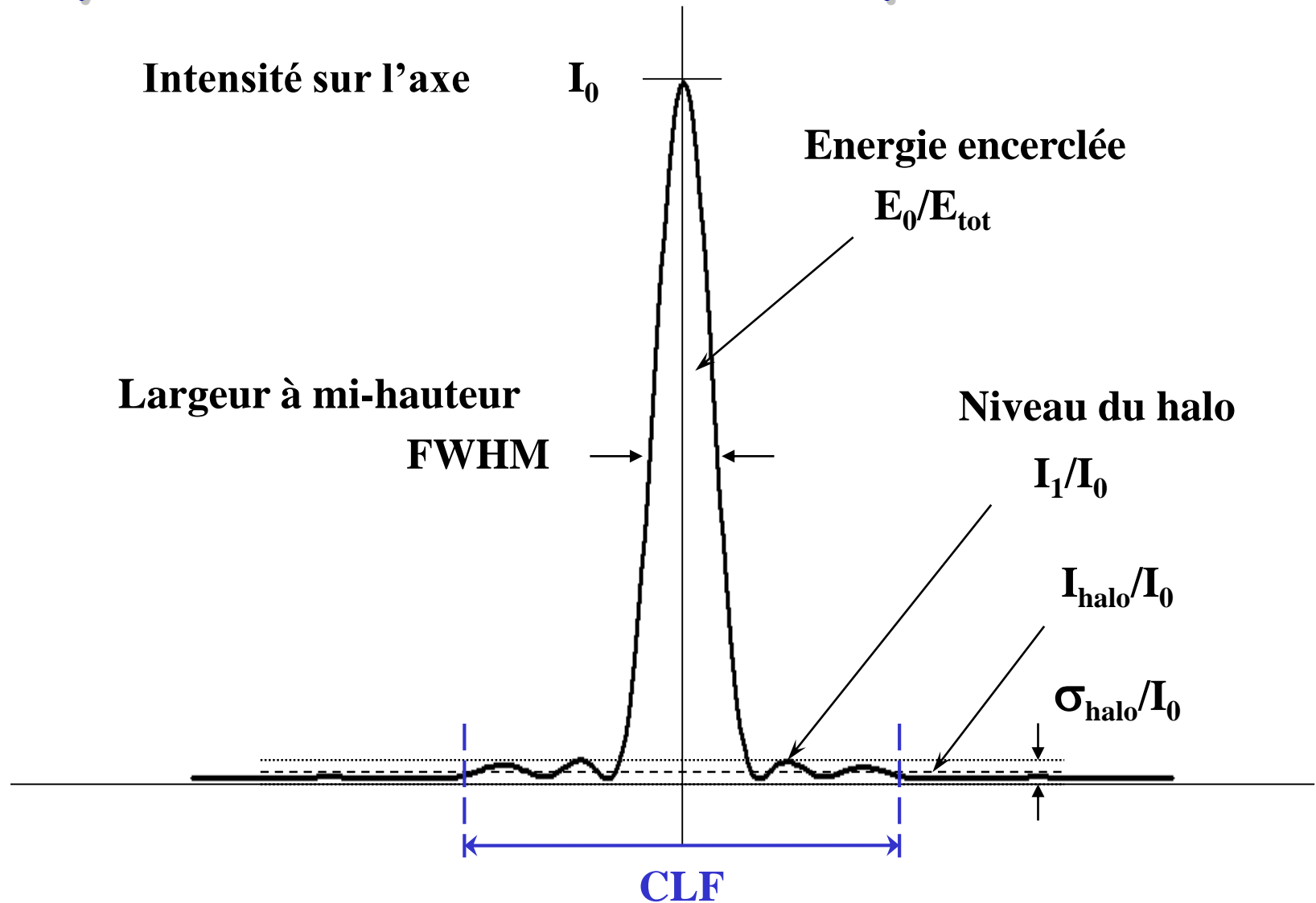
Geometry of the input pupil



Direct imaging examples



Quality criteria in the Point Spread Function



Quality versus number of sub-pupils

Fonction d'interférence

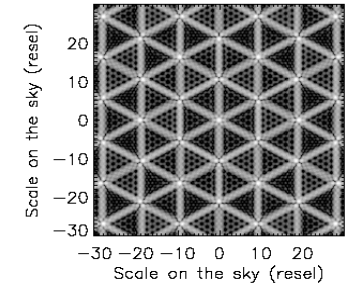
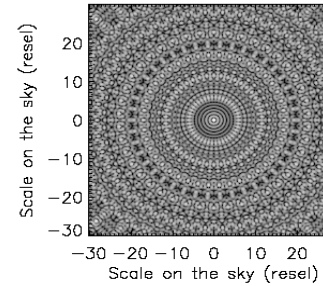
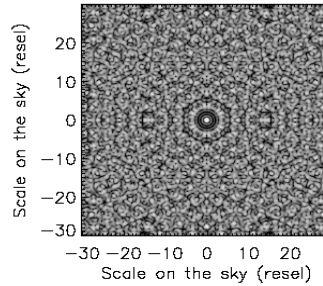
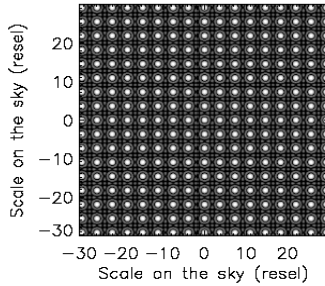
CARLINA

KEOPS

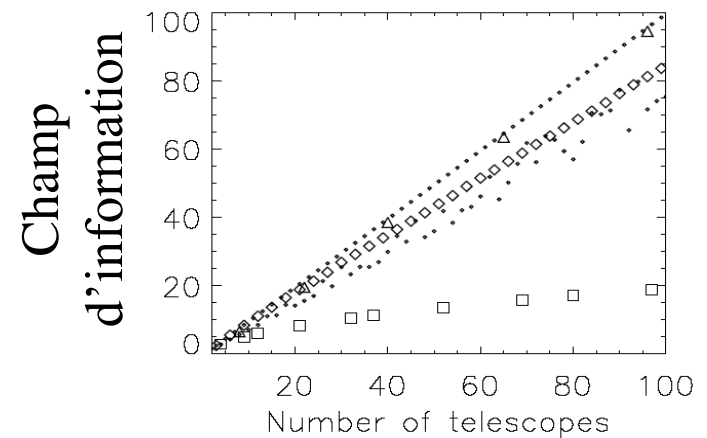
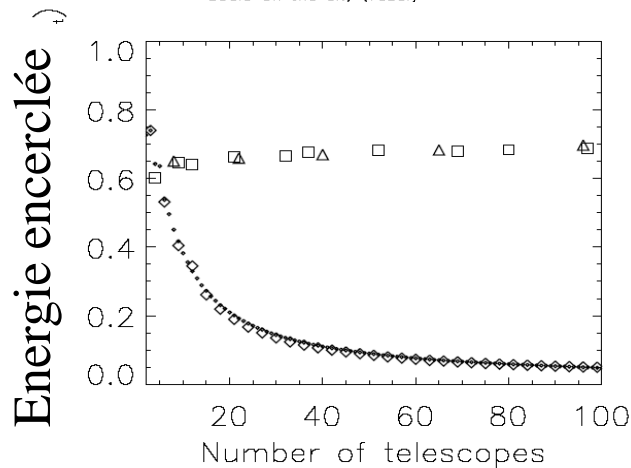
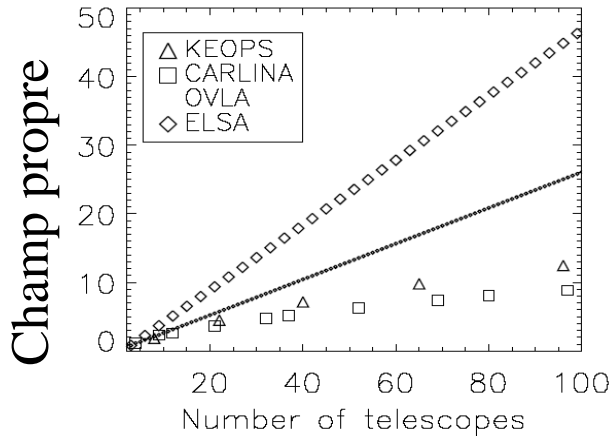
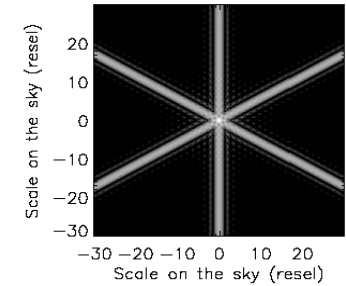
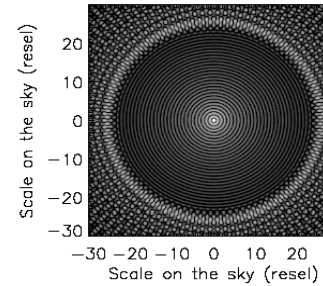
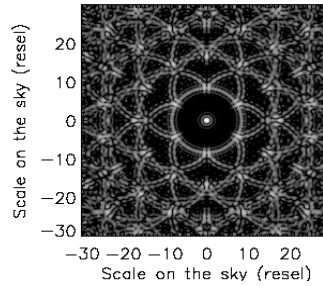
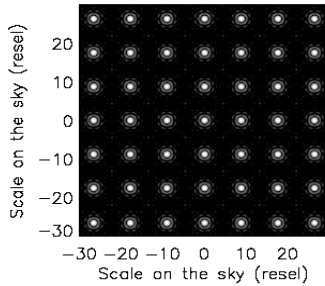
OVLA

ELSA

20 ouvertures



100 ouvertures



Where are we (3) ?

Ok Interferometry is, conceptually speaking, not different as any imaging telescope but...

Why has it been so difficult to get first images? And why do we continue to speak of fringes and visibilities?

Again a coherence problem...

but also a budget issue!

Coherence in reality

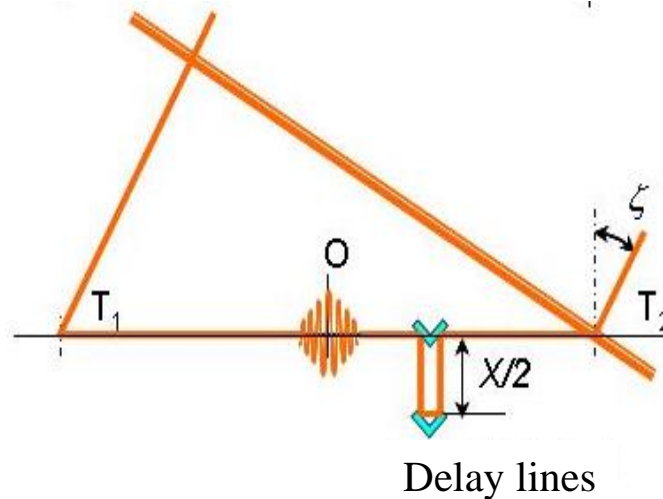
$$r_c = \frac{\lambda}{\pi\left(\frac{\theta}{2}\right)}$$

$$\Gamma_{12} = \frac{|\psi_1\psi_2^*|}{\sqrt{|\psi_1|^2|\psi_2|^2}}$$

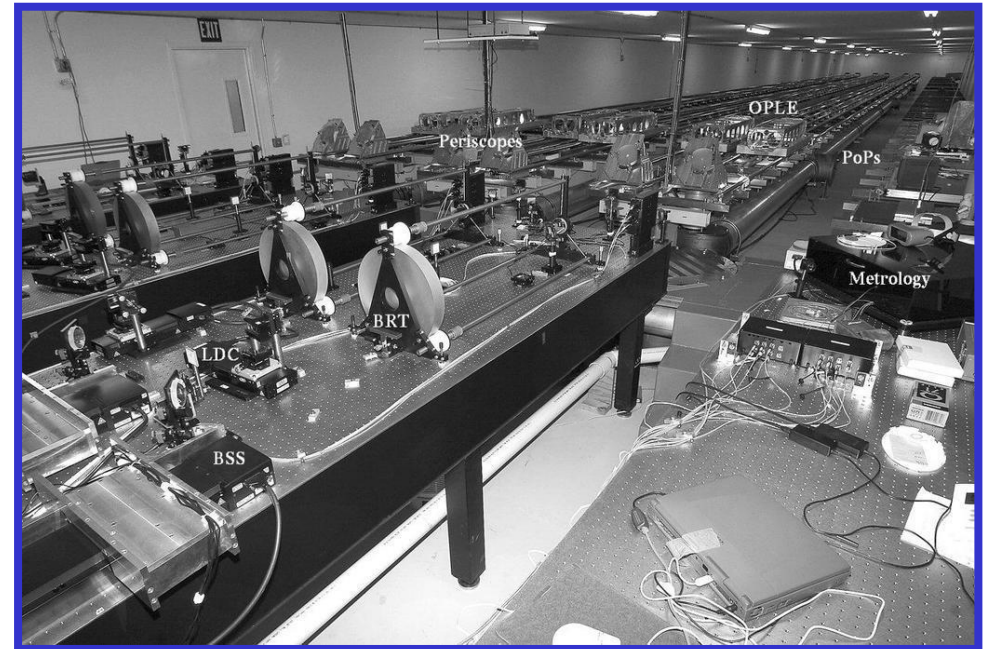
$$I = |\Psi_1 + \Psi_2 e^{i\theta}|^2$$

- N.A.: $\theta=10\text{mas}$, $\lambda=1\mu\text{m}$ → $r_c=13\text{m}$
 $\Delta\lambda=0.1\mu\text{m}$ and $t_c\Delta f=1$ → $t_c=3\cdot 10^{-14}\text{s}$
 $l_c=c\cdot t_c=\lambda^2/\Delta\lambda=R\cdot\lambda$ → $l_c=10\mu\text{m}$

First difficulty: equalizing the optical paths

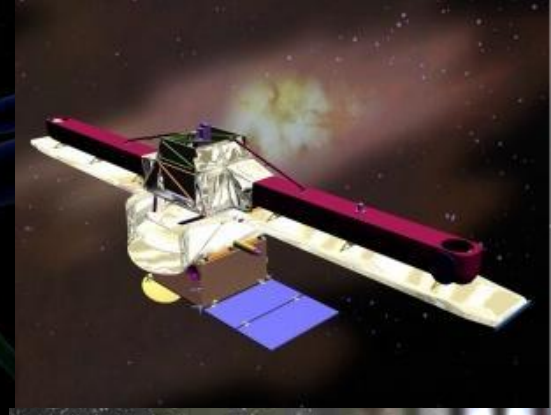
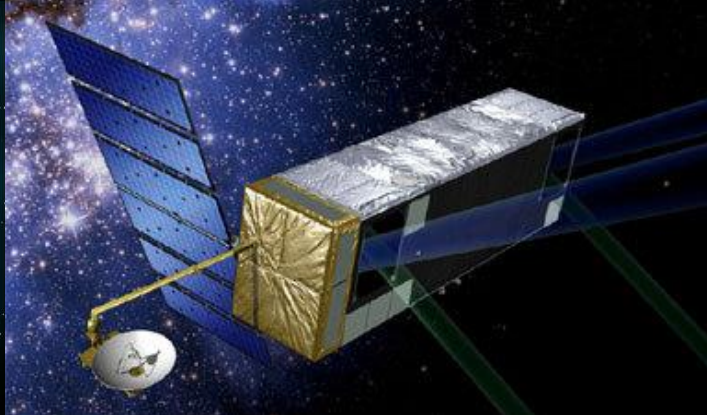


Exemples of delay lines

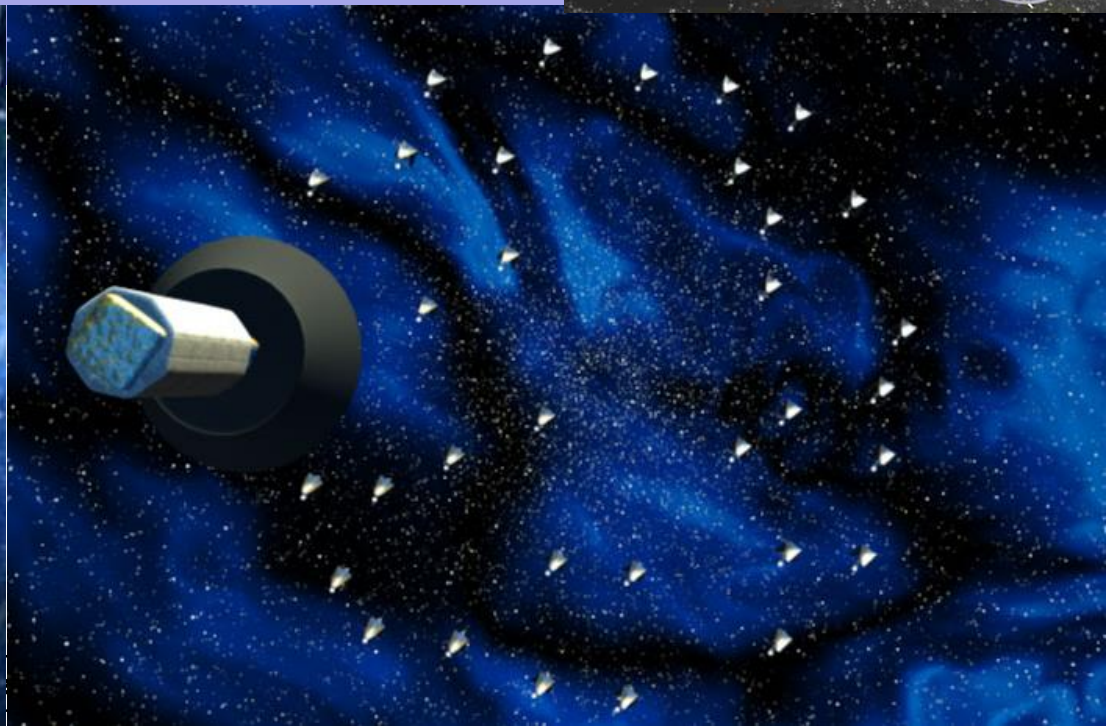
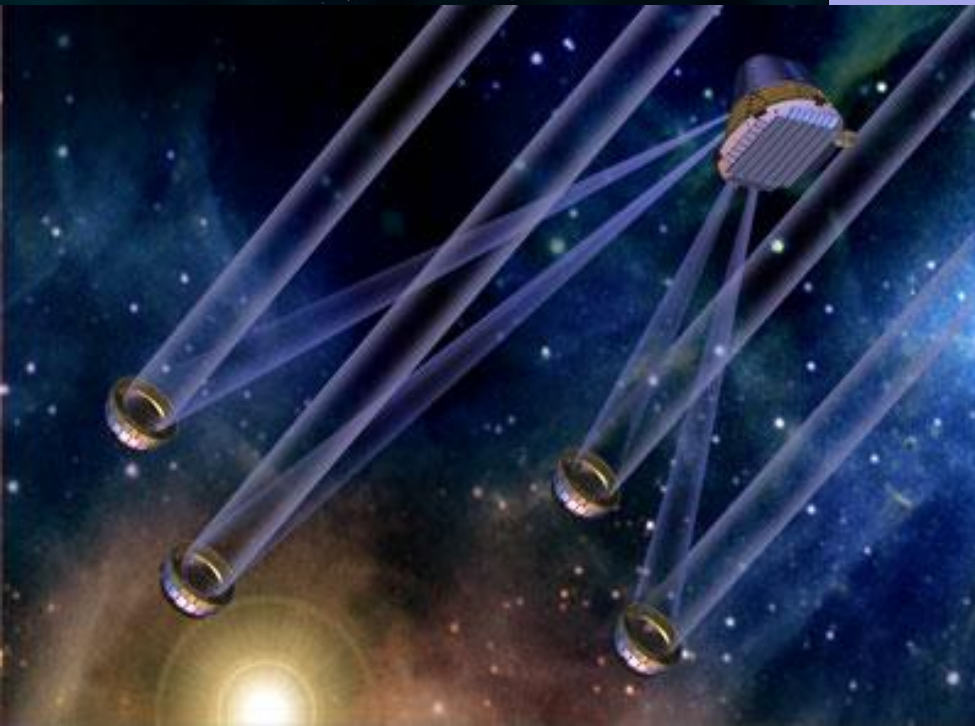
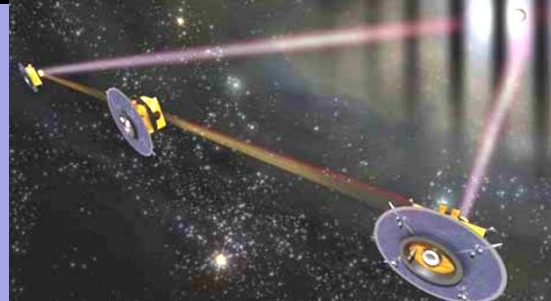


Second main difficulty: the atmospheric turbulence

- After passing through the turbulent atmosphere, the coherence is reduced:
 - Spatially: $r_0 = 10\text{cm}$
 - Temporarily: $t_0 = 5\text{ms}$
 - Spectrally: $\Delta\lambda = 30\text{nm}$ in the visible
- Note
 - hypervolume of coherence $\approx (\text{turbulence})^4!$
- Solutions
 - Space
 - Cophasing devices
 - Correct sampling of the corrugated wavefront



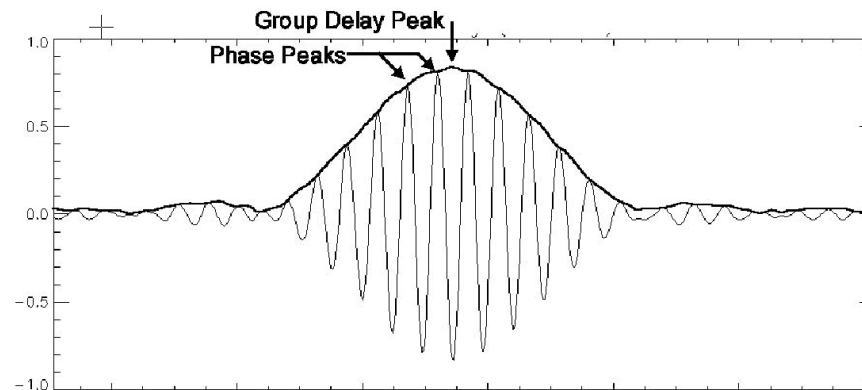
SPACE PROJECTS



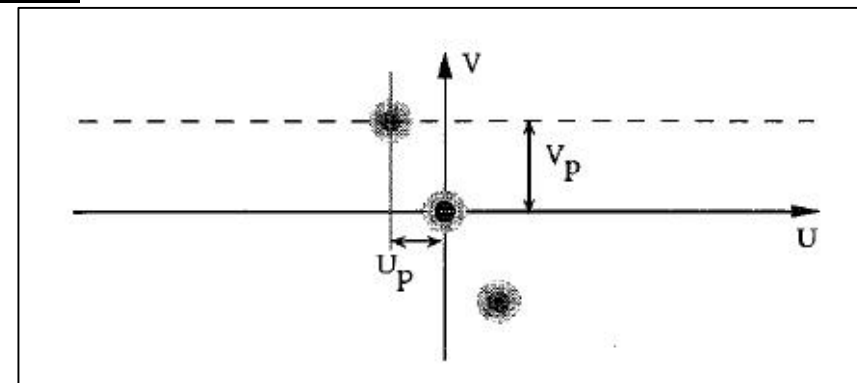
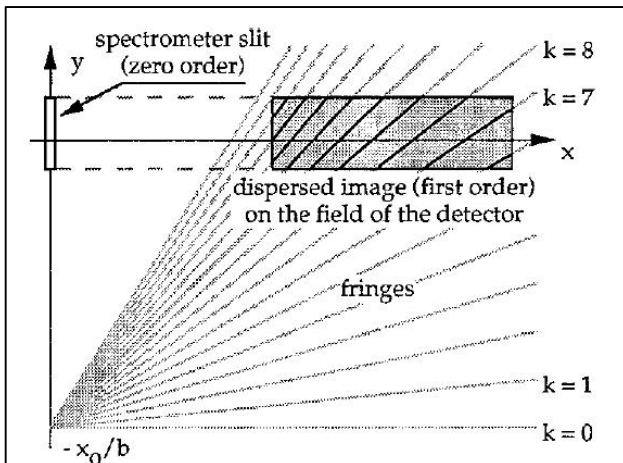
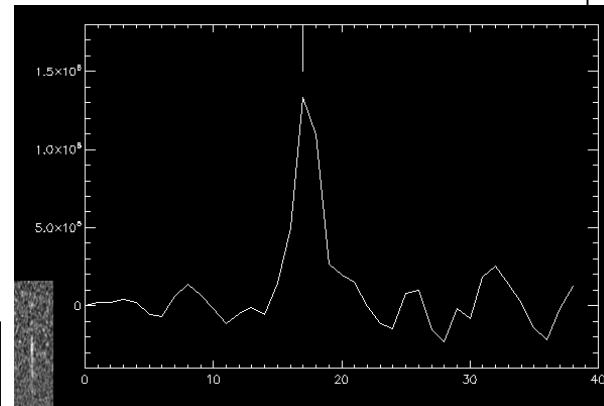
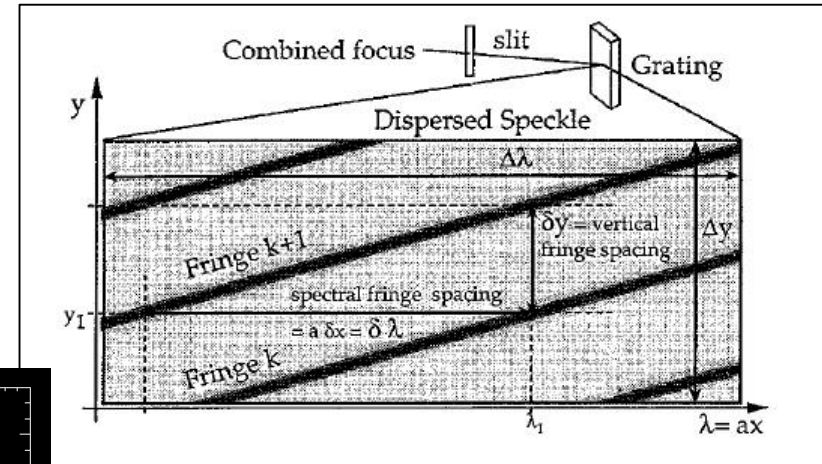
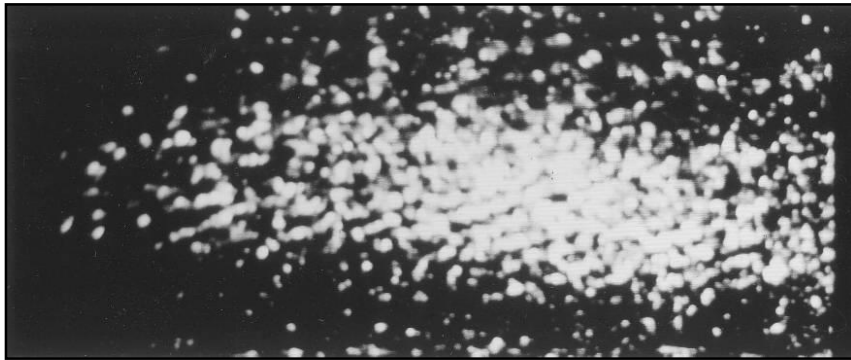
Cophasing devices (1)

$$I = (I_1 + I_2) * \left(1 + \frac{2\sqrt{I_1 I_2}}{I_1 + I_2} * \frac{\Psi_1 \Psi_2^*}{\sqrt{|\Psi_1|^2 |\Psi_2|^2}} * \cos(\theta) \right)$$

But θ contains a modulation term + a random atmospheric term



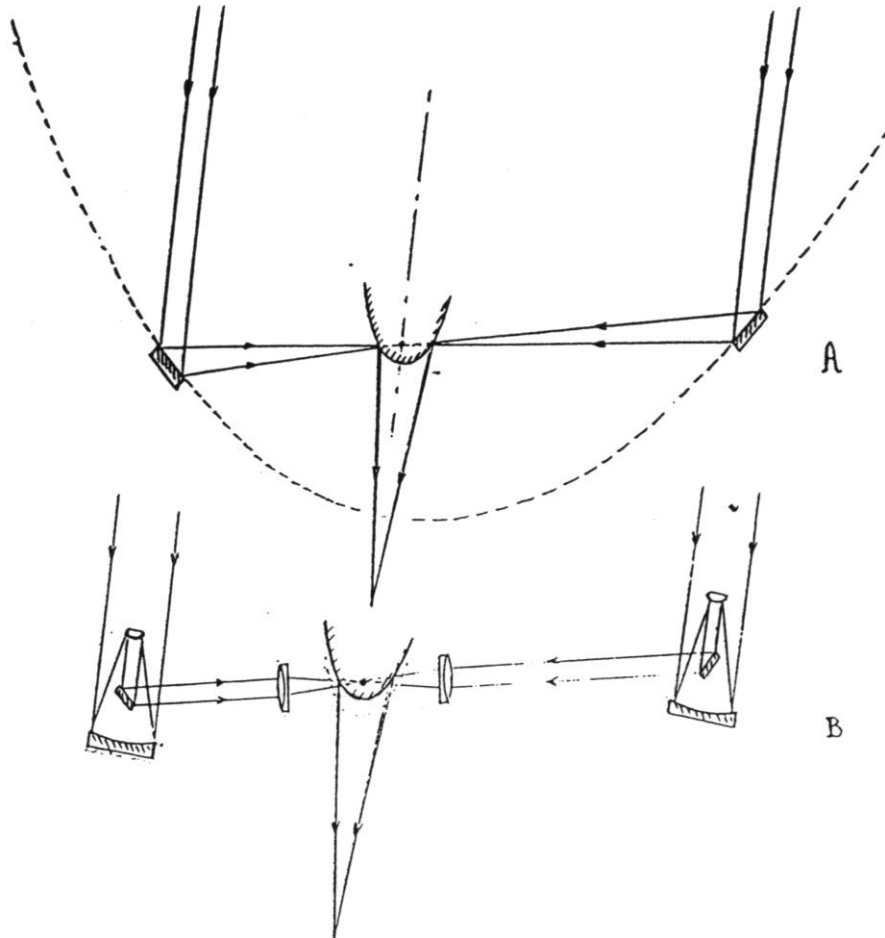
Cophasing devices, dispersed fringes (2)



Cophasing: does-it work?

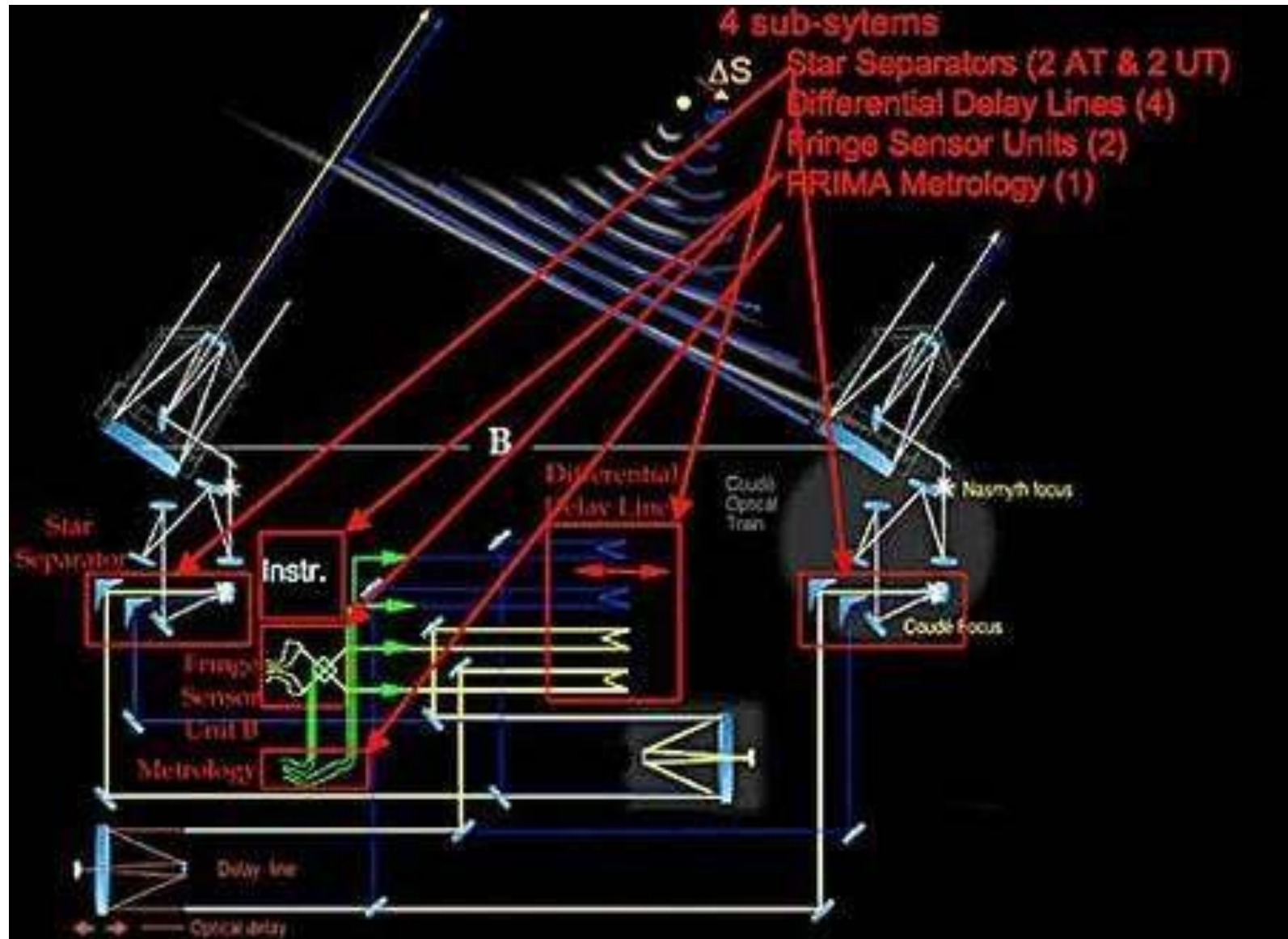
- Yes of course → *GRAVITY* is able to make long integrations of the fringe signal. But this is very recent and for the moment quite exceptional
- Short exposures are mandatory otherwise the high spatial frequency information is blurred and the image quality is lost
 - ↔ a telescope without AO but in speckle interferometry mode
 - Strong limitations in sensitivity, signal to noise ratio.

Interferometer=telescope? Not exactly in fact



- The pupil plane is made of independent subpupils
 - Control of the position of the subpupils
 - Control of the tip/tilt of the subpupils
 - Control of the piston between the subpupils
 - AO for an interferometer
 - The pupil plane is not perpendicular to the direction of pointing
 - Delay
 - Atmospheric dispersion
 - Fresnel diffraction
- Complex optical interfaces between the collection of the waves and the interferometric focus.

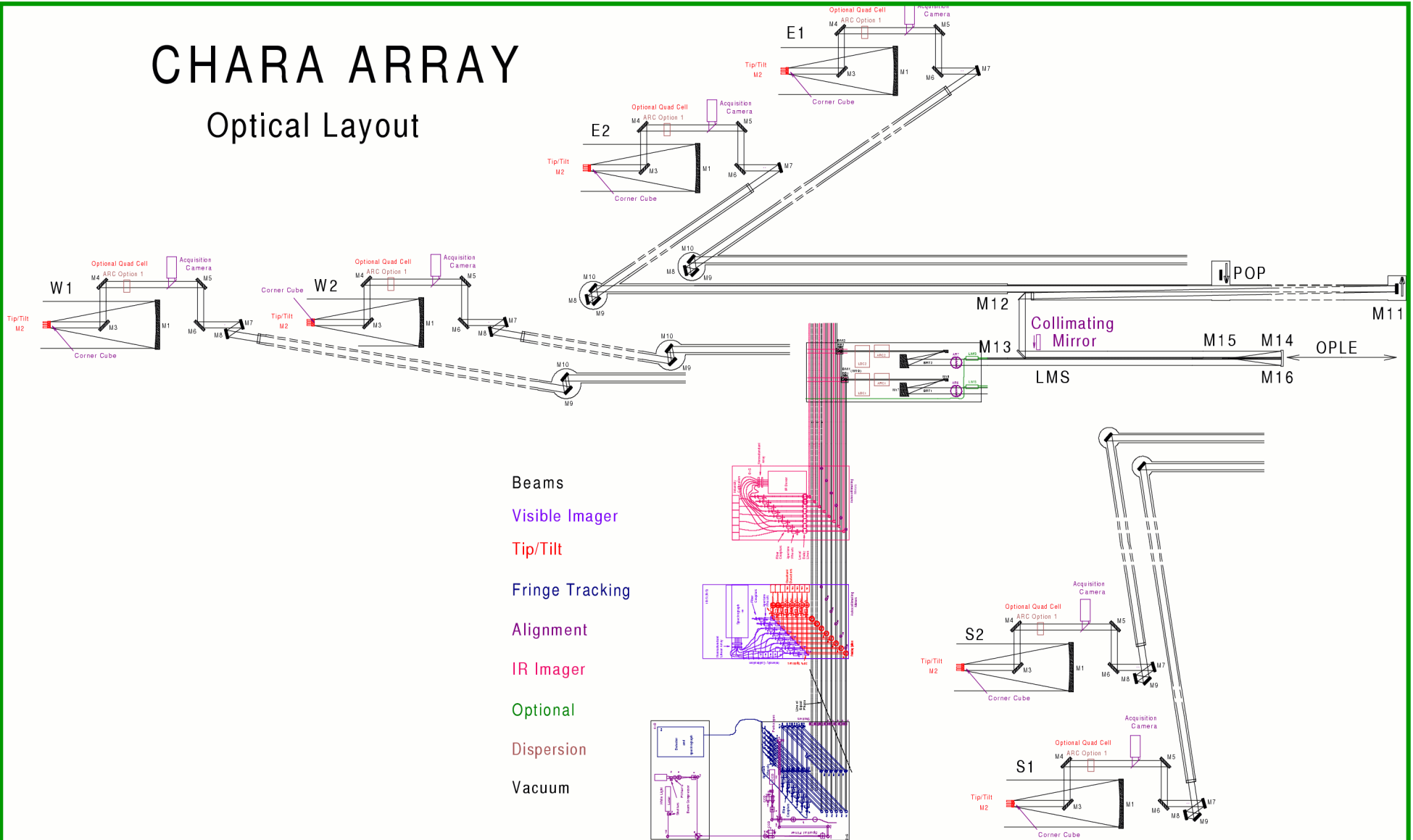
VLTI



CHARA

CHARA ARRAY

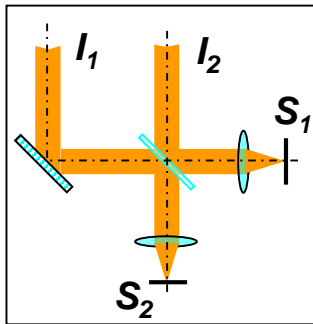
Optical Layout



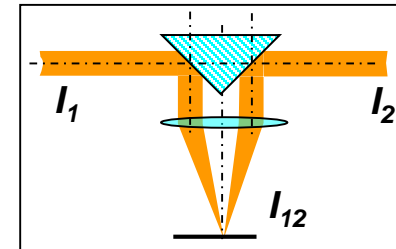
Encoding of fringes

$$I = |\Psi_1 + \Psi_2 e^{i\theta}|^2$$

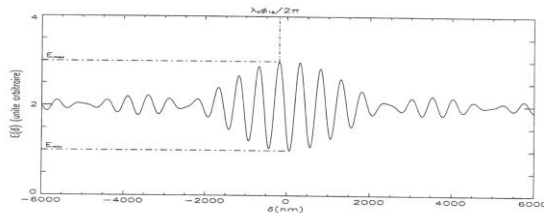
Coaxial



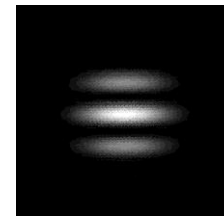
Multi-axial



Temporal sampling



Spatial sampling



Measuring the fringe contrast

$$I = (I_1 + I_2) * \left(1 + \frac{2\sqrt{I_1 I_2}}{I_1 + I_2} * \frac{\Psi_1 \Psi_2^*}{\sqrt{|\Psi_1|^2 |\Psi_2|^2}} * \cos(\theta) \right) \text{ with } \theta(t) \text{ or } \theta(x)$$

Contrast of the interference figure (with $I_1=I_2$)

$$C = \frac{I_{\max} - I_{\min}}{I_{\max} + I_{\min}} = \frac{|\Psi_1 \Psi_2^*|}{\sqrt{|\Psi_1|^2 |\Psi_2|^2}}$$

But this is practically not possible because of the fast turbulence motion

C is measured through the Fourier Transform of the image

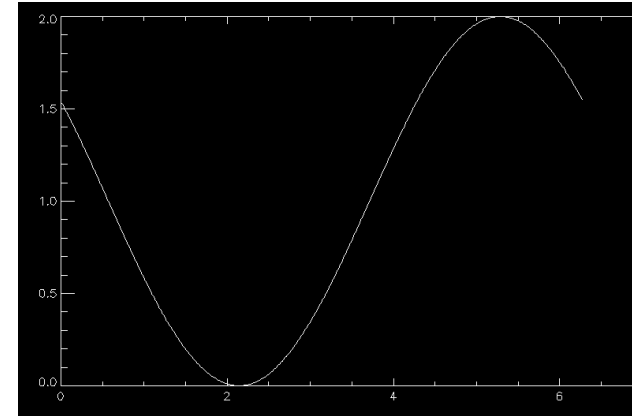
$$\left| \tilde{I} \right|^2 = 1 + \frac{C^2}{4} \delta(\pm f), \text{ } f \text{ being the frequency of the modulation}$$

More details in Roddier & Léna, 1994, Journal of Optics

A short digression...

$$I = 1 + V \cos(\omega t + \phi)$$

$$C = \frac{I_{\max} - I_{\min}}{I_{\max} + I_{\min}} = \frac{(1+V) - (1-V)}{(1+V) + (1-V)} = \frac{2V}{2} = V$$



$$I_A = I(0 - \pi/2), I_B = I(\pi/2 - \pi), I_C = I(\pi - 3\pi/2), I_D = I(3\pi/2 - 2\pi)$$

$$V = \frac{\pi}{\sqrt{2}} \frac{\sqrt{(I_A - I_C)^2 + (I_B - I_D)^2}}{I_{\text{tot}}}$$

Both methods are equivalent to a Fourier transform in fact!

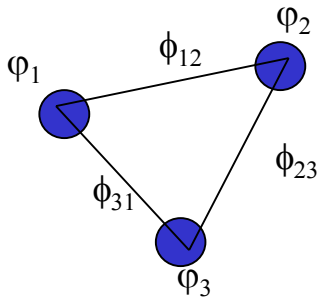
Measuring the phase

$$I = (I_1 + I_2) * \left(1 + \frac{2\sqrt{I_1 I_2}}{I_1 + I_2} * \frac{\Psi_1 \Psi_2^*}{\sqrt{|\Psi_1|^2 |\Psi_2|^2}} * \cos(\theta) \right) = (I_1 + I_2) * \left(1 + \frac{2\sqrt{I_1 I_2}}{I_1 + I_2} * \frac{|\Psi_1 \Psi_2^*|}{\sqrt{|\Psi_1|^2 |\Psi_2|^2}} * \cos(\theta + \phi) \right)$$

1) Differential phase:

$$\left\langle \tilde{I}_{\lambda_1} \tilde{I}_{\lambda_2}^* \right\rangle_{\frac{\vec{B}}{\lambda}} \Rightarrow \frac{\left| \tilde{O}_{\lambda_1} \left(\frac{\vec{B}}{\lambda} \right) \right|}{\left| \tilde{O}_{\lambda_2} \left(\frac{\vec{B}}{\lambda} \right) \right|} \text{ et } \text{Arg} \left(\tilde{O}_{\lambda_1} \left(\frac{\vec{B}}{\lambda} \right) \right) - \text{Arg} \left(\tilde{O}_{\lambda_2} \left(\frac{\vec{B}}{\lambda} \right) \right) = \phi_{B, \lambda_2} - \phi_{B, \lambda_1}$$

2) Phase closure:



Baseline 12: $\Psi_{12} = \Phi_{12} + \varphi_1 - \varphi_2$

Baseline 23: $\Psi_{23} = \Phi_{23} + \varphi_2 - \varphi_3$

Baseline 31: $\Psi_{31} = \Phi_{31} + \varphi_3 - \varphi_1$

with $\Phi_{ij} = \text{Arg} \left(\tilde{O} \left(\frac{\vec{B}_{ij}}{\lambda} \right) \right)$ and φ_i the turbulent phase on pupil i

Closure phase equation: $\Psi_{12} + \Psi_{23} + \Psi_{31} = \Phi_{12} + \Phi_{23} + \Phi_{31}$

Interferometric data

Visibility

$$V^2 = \frac{\left| \tilde{O}\left(\frac{B}{\lambda}\right) \right|^2}{\left| \tilde{O}(0) \right|^2}$$

Differential phase

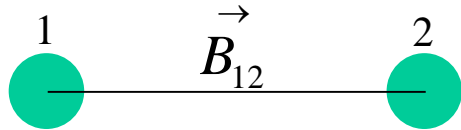
$$\text{Arg}\left(\tilde{O}_{\lambda_1}\left(\frac{\vec{B}}{\lambda}\right)\right) - \text{Arg}\left(\tilde{O}_{\lambda_2}\left(\frac{\vec{B}}{\lambda}\right)\right)$$

Phase closure

$$\Psi_{12} + \Psi_{23} + \Psi_{31} = \Phi_{12} + \Phi_{23} + \Phi_{31}$$

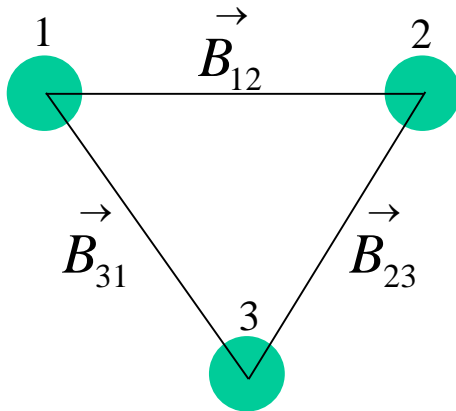
Number of observables

2 telescopes interferometer



$$\left| \tilde{O}(\vec{B}_{12} / \lambda) \right|^2$$

3 telescopes interferometer



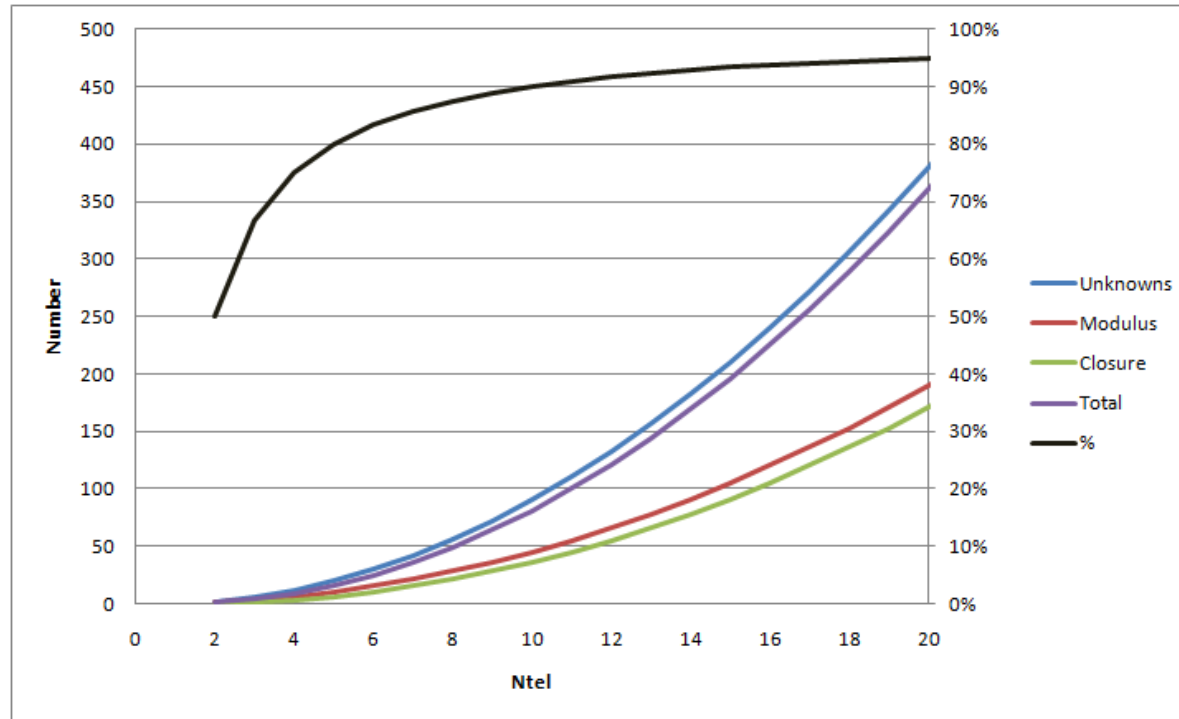
$$\left[\begin{array}{l} \left| \tilde{O}(\vec{B}_{12} / \lambda) \right|^2 \\ \left| \tilde{O}(\vec{B}_{23} / \lambda) \right|^2 \\ \left| \tilde{O}(\vec{B}_{31} / \lambda) \right|^2 \end{array} \right]$$

$$Arg(\tilde{O}(\vec{B}_{12} / \lambda)) + Arg(\tilde{O}(\vec{B}_{23} / \lambda)) + Arg(\tilde{O}(\vec{B}_{31} / \lambda))$$

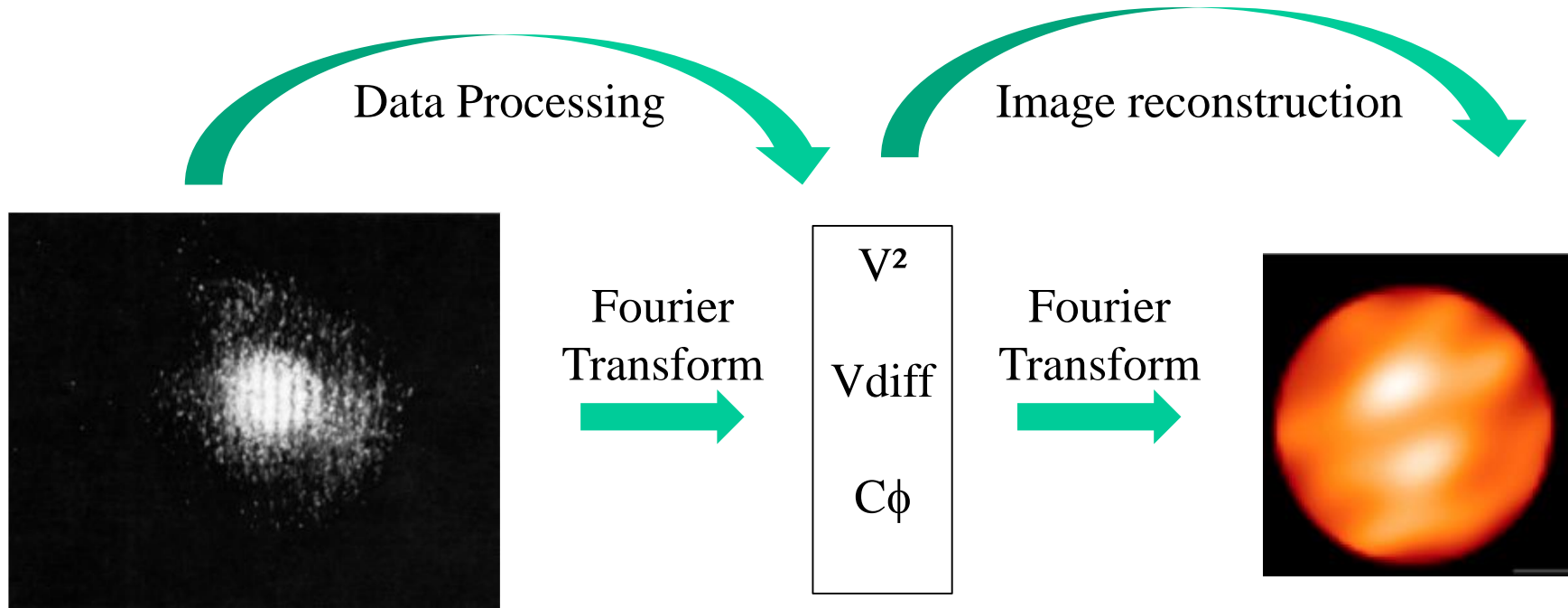
Generalization

An interferometer with n telescopes produces

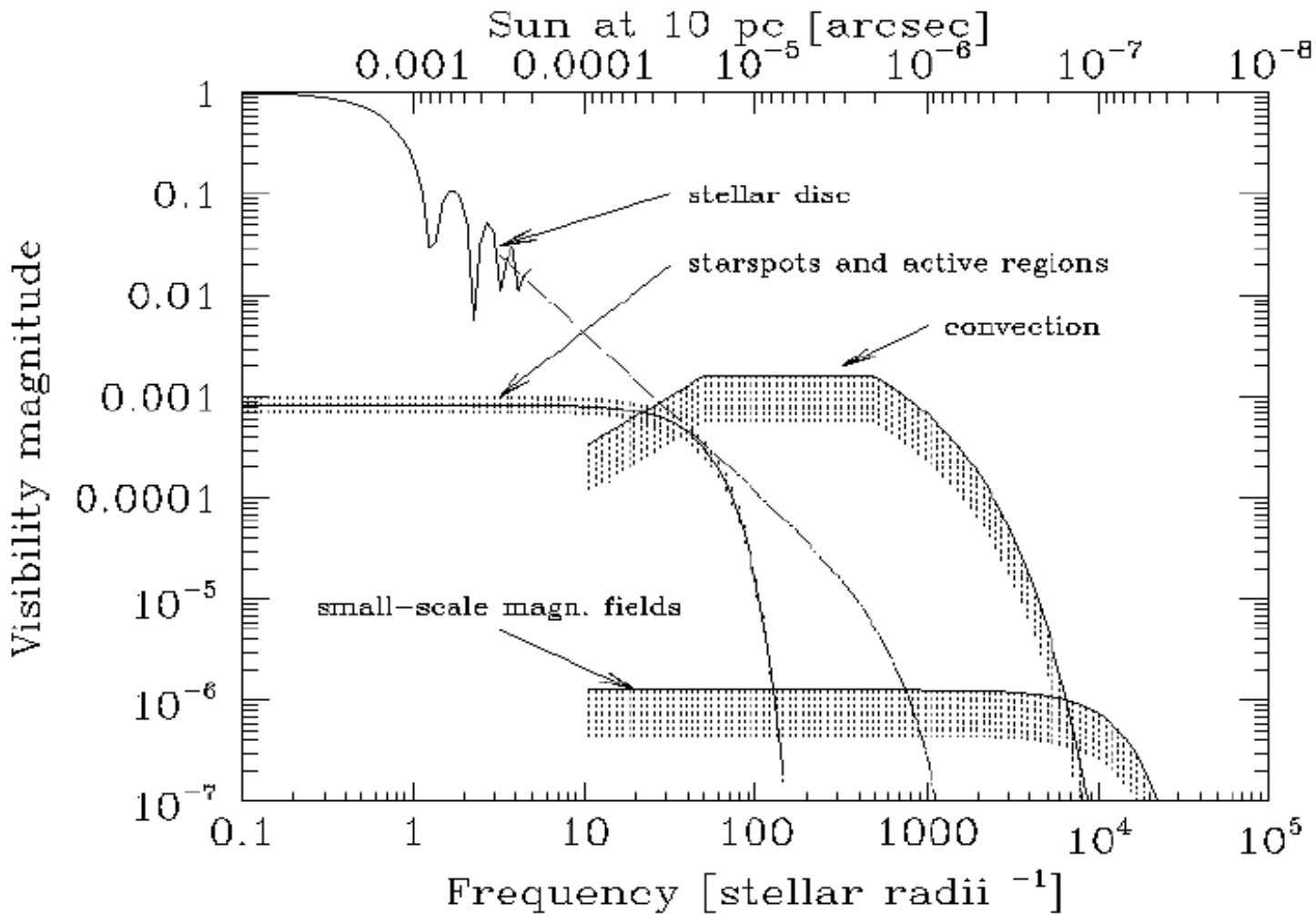
- $n(n-1)/2$ bases, so $[n(n-1)/2]$ complex quantities, so $n(n-1)$ unknowns
- $n(n-1)/2$ modulus measurements
- $(n-1)(n-2)/2$ closure phase measurements



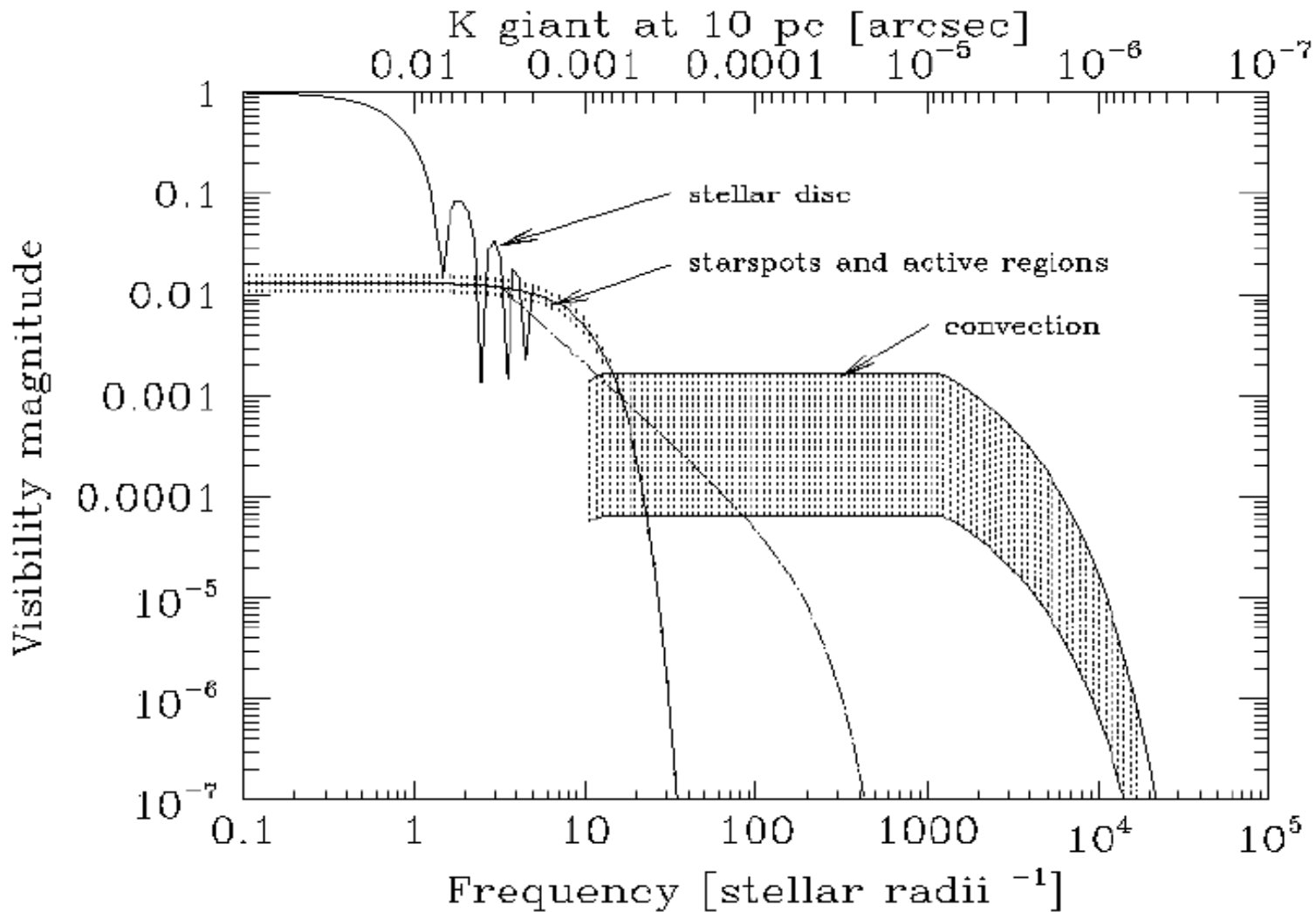
But do not remember that an interferometer is a direct imaging telescope!



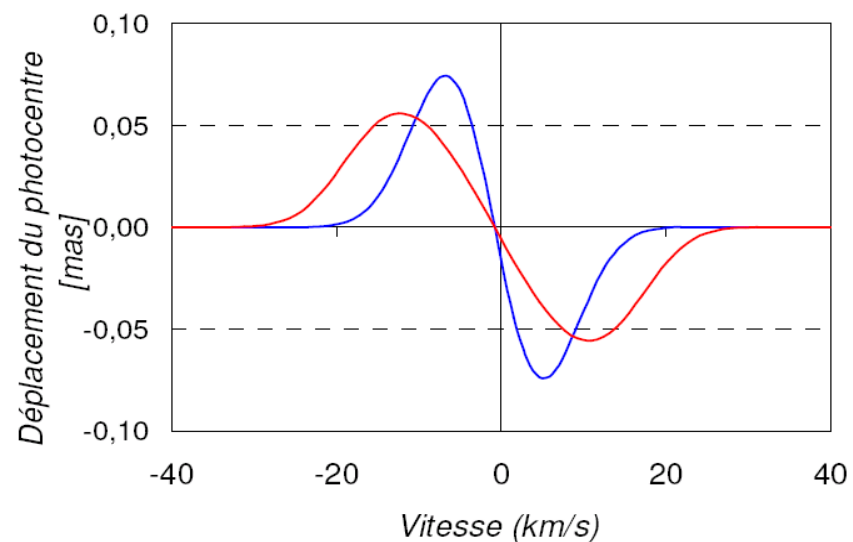
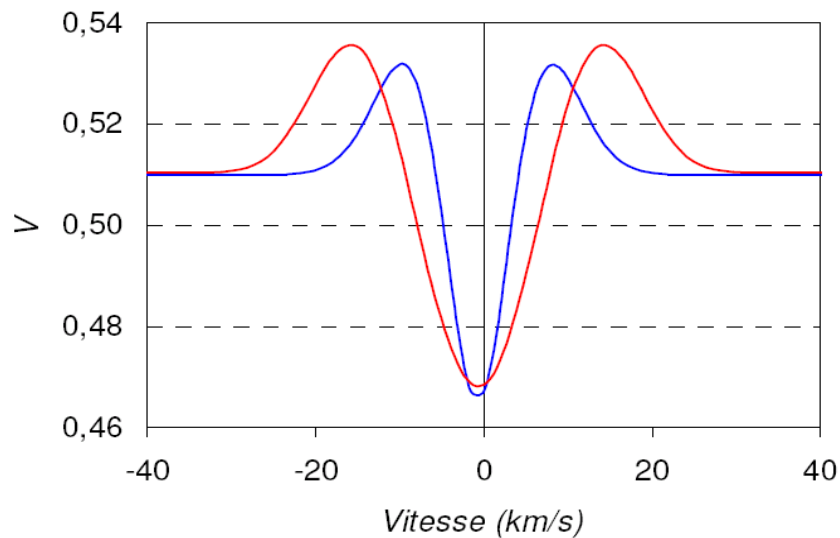
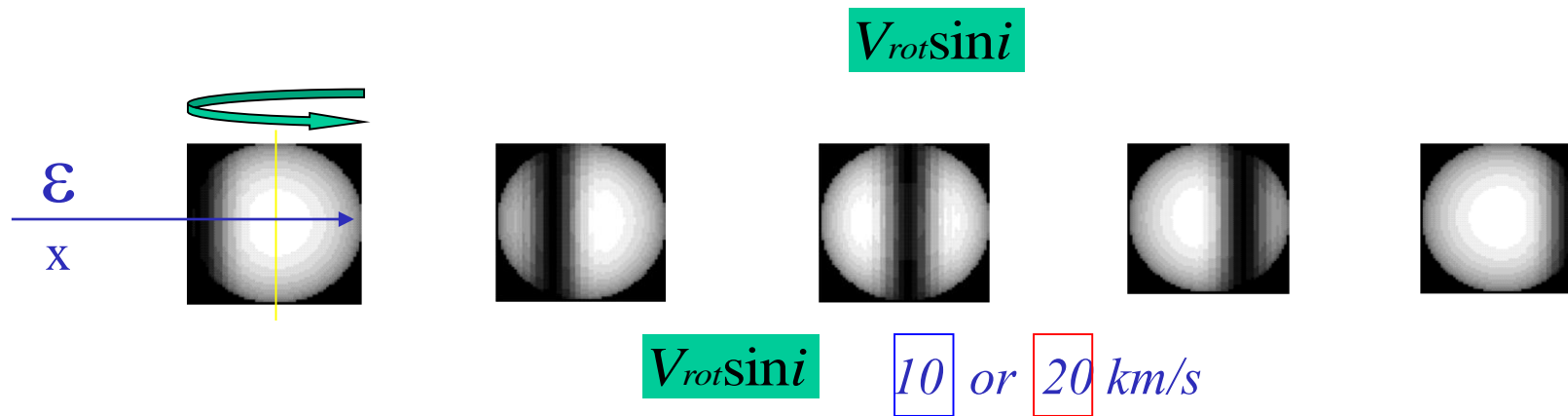
Visibility of a solar type star (1 R_{\odot}) at 10 pc ?



And a K giant ($25 R_{\odot}$) at 10 pc ?



Example of differential phase measurements



Different ways of considering interferometric observations

Everything is in $\frac{\vec{B}_p}{\lambda}$

↪ Spatial frequency sampling (*base, wavelength*)

↪ Spectral sampling

↪ Field sampling

↪ Time sampling

↪ Polarisation sampling

➔ Complementary data are usually considered

Some examples of preparation tools

JMMC

NexSCI

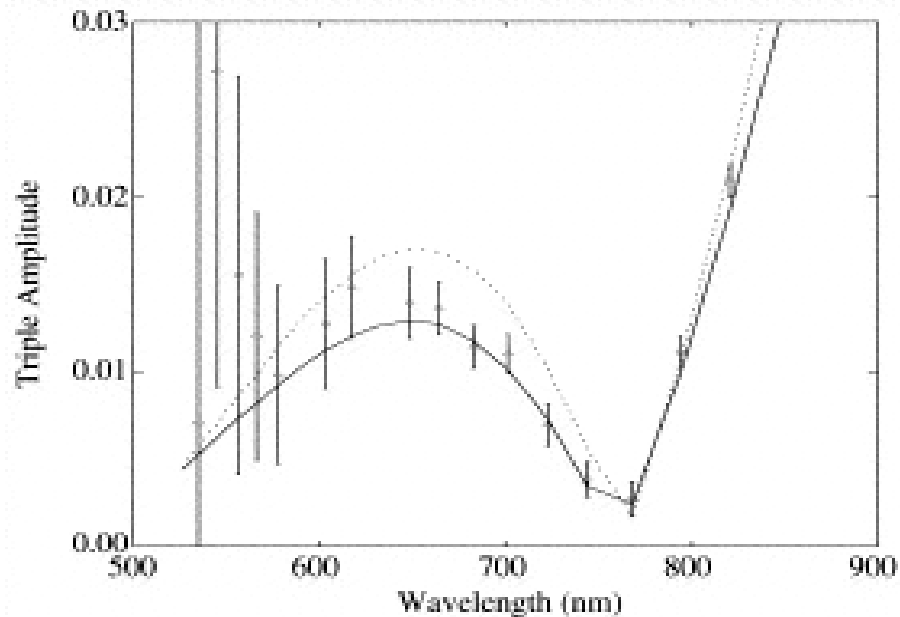
ASPRO2

VMT

Publications and science database: [JMMC-BIBDB](#)

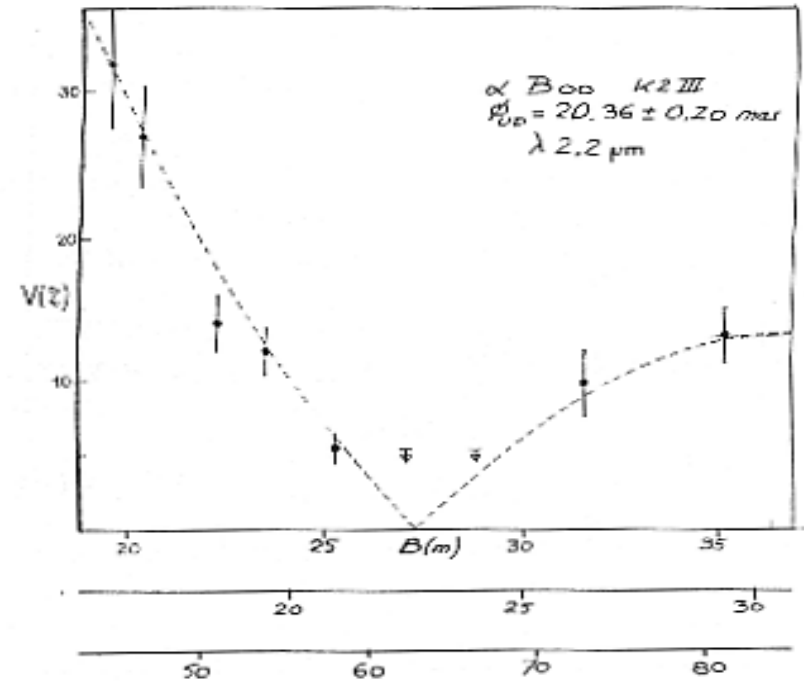
Limb darkening measurements

α Cas



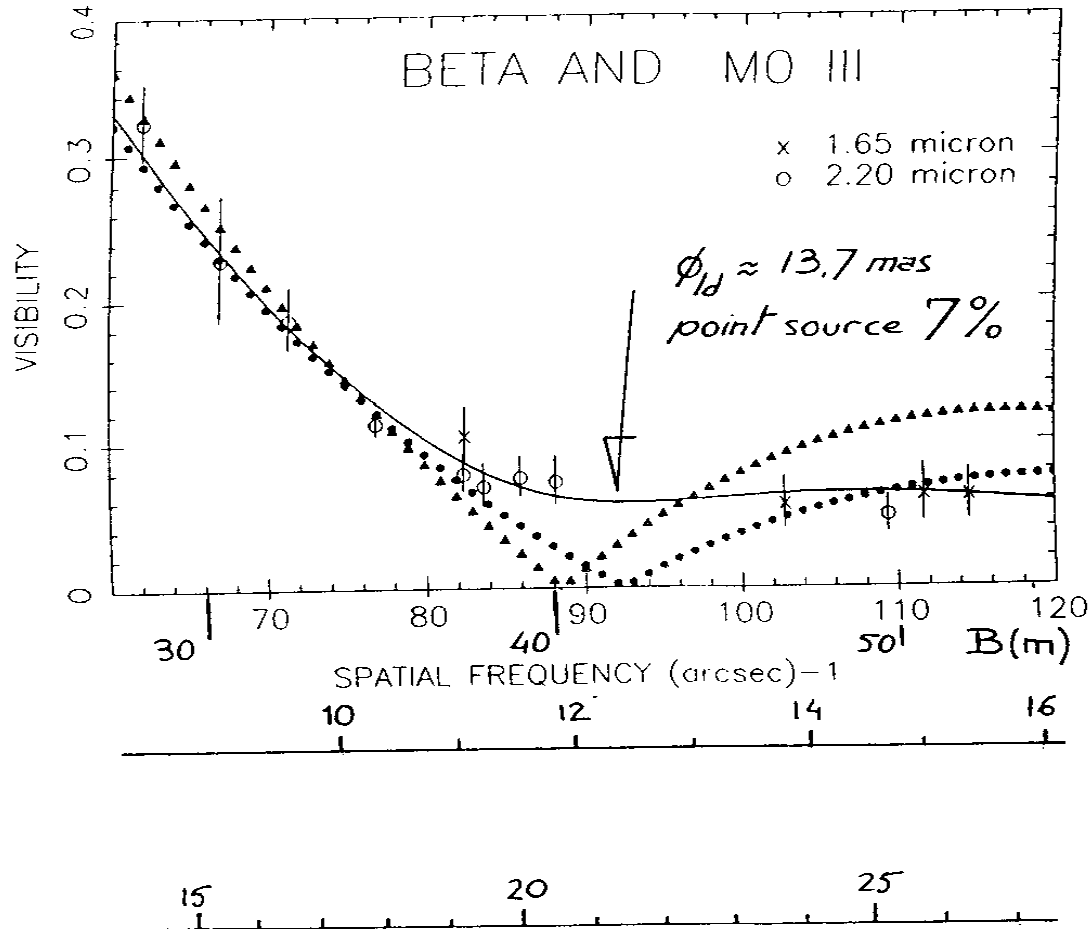
Hajian et al. 1998, ApJ, 496, 484 (NPOI)

α Boo



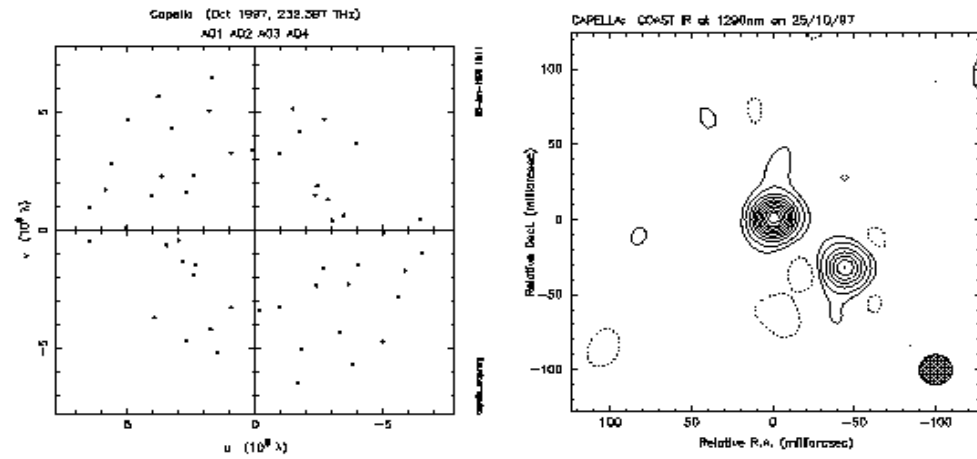
Di Benedetto & Foy 1986,
A&A, 166, 204, (I2T)

Stellar structure detection

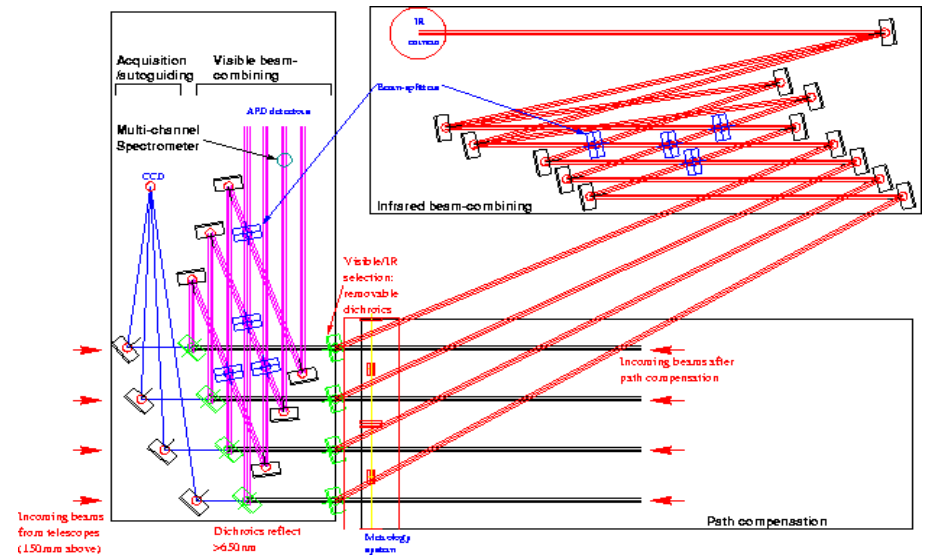


Di Benedetto & Bonneau, 1990, A&A, 358, 617

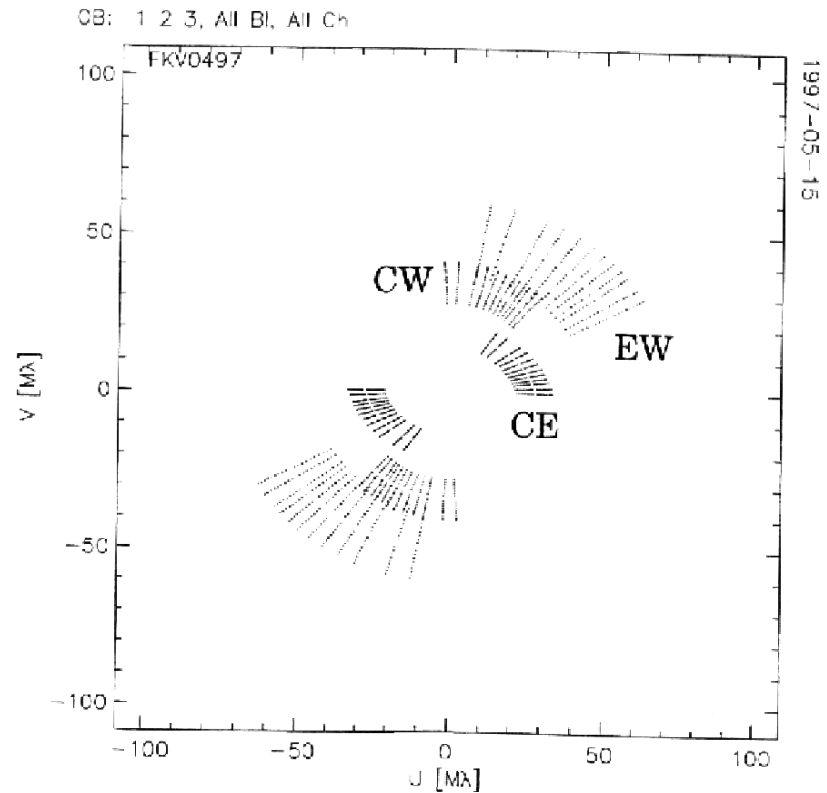
COAST (Cambridge, MRAO)



First reconstructed image: Capella



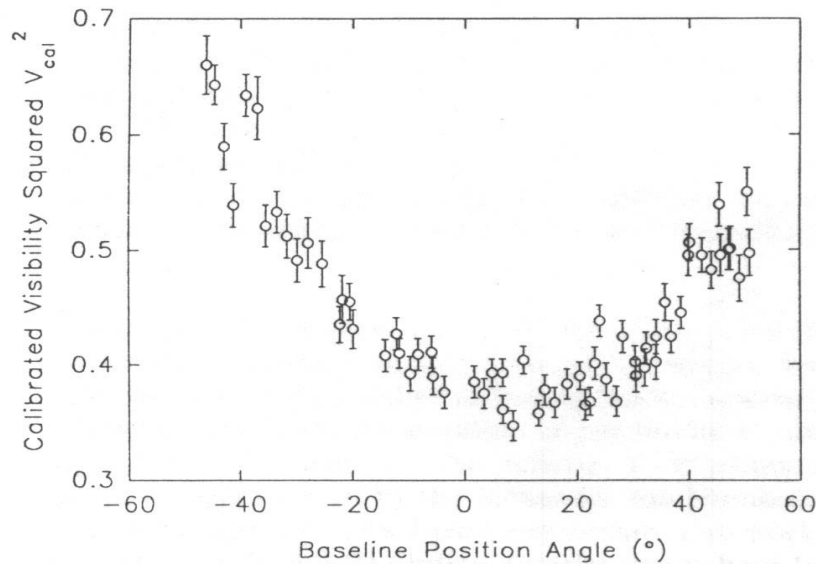
Sampling the (u,v) plane



NPOI observation of the binary star mizar

Supersynthesis effect

γ Cas

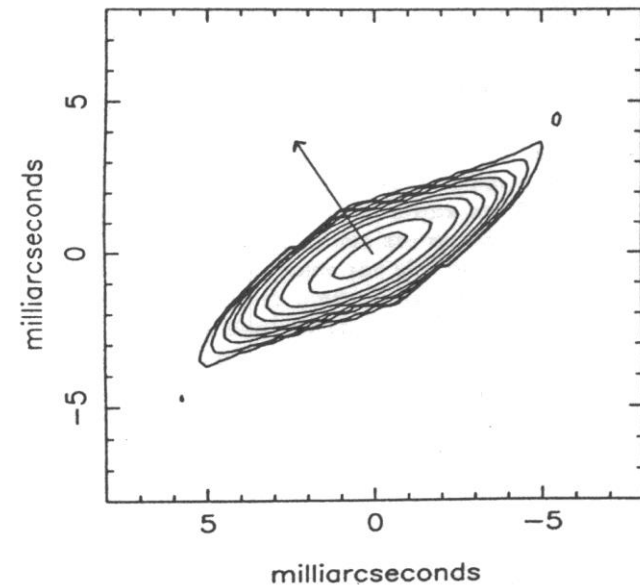


Non-spherical envelope

(Quirrenbach et al. 1993, ApJ, 416, L25)

$e=0.74$, Major axis= 3.2 mas

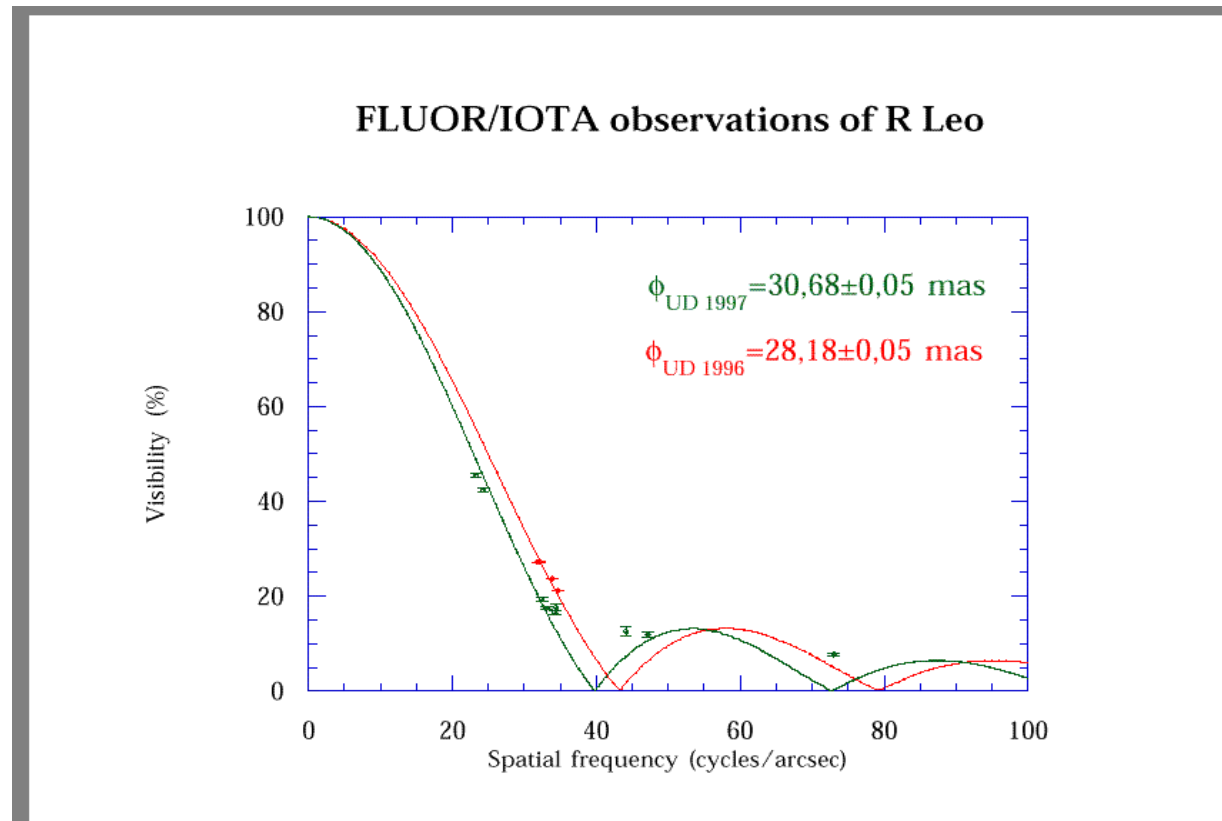
ζ Tau



Flattened envelope

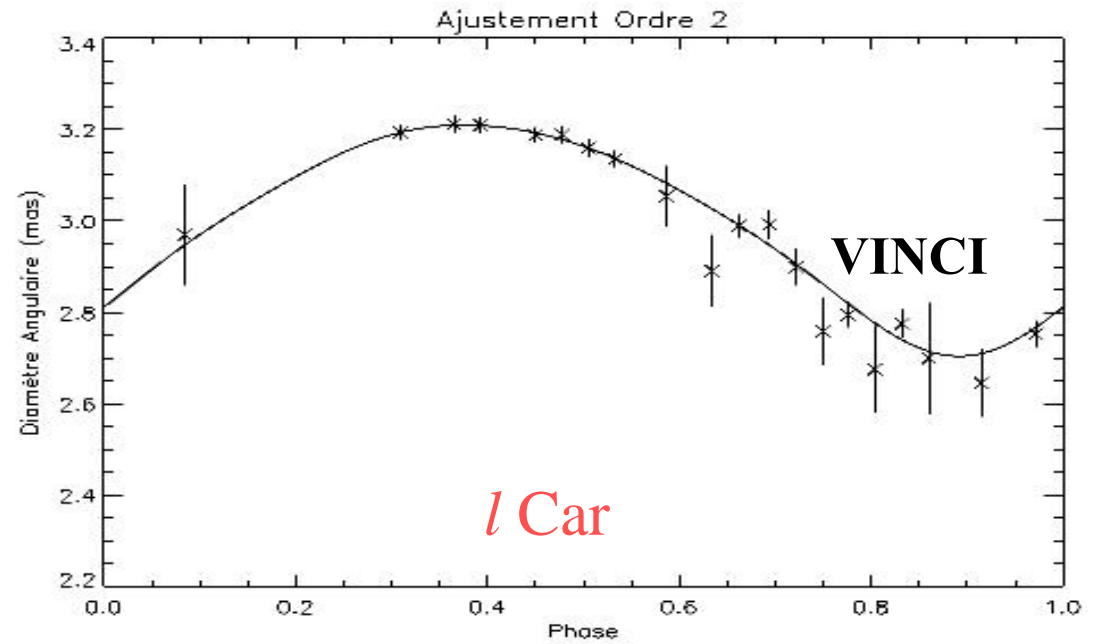
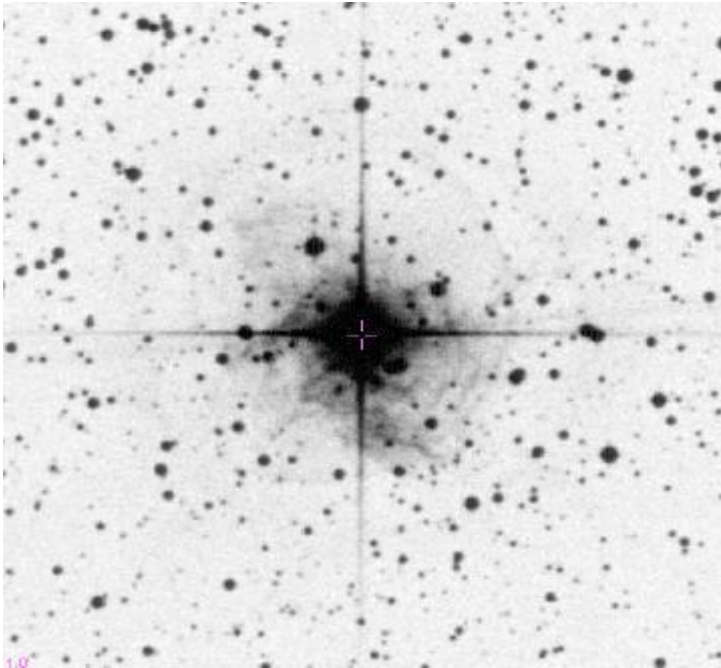
(Quirrenbach et al., A&A, 283, L13)

Time sampling



Variation of the angular diameter of R Leo as a function of time IOTA/FLUOR

Cepheids stars



Calibration of the measurements

- On a point-like source, $V^2=1$ in theory, much less in actual conditions
- 1/2 to 2/3 of the observing time is spent on calibrators.

$$V_{m,cal}^2 = V_{th,cal}^2 x T^2$$

$$\implies V_{th,target}^2 = V_{m,target}^2 x \frac{V_{th,cal}^2}{V_{m,cal}^2}$$

$$V_{m,target}^2 = V_{th,target}^2 x T^2$$

- What is a good calibrator?

$$\sigma V_{th}^2 \text{ and } \sigma V_m^2$$

[SearchCal](#)

[getCal](#)

Starting the interpretation

- Calibrated visibilities and limited (u,v) coverage.
- Interferometric measurements are usually stored in OIFITS file (international norm for data exchange).

Model fitting is a first step solution

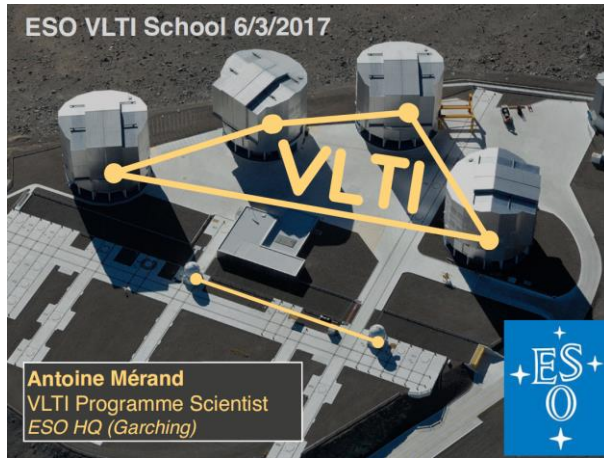
[LITPRO \(JMMC\)](#)

More elaborated models are usually necessary

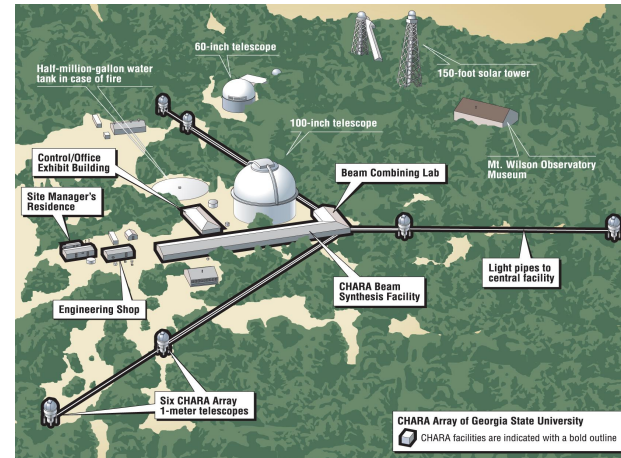
Image reconstruction

Now the reality

ESO/VLTI



CHARA



NPOI



MROI





437m (17,200")
Navy Precision
Optical Interferometer

NPOI: The Basics



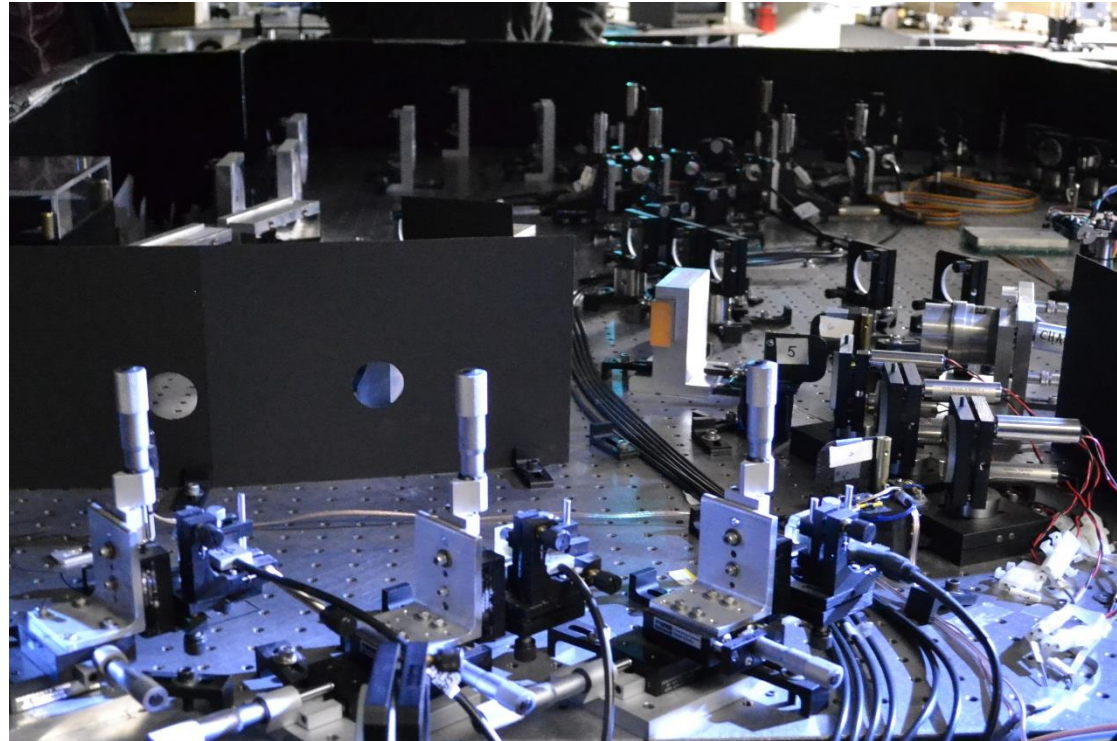
NPOI Array Center

- NPOI = Navy Precision Optical Interferometer
 - Major funding by Oceanographer of the Navy and Office of Naval Research
 - Additional instrument funding from National Science Foundation
- NPOI is collaboration between US Naval Observatory (USNO), Naval Research Lab (NRL) & Lowell Observatory
- Lowell is both a science partner, and a contractor to USNO (infrastructure & ops) & NRL (site projects)

60

NPOI Current Performance

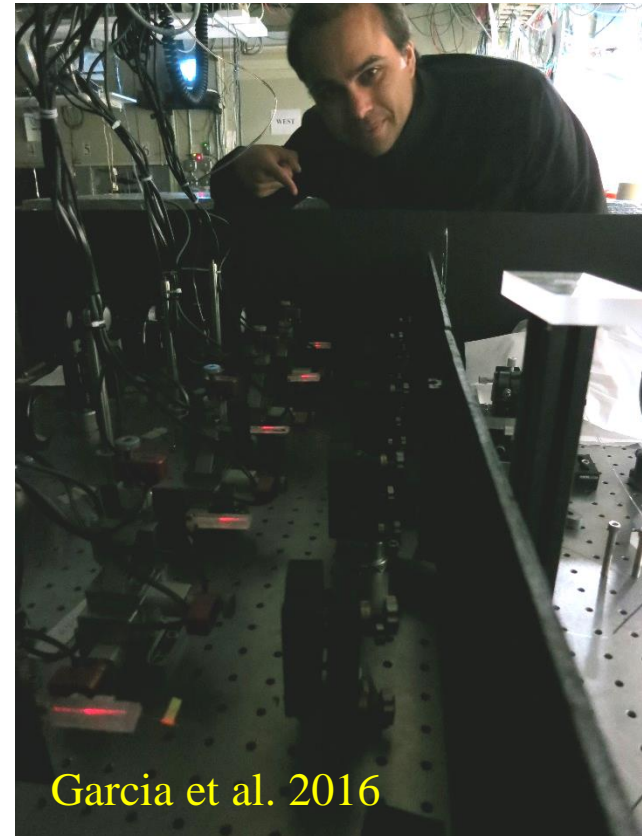
- 'Classic' Combiner
 - APD-based temporally modulating combiner
 - Spectral resolution: $R=40$ (16 channels) over 550-850nm
 - Collects many N-way permutations
 - 1/3 of data dropped
 - Sensitivity limit of $m_V \approx 5.5$



Armstrong et al. 1998, 2013

NPOI Current Performance

- VISION
 - EMCCD-based spatially modulating combiner
 - Spectral resolutions: $R=200, 1000$ over 570-850nm
 - Collects *all* N-way permutations
 - Automatic data pipeline adapted from MIRC
 - Sensitivity limit of $m_V \approx 6$



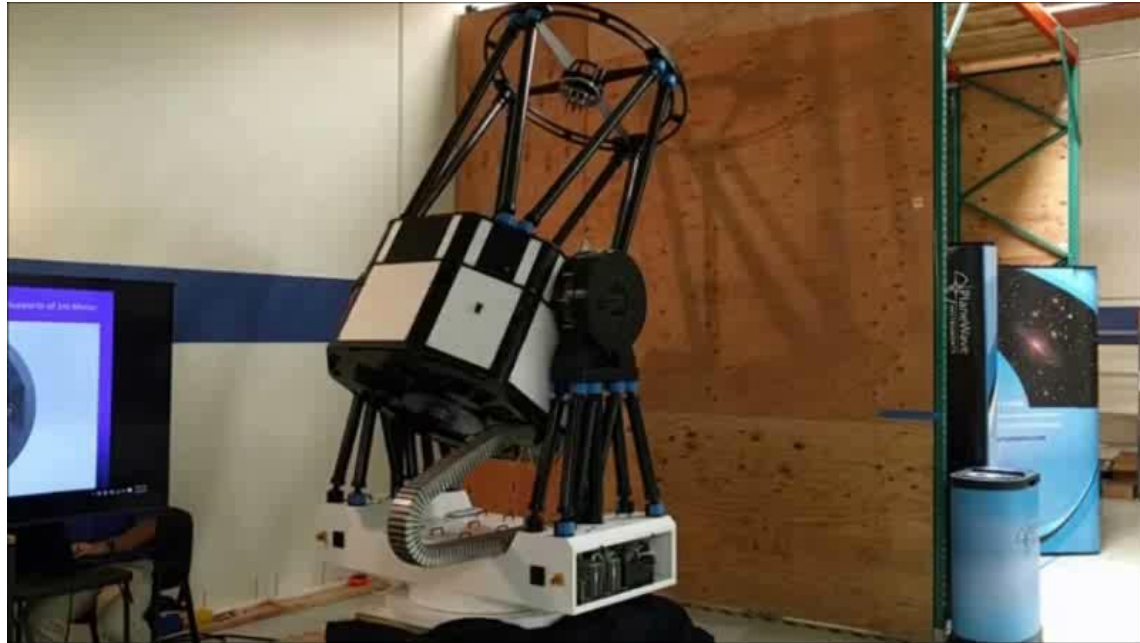
Current Infrastructure

- Siderostats
 - Six 12-cm 'imaging' apertures
 - Four 12-cm 'astrometric' apertures
- FDLs
 - Six variable optical delay lines
- LDLs
 - Not yet online
 - Limits sky coverage
- Astrometric metrology
 - Mothballed

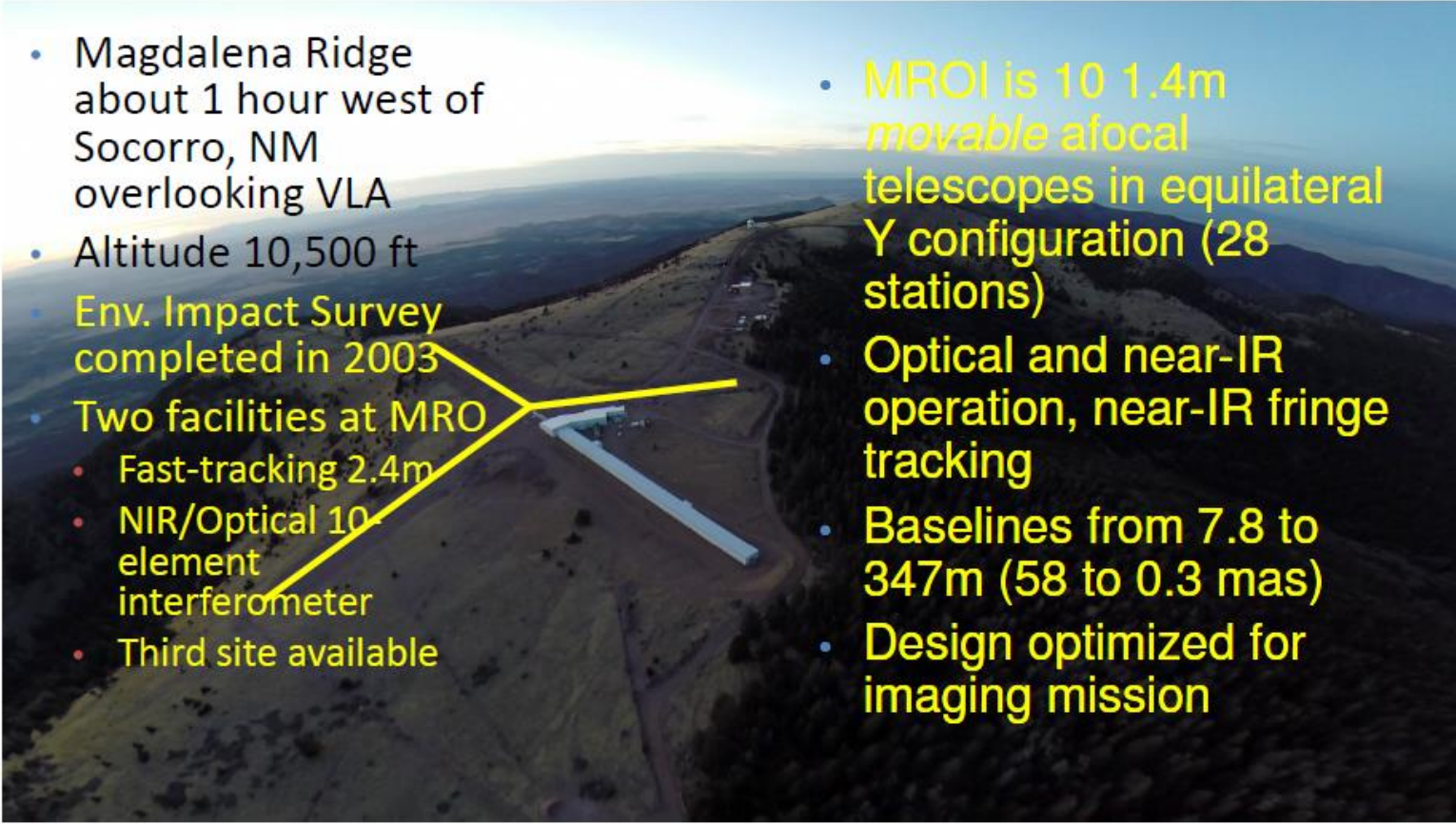


Large Apertures for NPOI

- NRL support for development of geosat imaging technology
 - Capital construction for 3×1.0 m telescopes
- New large model from PlaneWave Instruments for 1.0 m
 - Robust, turnkey operations
 - CDK700 proven with MINERVA and other projects
- 70× increase in collecting area: Δm of up to +4.5mag

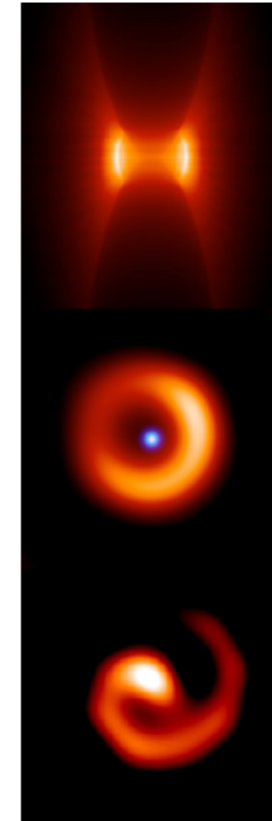


Overview of the Observatory

- 
- Magdalena Ridge about 1 hour west of Socorro, NM overlooking VLA
 - Altitude 10,500 ft
 - Env. Impact Survey completed in 2003
 - Two facilities at MRO
 - Fast-tracking 2.4m
 - NIR/Optical 10-element interferometer
 - Third site available
 - MROI is 10 1.4m *movable afocal* telescopes in equilateral Y configuration (28 stations)
 - Optical and near-IR operation, near-IR fringe tracking
 - Baselines from 7.8 to 347m (58 to 0.3 mas)
 - Design optimized for imaging mission

MROI Science Case

- AGN:
 - Verification of the unified model.
 - Determination of nature of nuclear/extra-nuclear starbursts.
 - H = 14 gives >100 targets.
- Star and planet formation:
 - Protostellar accretion, imaging of dust disks, disk clearing as evidence for planet formation.
 - Emission line imaging of jets, outflows and magnetically channeled accretion.
 - Detection of sub-stellar companions.
- Stellar accretion and mass loss:
 - Convection, mass loss and mass transfer in single and multi-star systems.
 - Bipolarity and collimation of circumstellar material, wind and shock geometries, interacting binary systems
 - Pulsations in Cepheids, Miras, RV Tauris, etc.

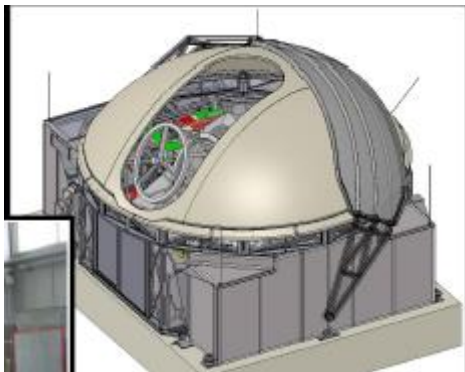


MROI current situation

1st telescope Nov. 16



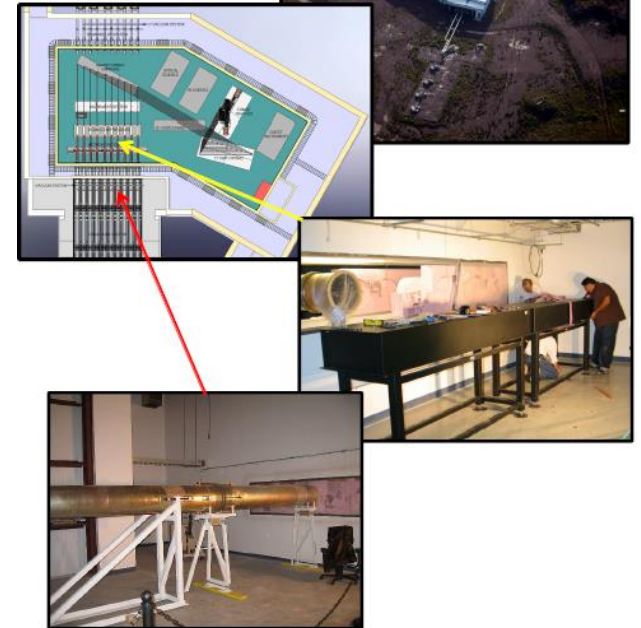
1st Dome Nov. 17



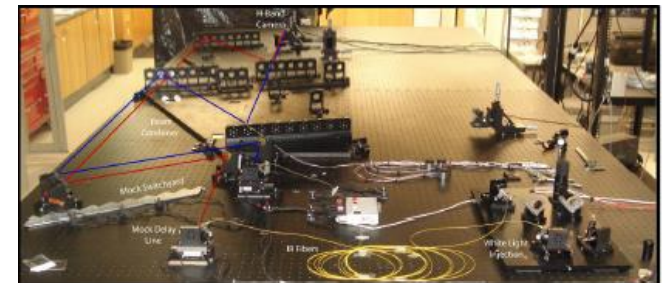
1st cart delivered



Building in completion



Prototype of fringe tracker



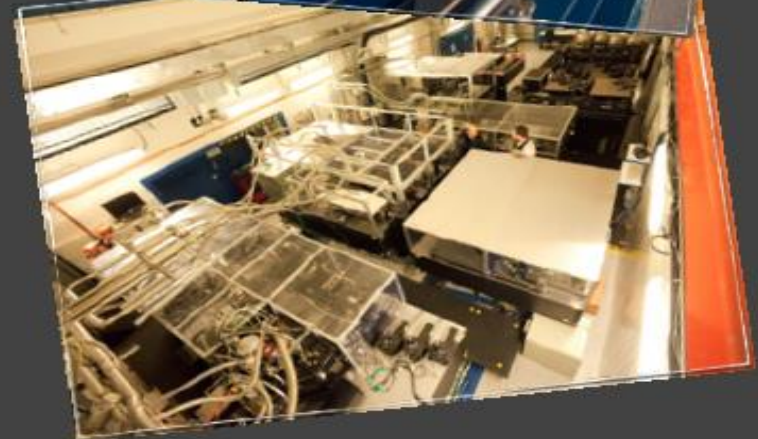
Timeline for Future Development

- Funding under \$25M cooperative agreement with AFRL supports deploying first 3 telescopes
 - First telescope and enclosure deployed on array arms next spring – will characterize light into beam combining facility
 - Fringes anticipated in 2019 and three-telescope measurements in 2020
 - More funding needed to complete 10 telescope facility – looking to NSF, alumni, philanthropy
 - Costs are ~\$8M per “beamline” – looking for partners for new beamlines as well as operations
-

ESO/VLTI Paranal Observatory



- Up to 4 telescopes simultaneously
- UTs (8.2m) and movable ATs (1.8m)
- Wavelength coverage from $1.5\mu\text{m}$ to $12\mu\text{m}$
- Baselines from 11m to 140m
- Angular resolution in the $0.001''$ (1mas) regime

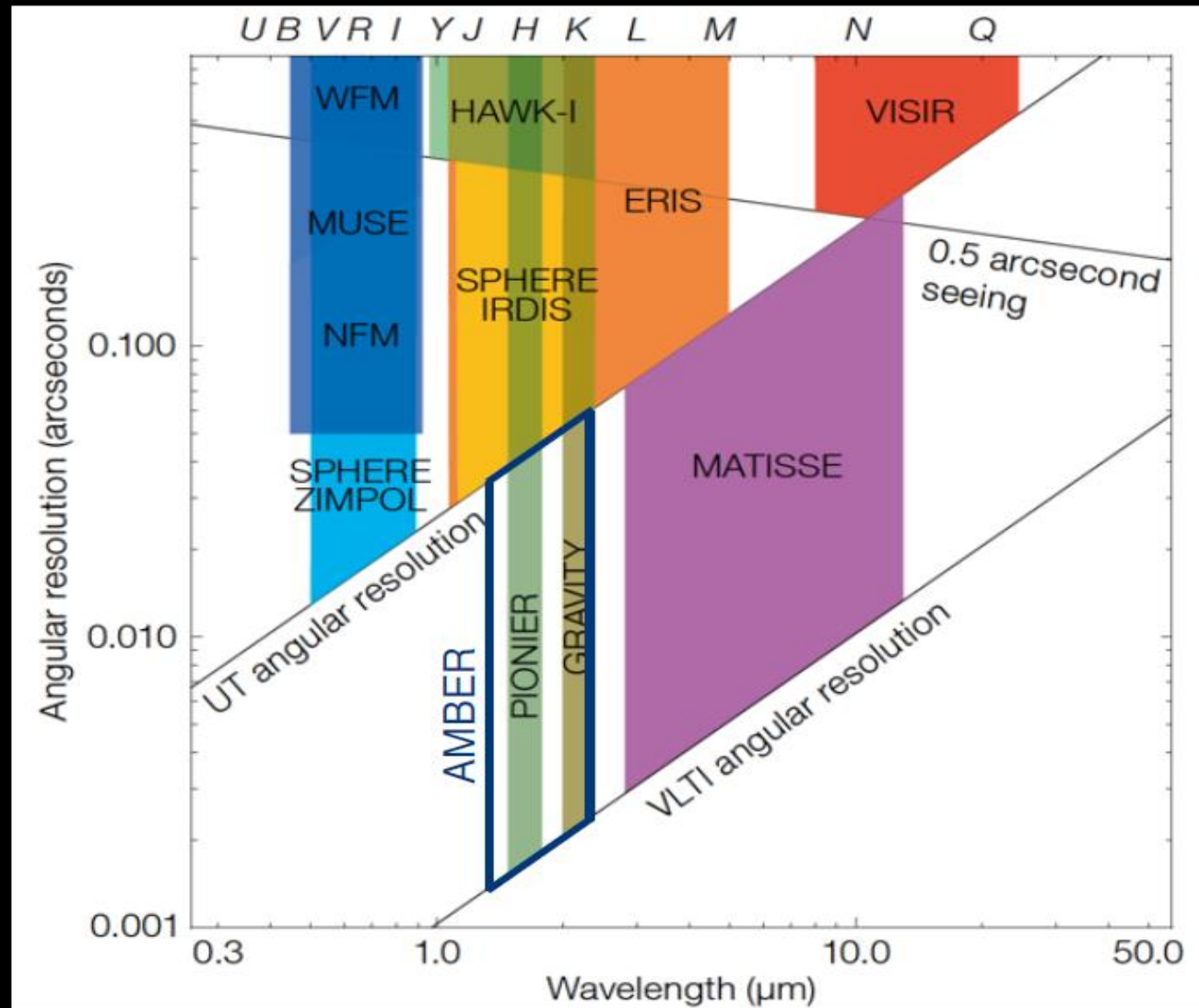




Instrument overview

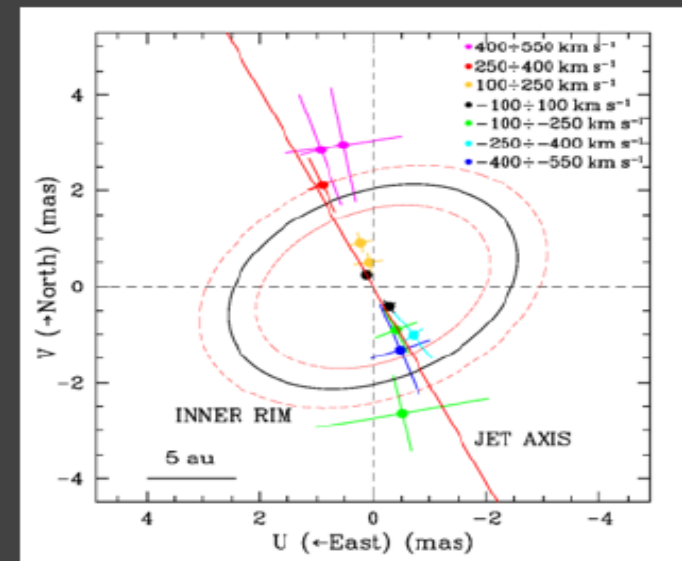
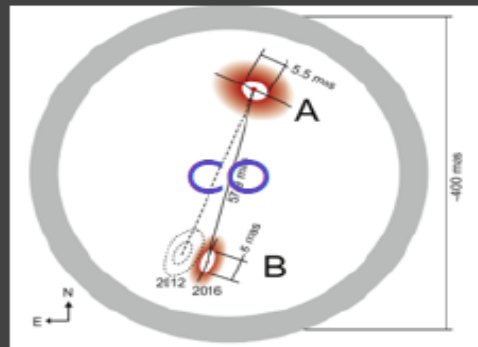
	AMBER	PIONIER	GRAVITY	MATISSE
# of combined telescopes (ATs or UTs)	3	4	4	4
Spectral range and resolution	H-K (35,1500,12000)	H (none,30)	K (22,500,4000)	L,M,N (30-5000)
Fringe tracker	FINITO		Dedicated internal FT (on/off-axis)	GRA4MAT

+ astrometry offered in the near-future

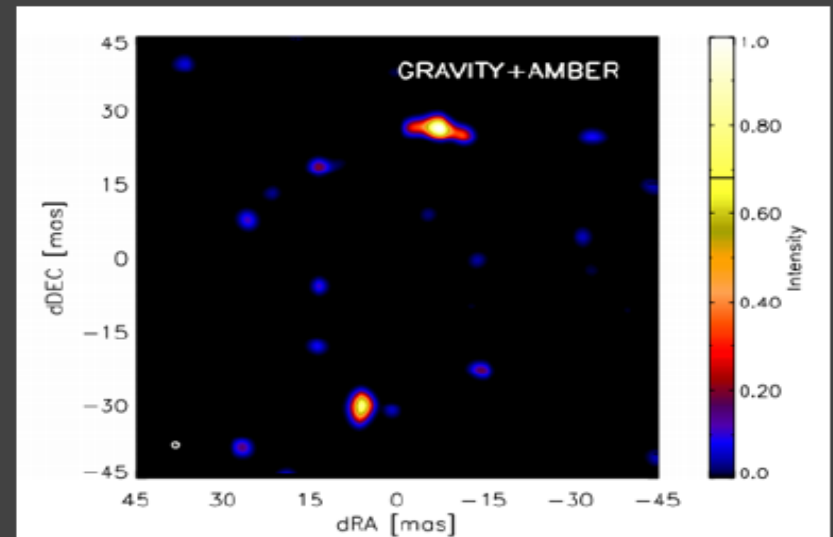


Massive YSOs

- AMBER resolves a jet for IRAS 13481-6124
- AMBER+GRAVITY image a of Massive YSO binary



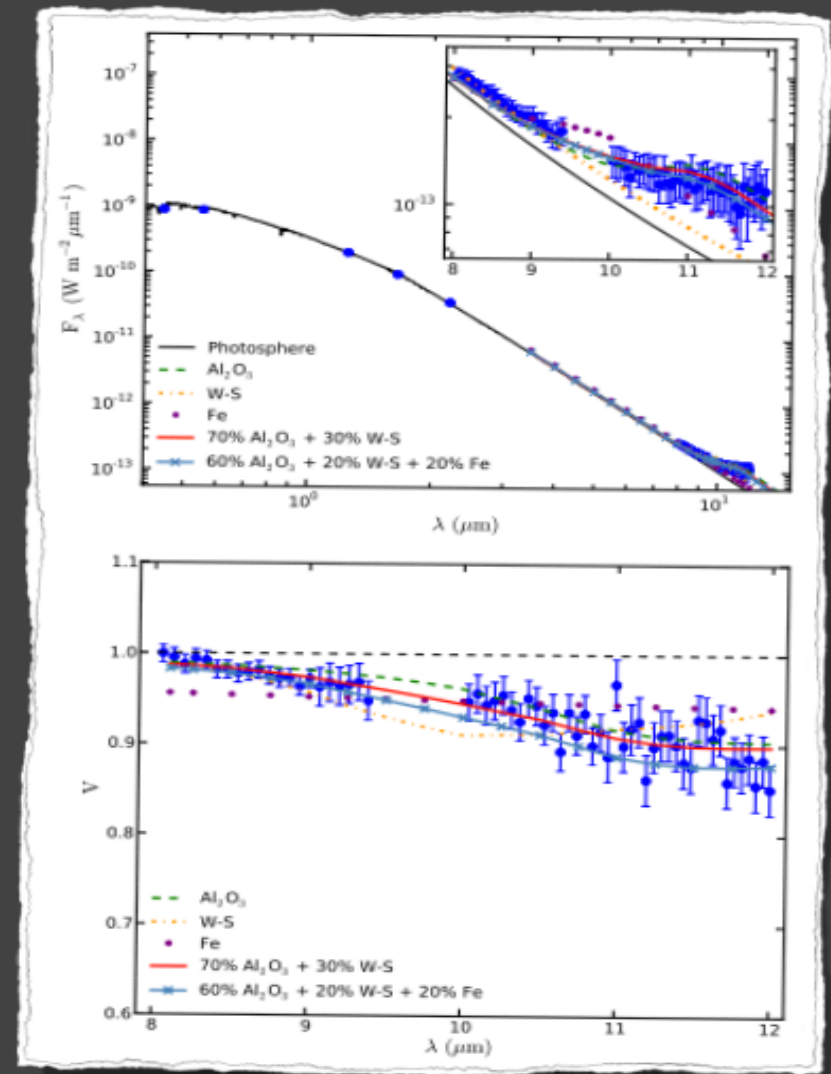
Caratti o Garatti+ 2016



Kraus+ 2017

Cepheids' mass loss

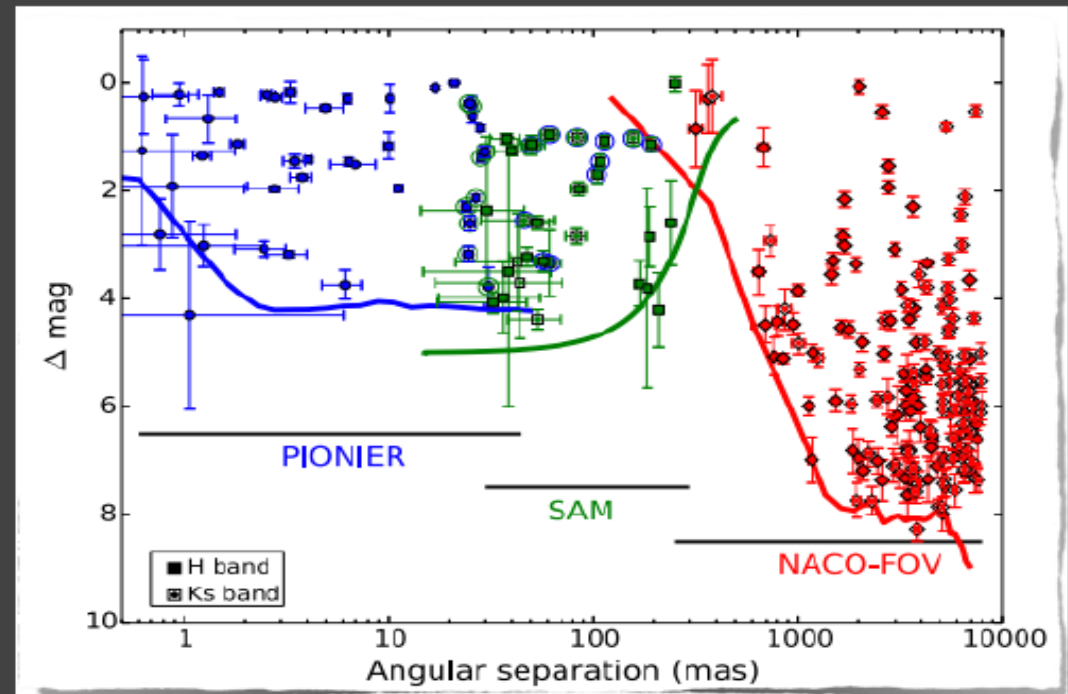
- MIDI resolved known IR excess
- Modelled using DUSTY code
- Mineralogy not well constrained yet (MATISSE)



Gallenne et al. (2013)

Binarity of massive stars

- $\sim 45\%$ of O stars are in multiple systems according to RV
- PIONIER+NACO survey showed 100% of O stars are in multiple systems



Sana + 2014

Interacting Binary

Image reconstruction (PIONIER)
unexpected mass ratio (fact. of 2)

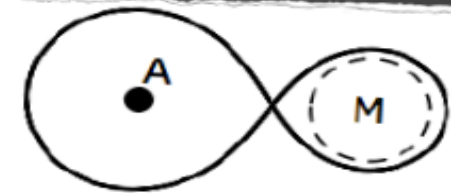
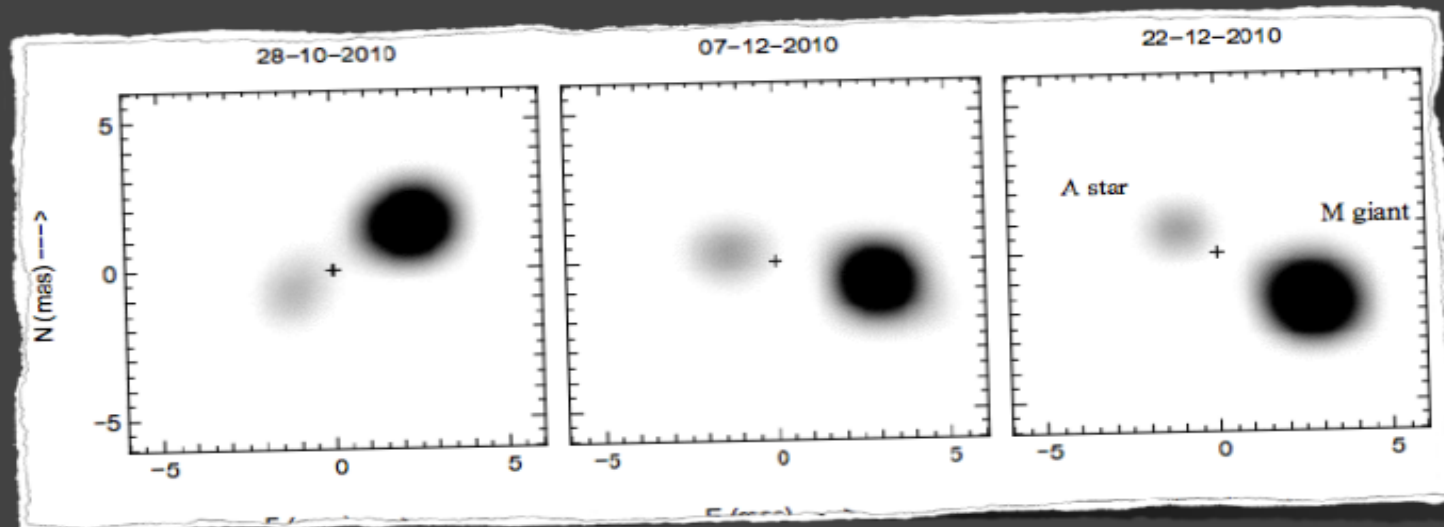


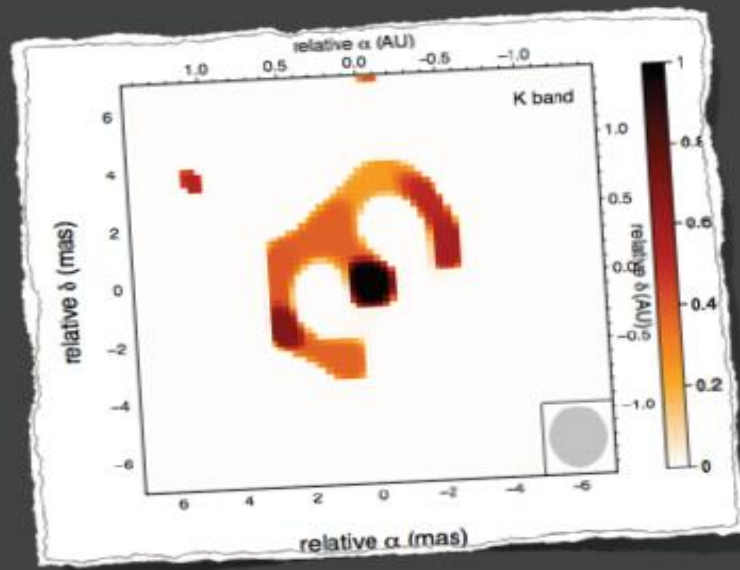
Fig. 5. Representation of the modified Roche equipotential (solid line) for a mass ratio $1/q = 2.2$. The limb-darkened diameter of the M giant is the dashed line, while the A star one is the dark dot.



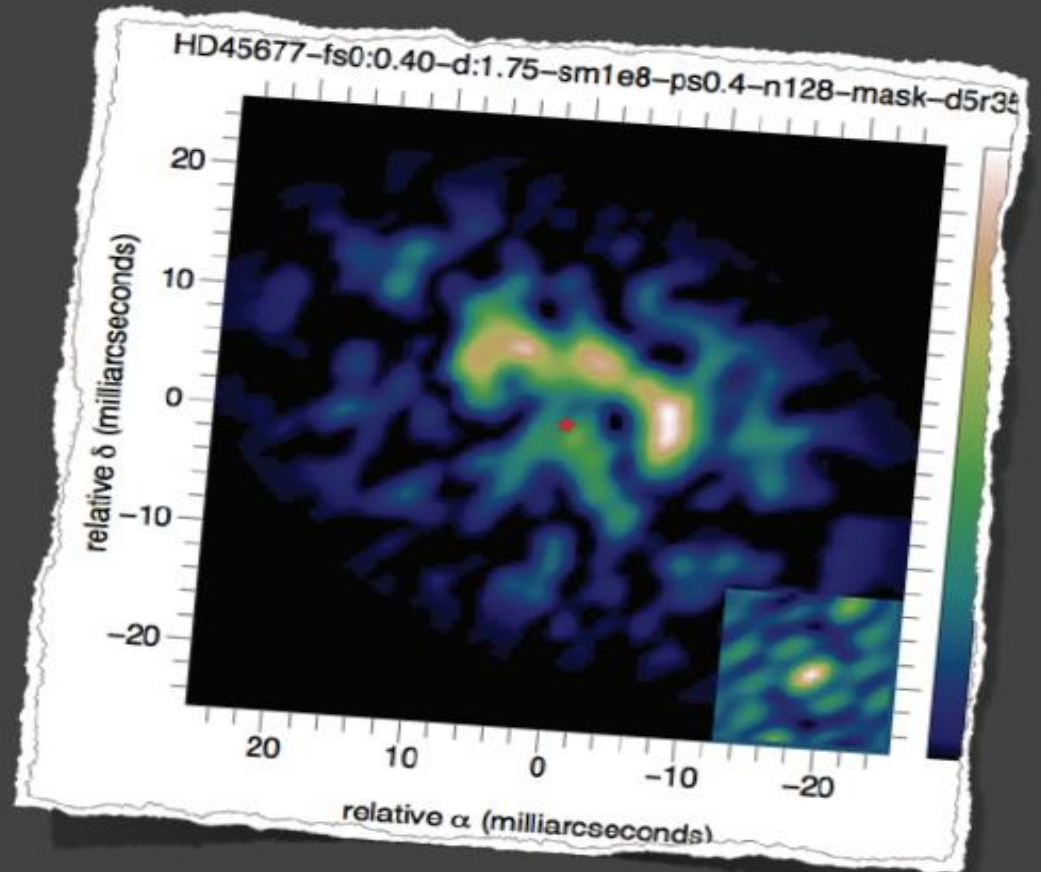
Blind, Boffin et al. (2011)

Disks & young stars

- Disk inner rim reconstructed images
- “the first AU”



Benisty et al. (2011): AMBER

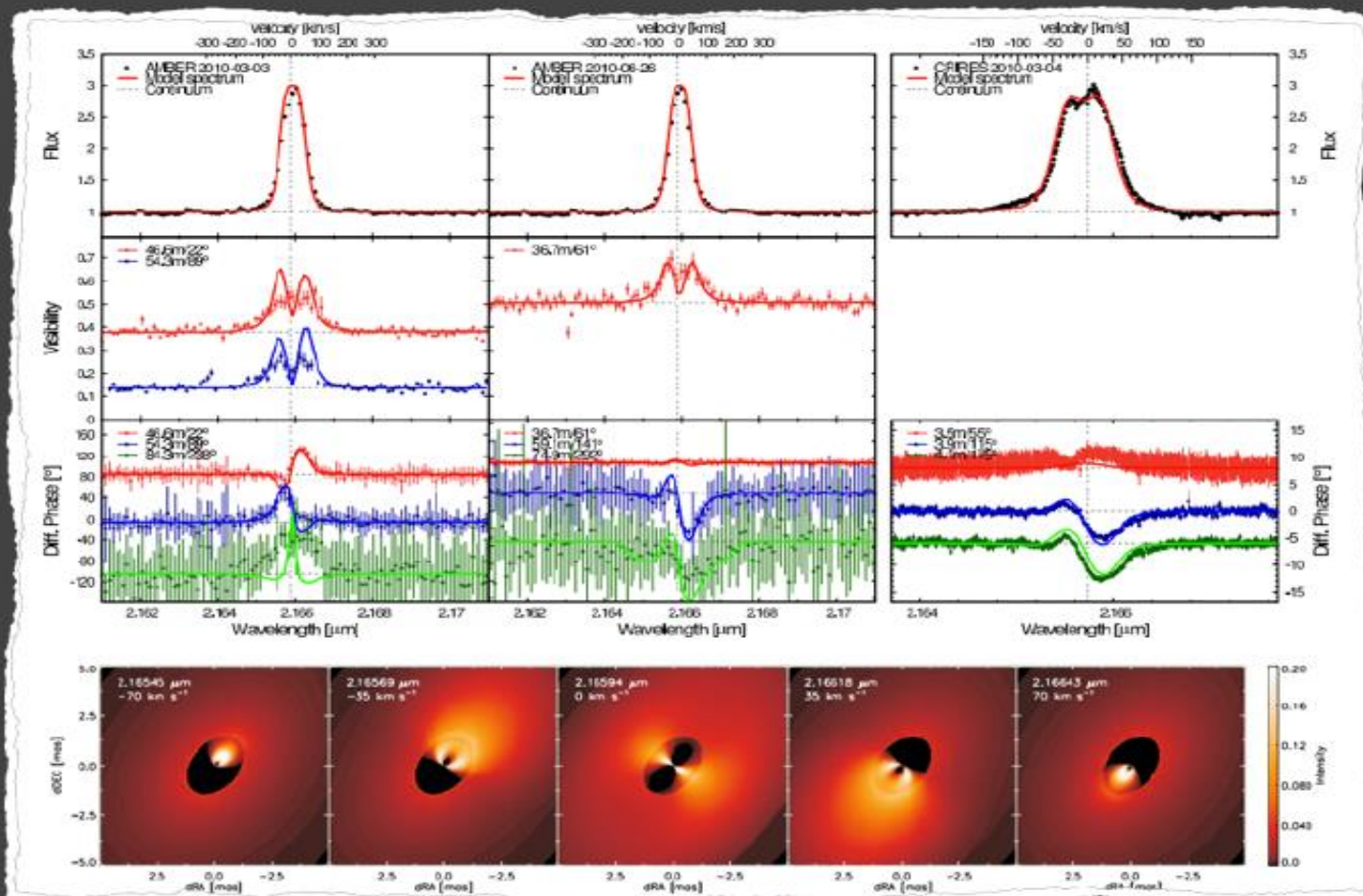


Kluska et al. (in prep): PIONIER

Be stars

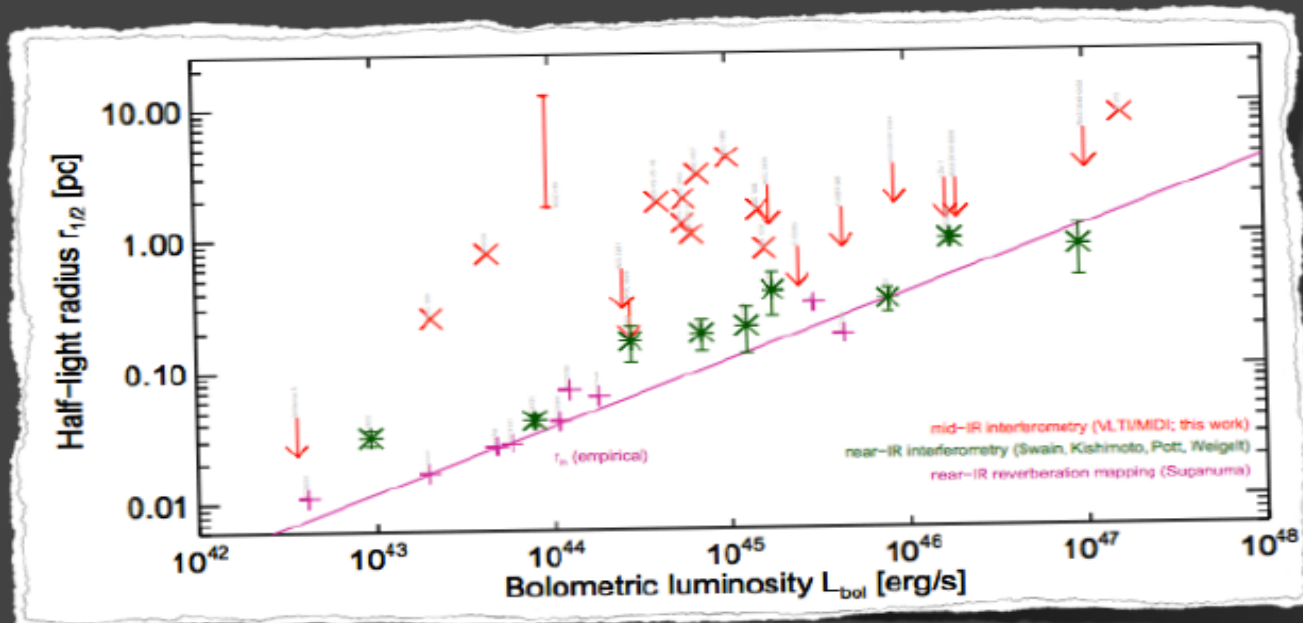
(Keplerian) disks and companions

Kraus et al. 2012

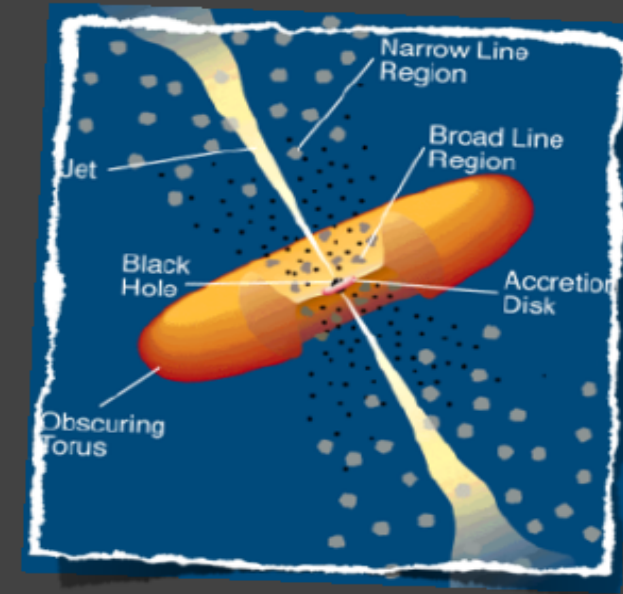


AGNs

- No morphological differences between type 1 and type 2 (!)
- Radius/Luminosity relation



Burtscher et al. 2013 (MIDI)



The GRAVITY instrument in short

Very challenging science cases

Demanding requirements

- High sensitivity in K-band: **K ~ 10** (fringe tracking)
K ~ 16 (long-integration imaging)
- Astrometry at **10- μ as** accuracy \rightarrow control of aberrations, image and pupil positioning and control, metrology, ... **at nm-level!**

Technical challenges Innovative R&D

- Fast low-noise detectors
- Ultra-stable metrology laser
- **Integrated optics combiners**

Key-figures

- A cryostat of **2.3 tons**
- **2-m long and diameter of 1.5-m**
- **Under vacuum**
- Controlled temperatures : **80, 200, 240 K**

Le consortium GRAVITY

Frank Eisenhauer, **Guy Perrin**, Wolfgang Brandner, Christian Straubmeier , **Karine Perraut** , Antonio Amorim , Markus Schöller, Reinhard Genzel, **Pierre Kervella** , **Myriam Benisty**, Sebastian Fischer , **Laurent Jocou**, Paulo Garcia, Gerd Jakob, Stefan Gillessen, **Yann Clénet** , Armin Boehm, Constanza Araujo-Hauck, Jean-Philippe Berger, Jorge Lima, Roberto Abuter, Oliver Pfuhl, **Thibaut Paumard**, Casey P. Deen, Michael Wiest , **Thibaut Moulin**, Jaime Villate, Gerardo Avila, Marcus Haug, **Sylvestre Lacour** , Thomas Henning, Senol Yazici , Axelle Nolot , Pedro Carvas, Reinhold Dorn, Stefan Kellner, **Eric Gendron**, Stefan Hippler, Andreas Eckart , Sonia Anton, Yves Jung, Alexander Gräter, **Élodie Choquet** , Armin Huber, Narsireddy Anugu , Philippe Gitton, Eckhard Sturm, **Frédéric Vincent** , Sarah Kendrew, Stefan Ströbele, Clemens Kister, **Pierre Fédou**, Ralf Klein, Paul Jolley, Magdalena Lippa, **Vincent Lapeyrère**, Natalia Kudryavtseva, Christian Lucuix, Ekkehard Wieprecht, **Frédéric Chapron**, Werner Laun, Leander Mehrgan, Thomas Ott, **Gérard Rousset** , Rainer Lenzen, Marcos Suarez, Reiner Hofmann, **Jean-Michel Reess**, Vianak Naranjo, Pierre Haguenaer, Oliver Hans, **Arnaud Sevin** , Udo Neumann, Jean-Louis Lizon, Markus Thiel, **Claude Collin** , Jose Ricardo Ramos, Gert Finger, David Moch, **Daniel Rouan**, Ralf-Rainer Rohloff, Markus Wittkowski, Richard Davies, **Denis Ziegler** , Karl Wagner, Henri Bonnet, Katie Dodds-Eden, **Frédéric Cassaing**, Pengqian Yang, Florian Kerber, Sebastian Rabien, **Nabih Azouaoui**, Frederic Gonte, Josef Eder, **Vartan Arslanyan**, Willem-Jan de Wit, Frank Hausmann, **Roderick Dembet**, Luca Pasquini, Harald Weisz, **Pierre Lena**, Mark Casali, **Bernard Lazareff**, **Zoltan Hubert**, **Jean-Baptiste Le Bouquin**

7 institutes over 4 countries

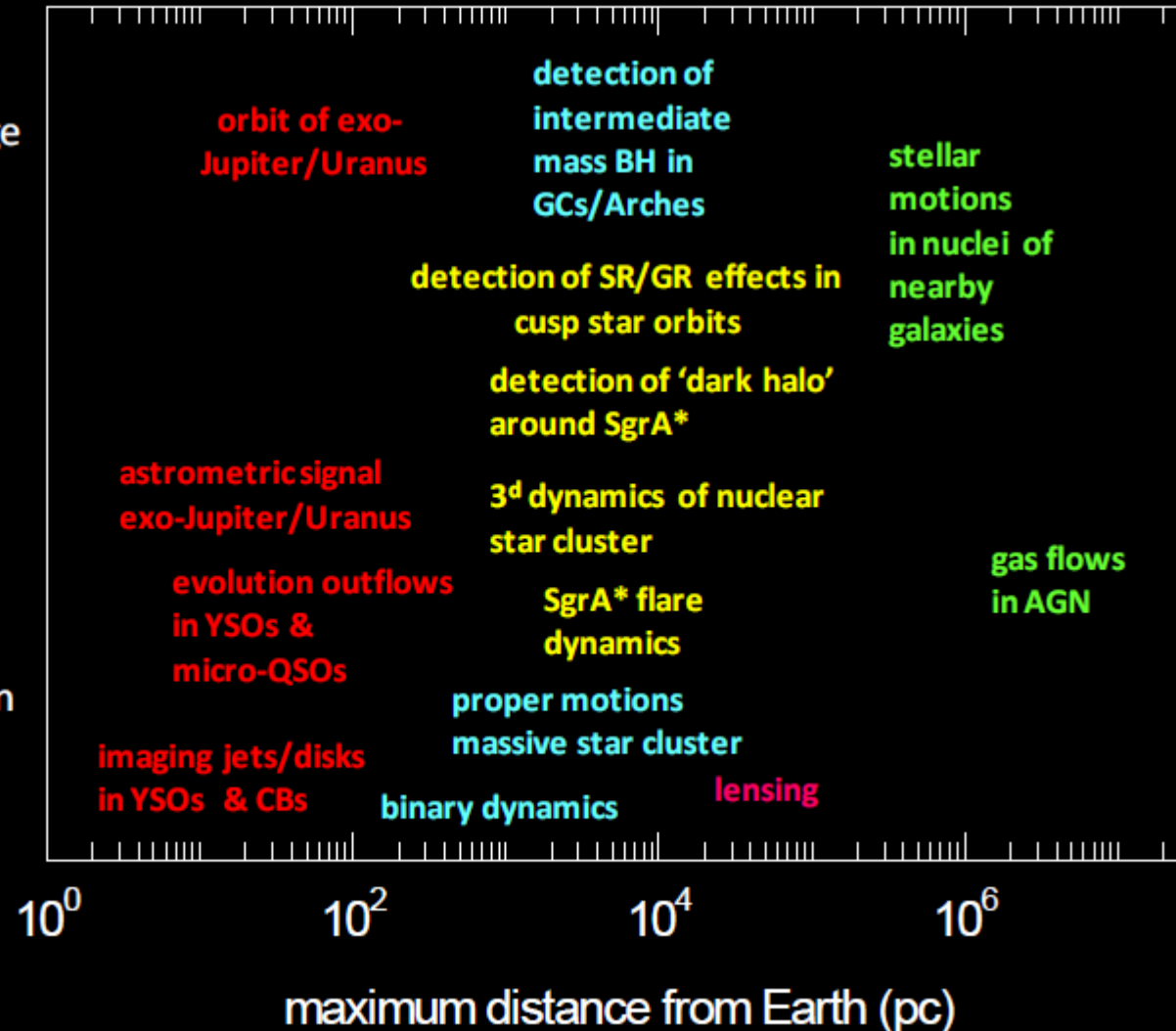
Whole project: ~10 M€ and 160 FTE

INSU/CNRS : 1.5 M€ and ~55 FTE

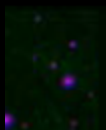
Duration ~ 10 years

GRAVITY science cases

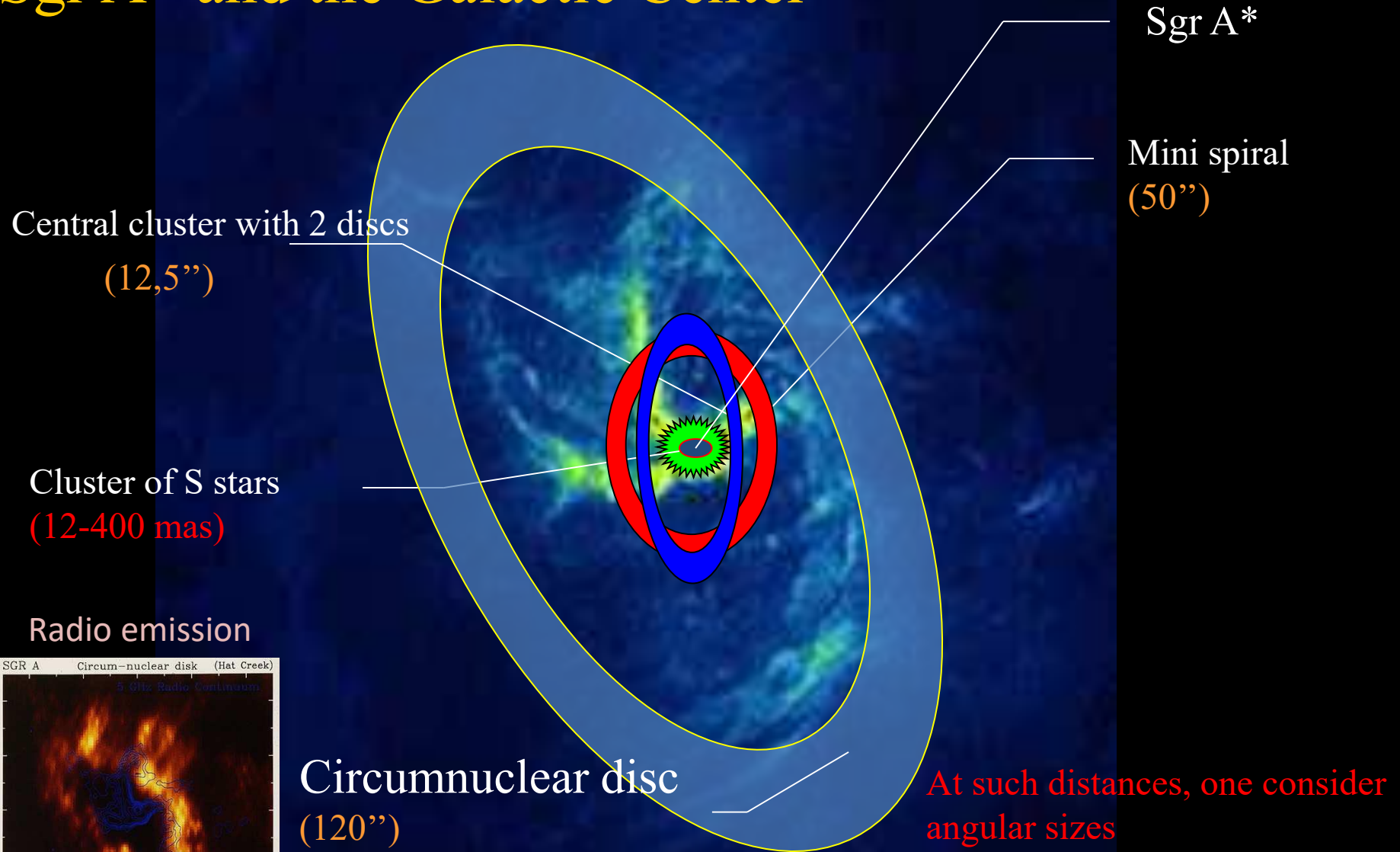
- U_1 ten year large program
- M
- R_{ϵ}
 - three year program
 -
- Te
 - single season campaign
- O_1



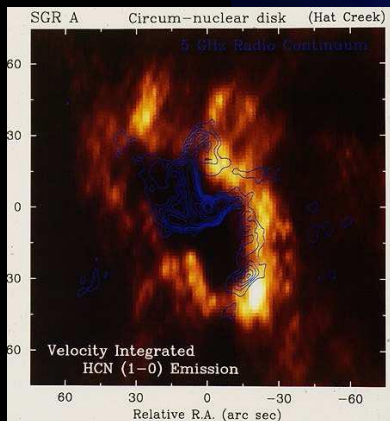
role
at
centricities



Sgr A* and the Galactic Center



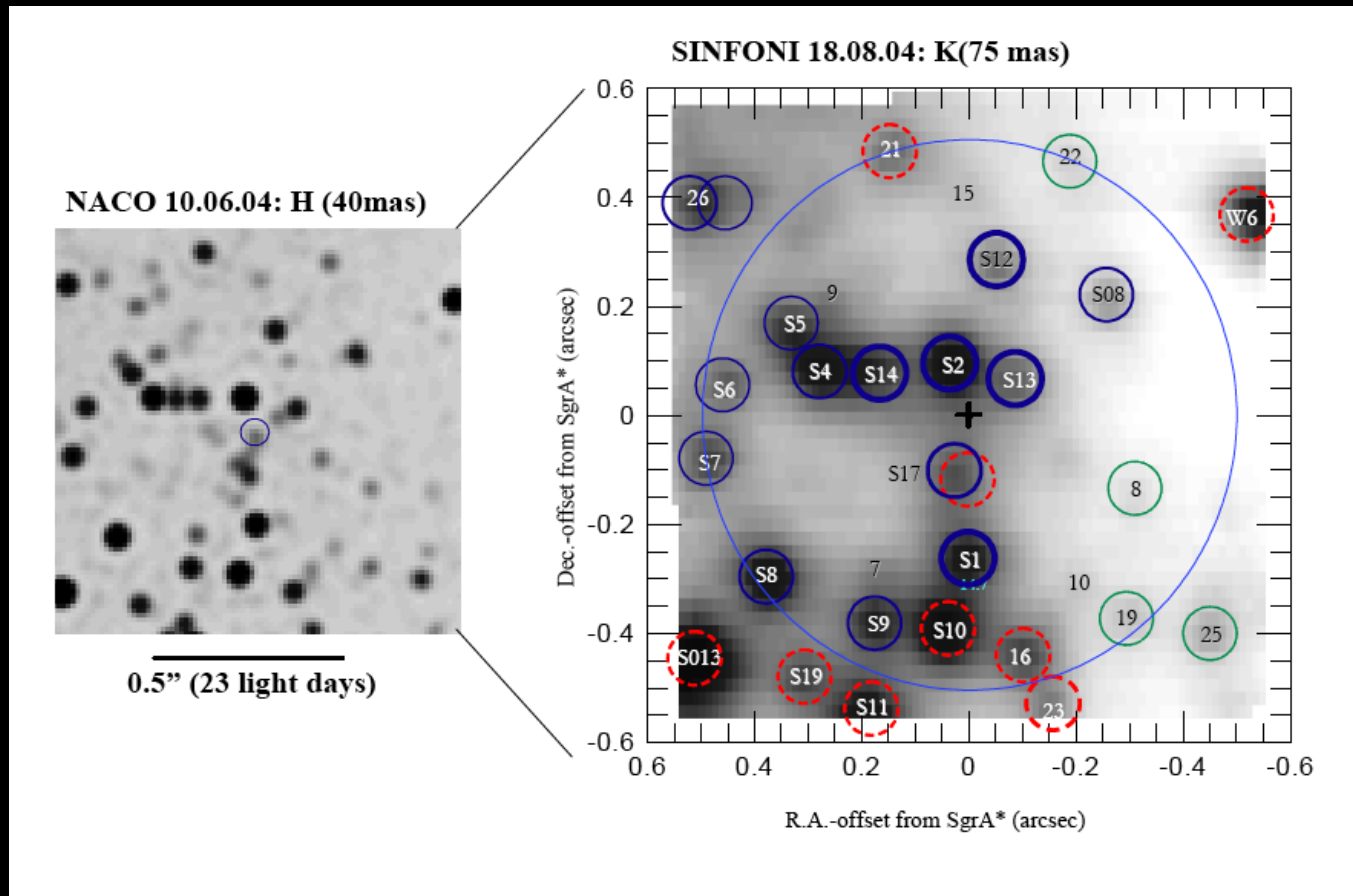
Radio emission



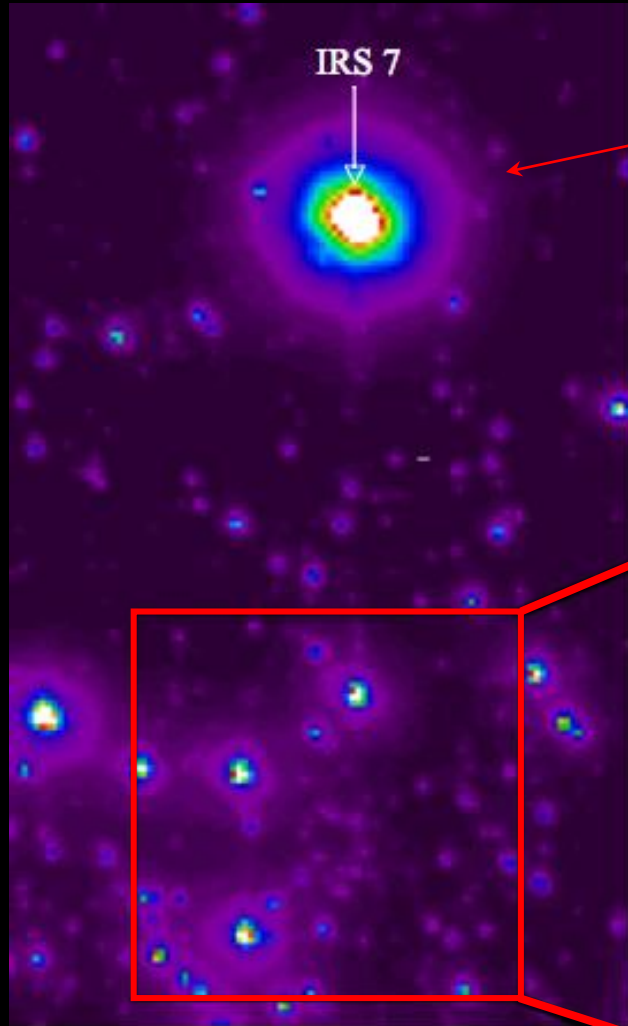
1'' = 4,85 10⁻⁶ rad = 1 man at Paris
 1 mas = 1 man on the Moon
 20 μas = 1 hair at Paris

The Galactic Center: a very star-crowded field

Observation in the near-infrared by adaptive optics and spectroscopy at the VLT

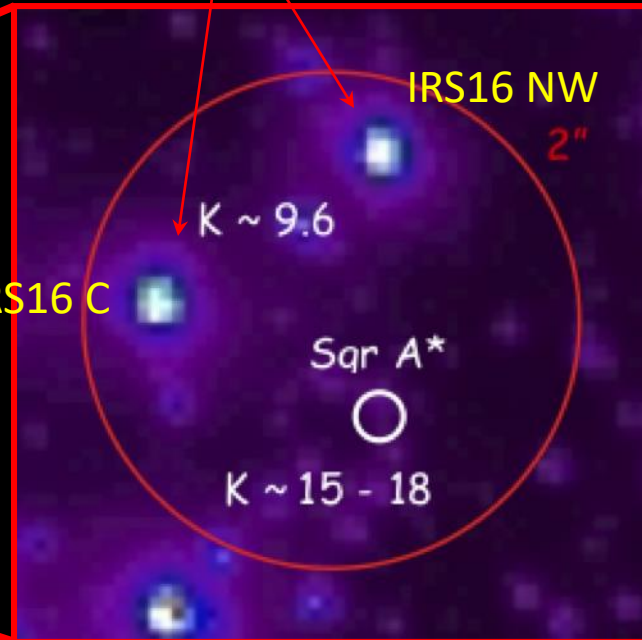
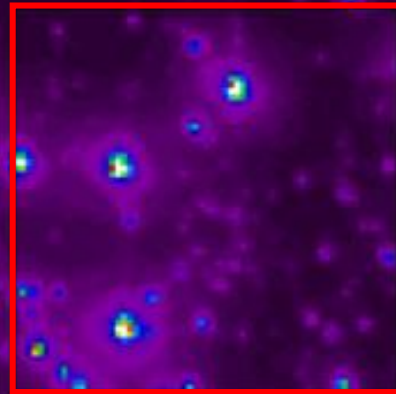


Two GRAVITY modes

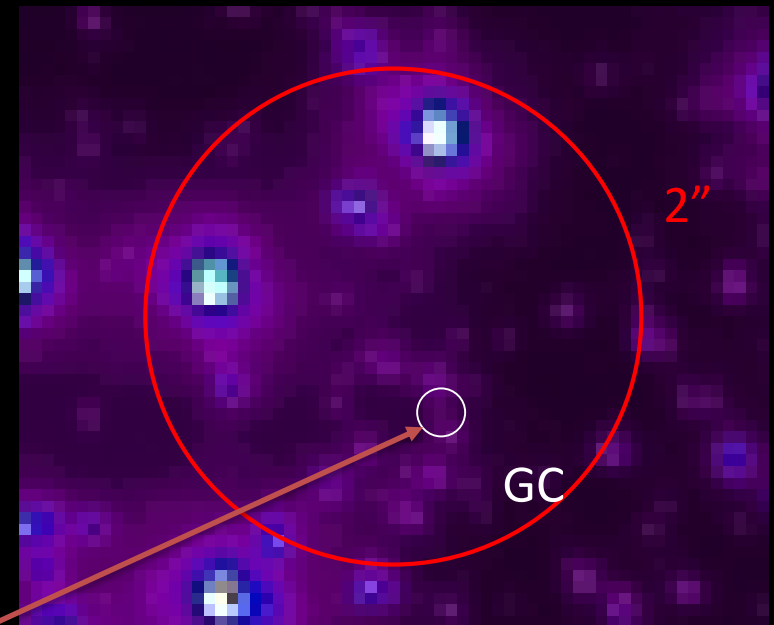
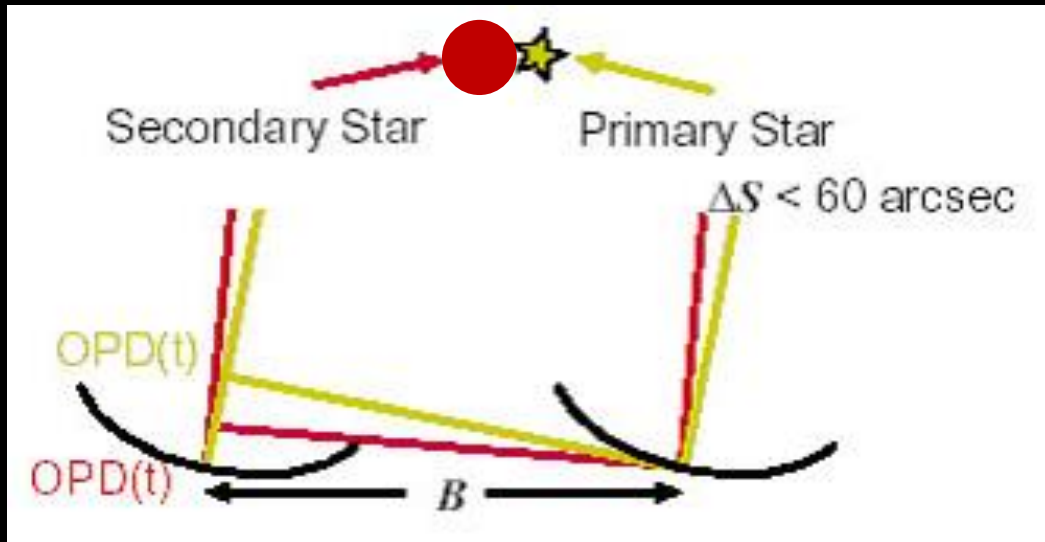


Reference source for
infrared adaptive optics

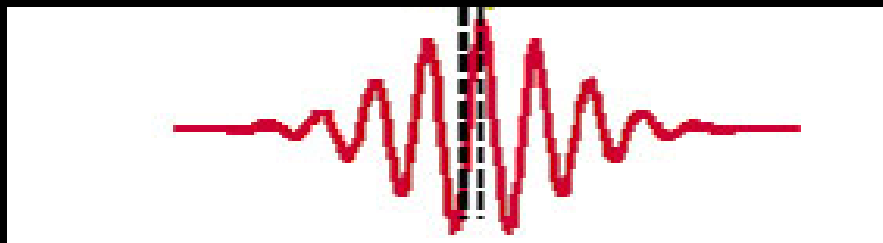
Reference sources for
imaging and astrometry



The GRAVITY imaging mode

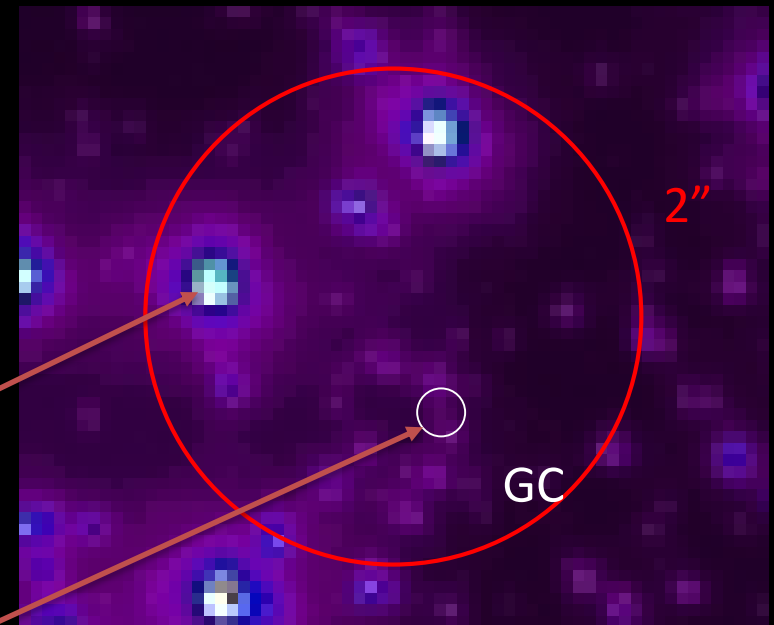
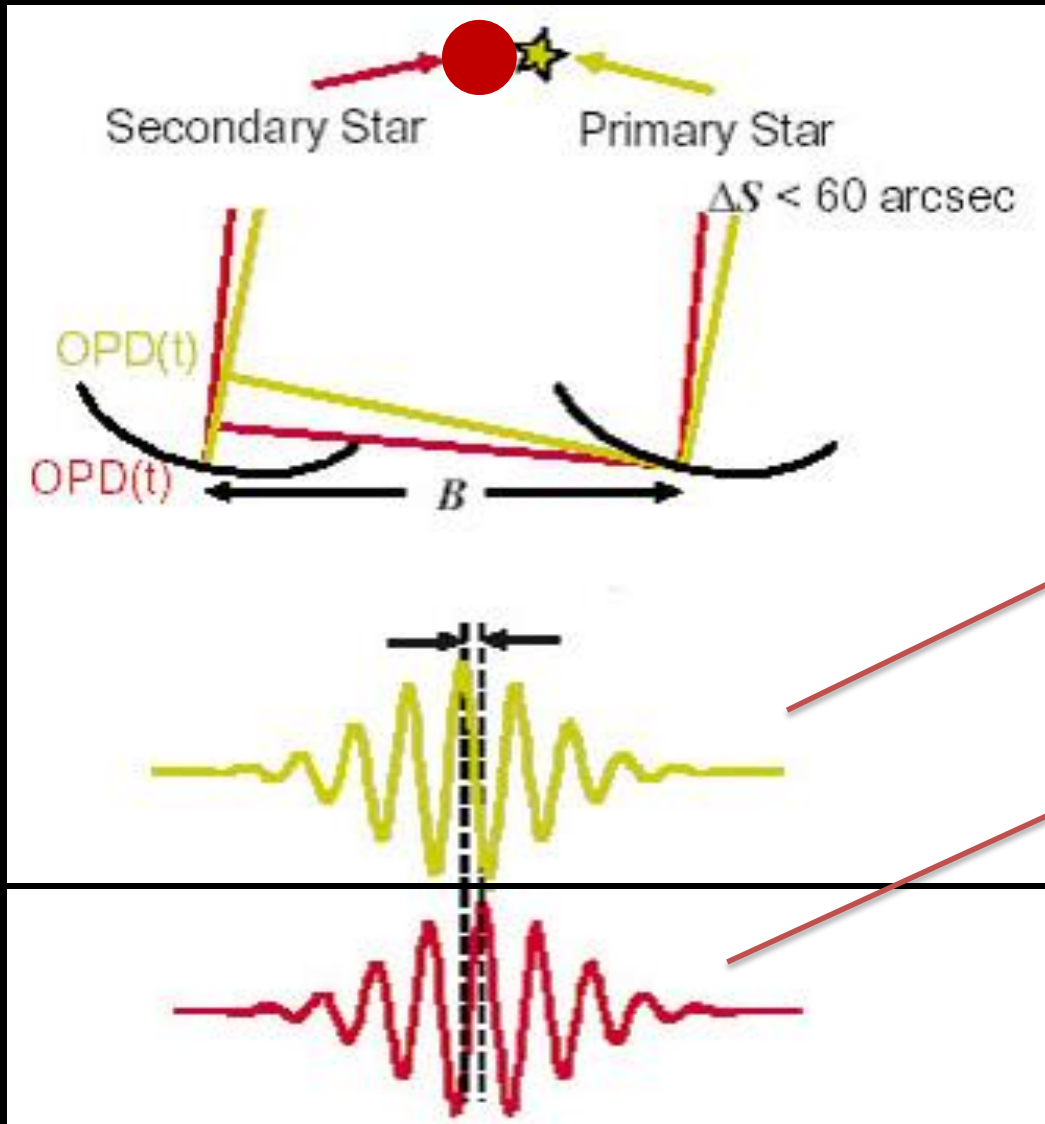


Contrast (B) \leftrightarrow F. T. (Object)



The GRAVITY astrometric mode

$$\delta OPD = \vec{B} \cdot \vec{\alpha} - \vec{B} \cdot \vec{\beta} = \vec{B} \cdot (\vec{\alpha} - \vec{\beta})$$

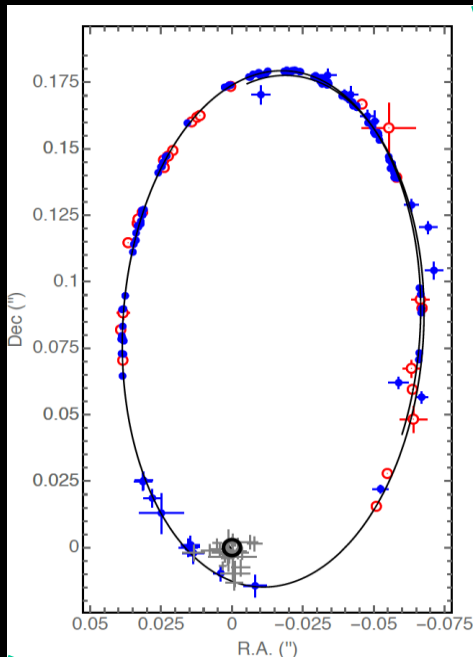


The GRAVITY tour

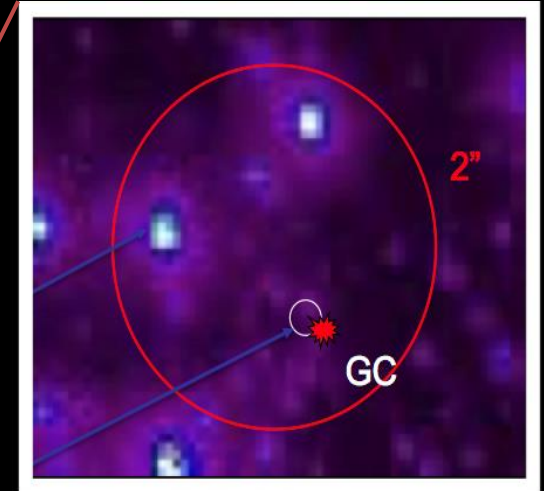


Max-Planck-Institut für
extraterrestrische Physik

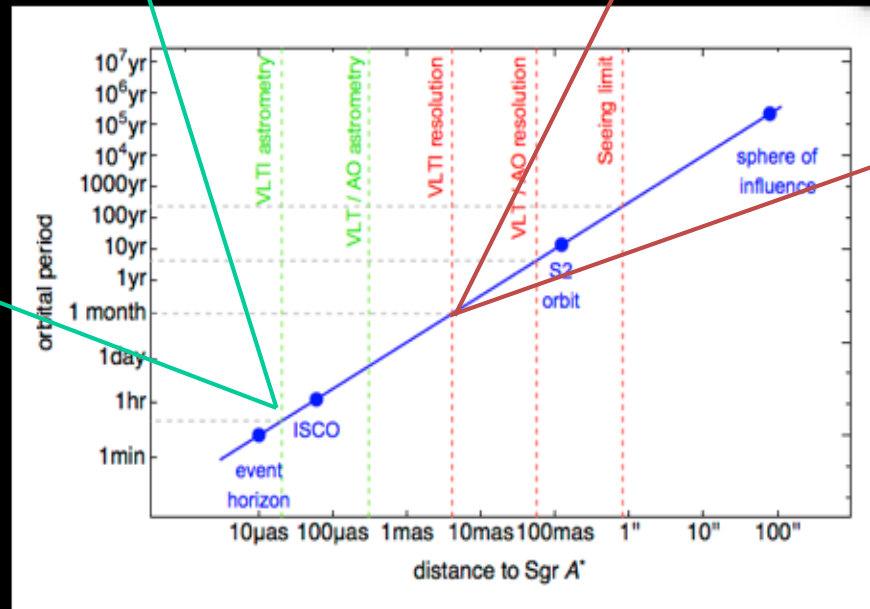
First results on the Galactic Center



Astrometry

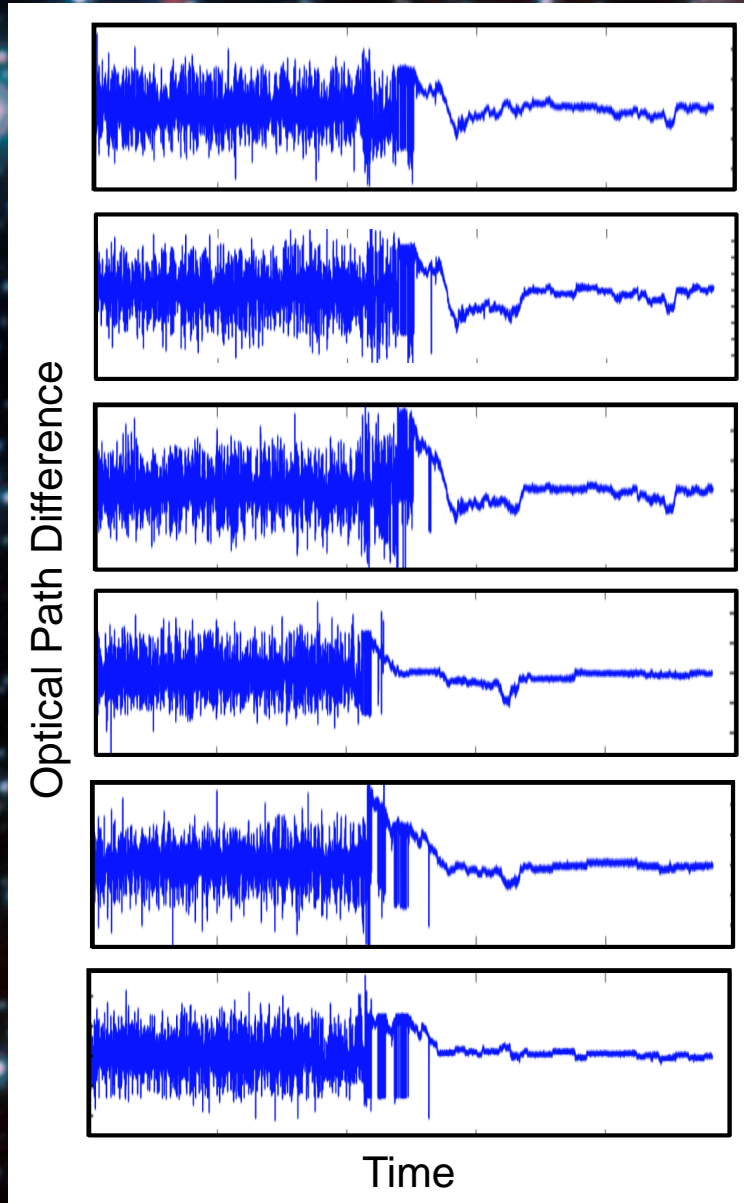


Imaging

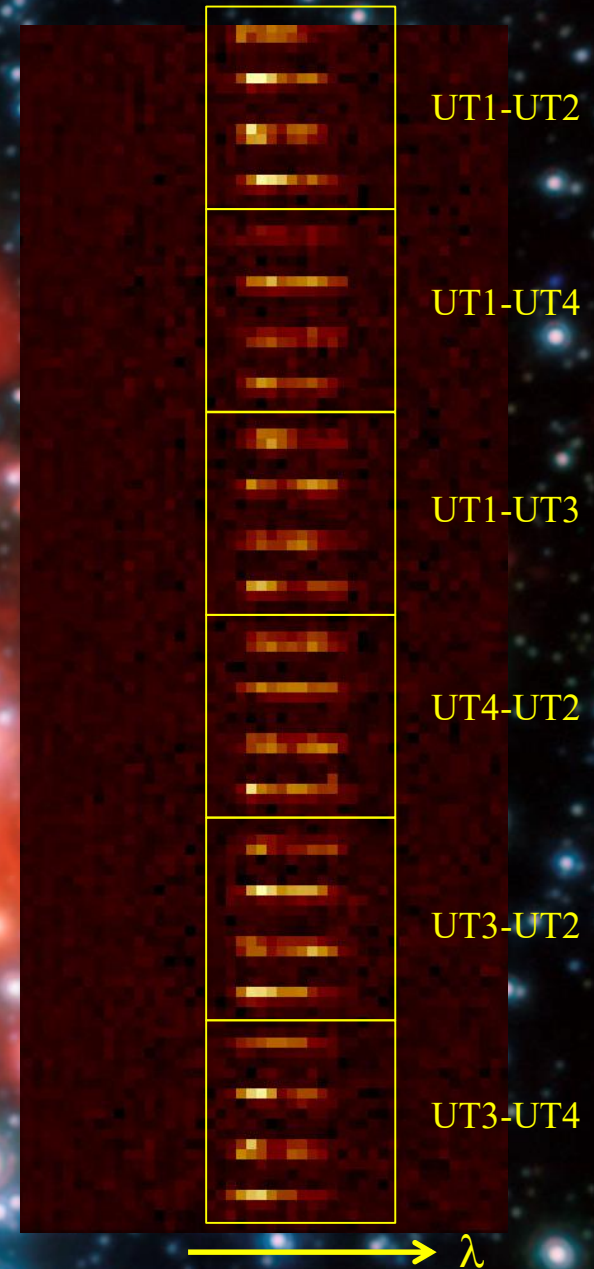
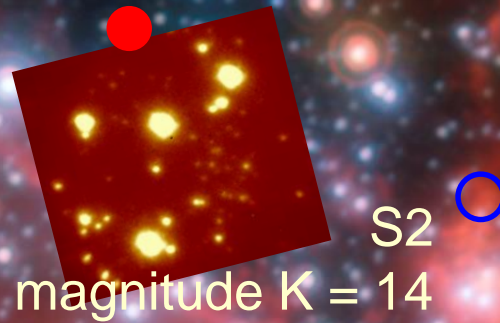


First observations of the Galactic Centre

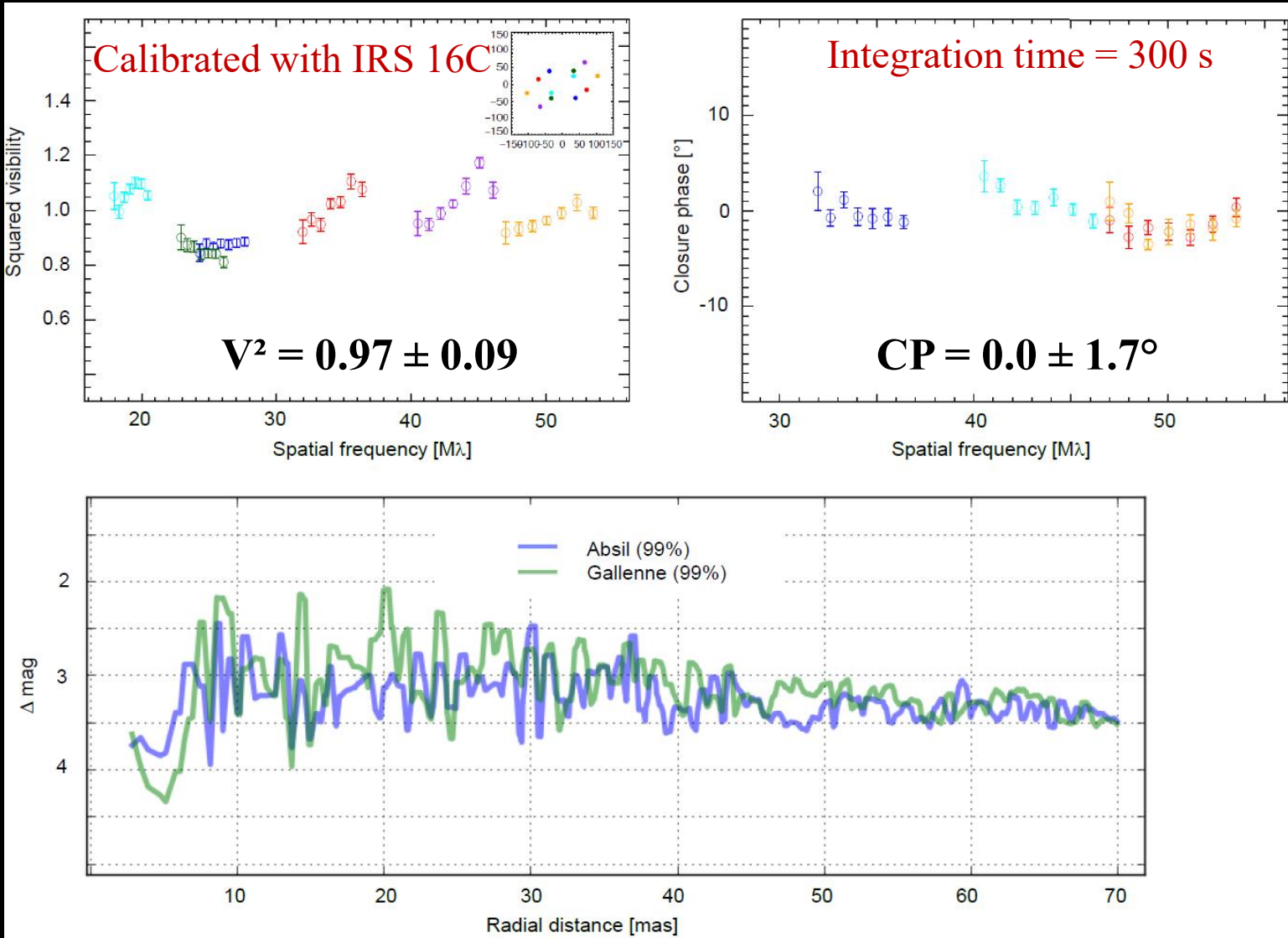
Fringe tracking on IRS16C ($\lambda/10$ rms) (2016, May 17th)



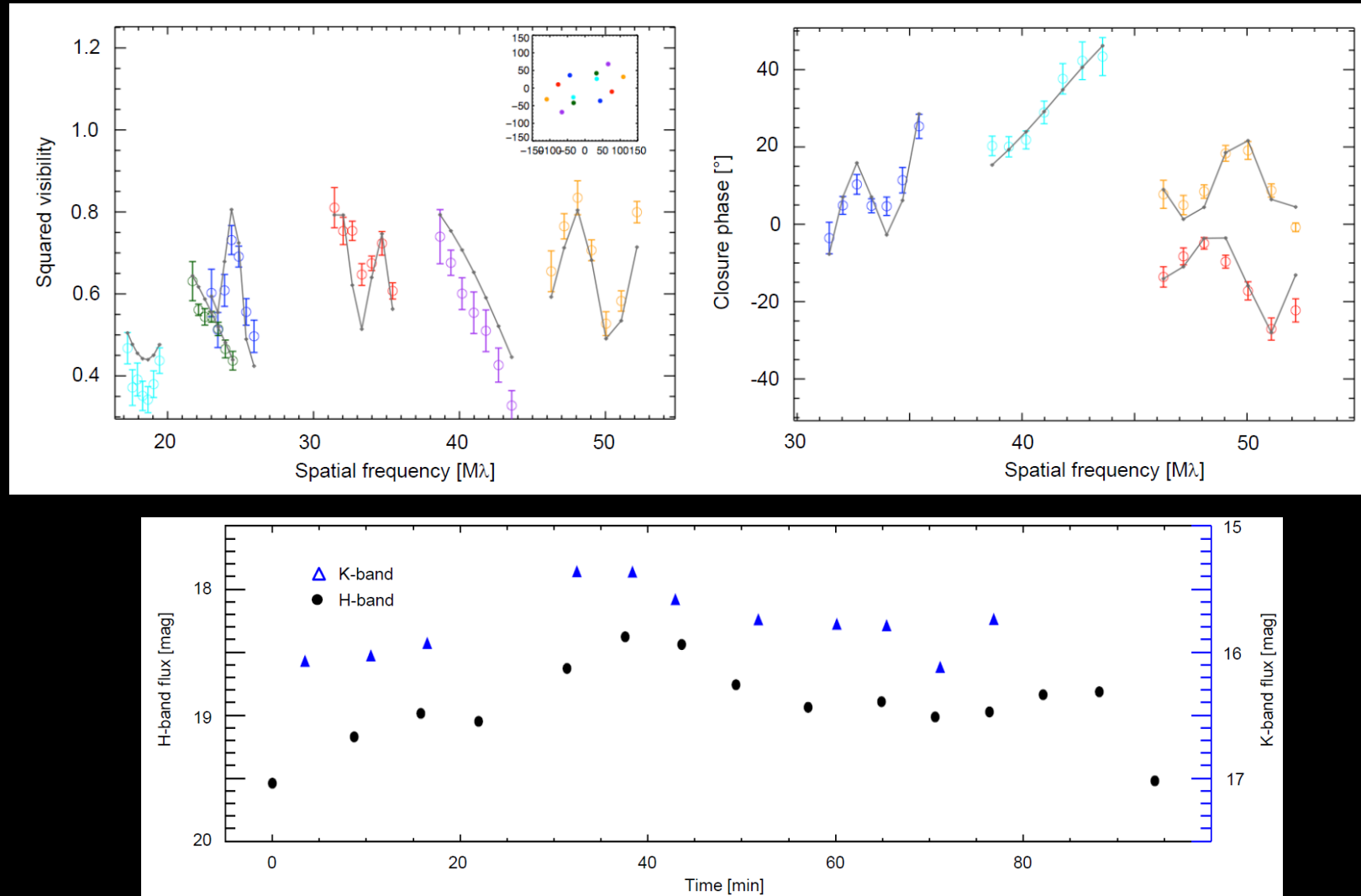
reference star
IRS16C
magnitude K = 10



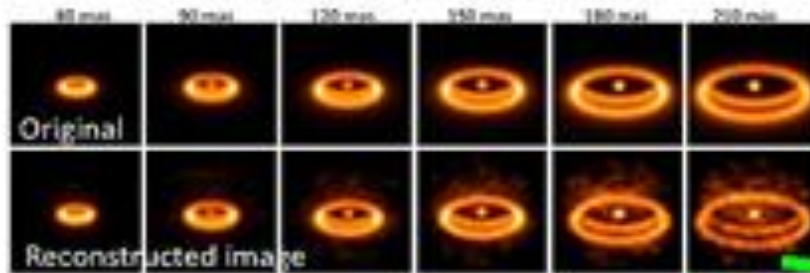
No stars brighter than $m_K = 17.1$ mag near S2



First detection of Sgr A* in infrared interferometry

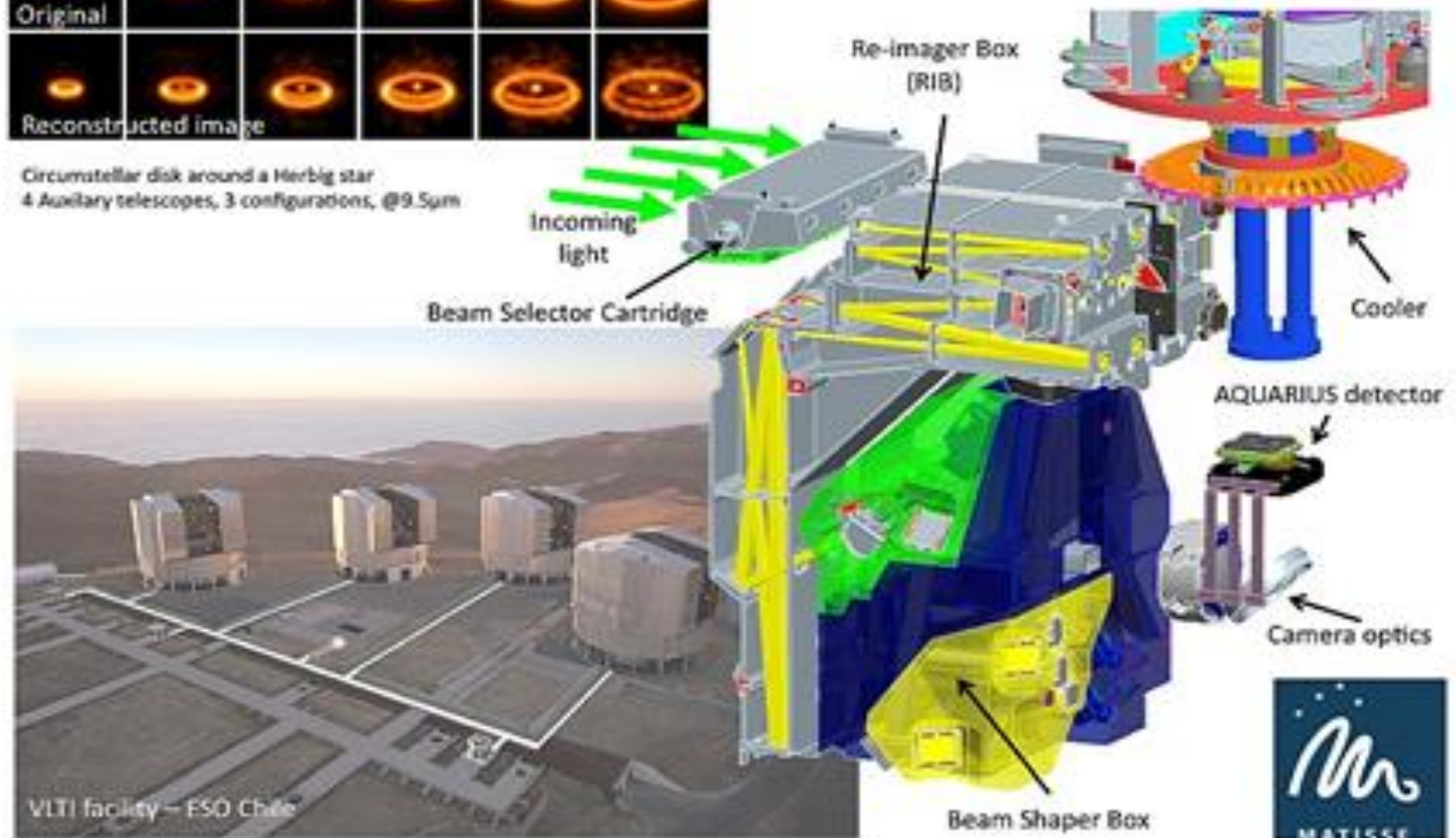








Simulation image capabilities MATISSE

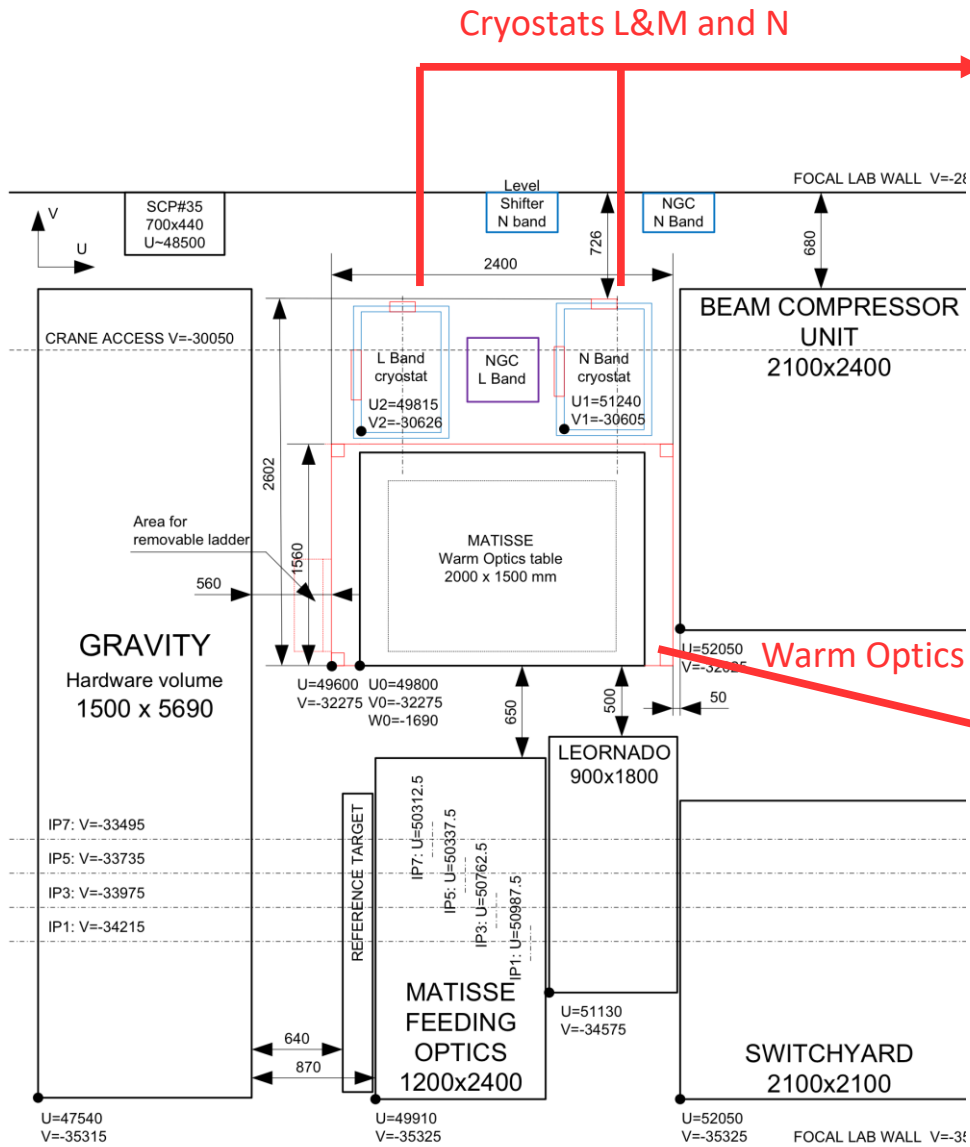


Circumstellar disk around a Herbig star
4 Auxiliary telescopes, 3 configurations, @9.5 μ m

MATISSE Cold Optical Bench

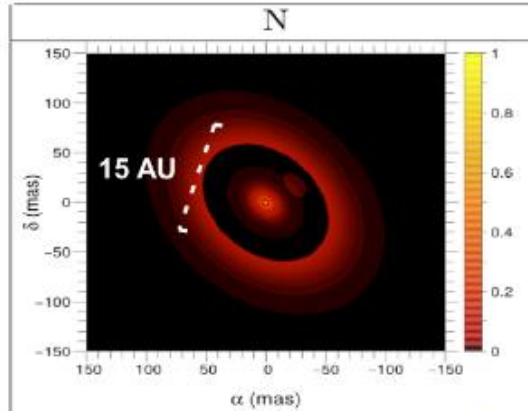


	<p>Observatoire Côte d'Azur Laboratoire Lagrange Université de Nice IPAG & CEA Saclay (France) *</p>	<p>Science – General concept & system – Management – Warm Optics – Control Command – Data reduction – Assembly, Integration, Tests - Commissioning</p>
	<p>Université de Leiden ** ASTRON (Netherlands)</p>	<p>Science – Cold optics – Interfaces</p>
	<p>Max Planck Institut Heidelberg (Germany)</p>	<p>Science – Cryogenics – Electronics</p>
	<p>Max Planck Institut Bonn (Germany)</p>	<p>Science – Detector – Image reconstruction</p>
	<p>Universität Vienne (Austria) Universität de Kiel (Germany)</p>	<p>Science</p>
	<p>European Southern Observatory (Germany)</p>	<p>Science- Detector – Infrastructure and VLTI logistics</p>

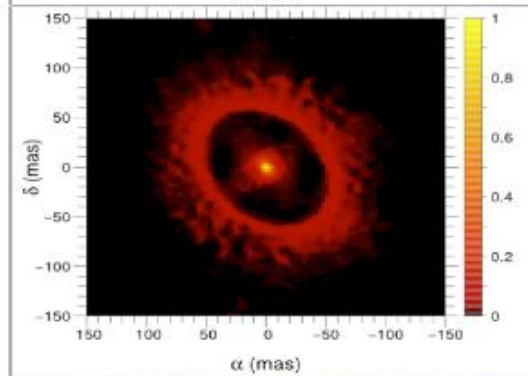


Observation of the inner protoplanetary disk regions

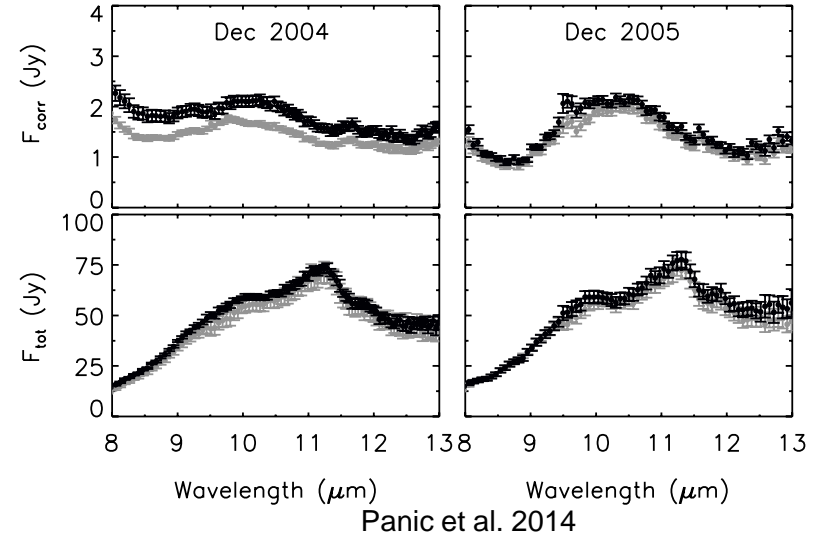
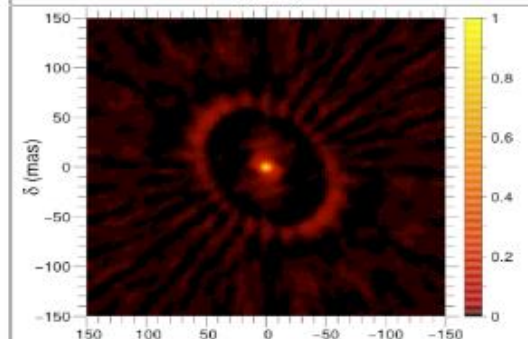
Analytical model of HD100546 disk + gap + clump



Reconstructed N band image (AT: 1.8m VLT telescope)
3 nights



Reconstructed N band image (UT: 8m VLT telescope)
1 night

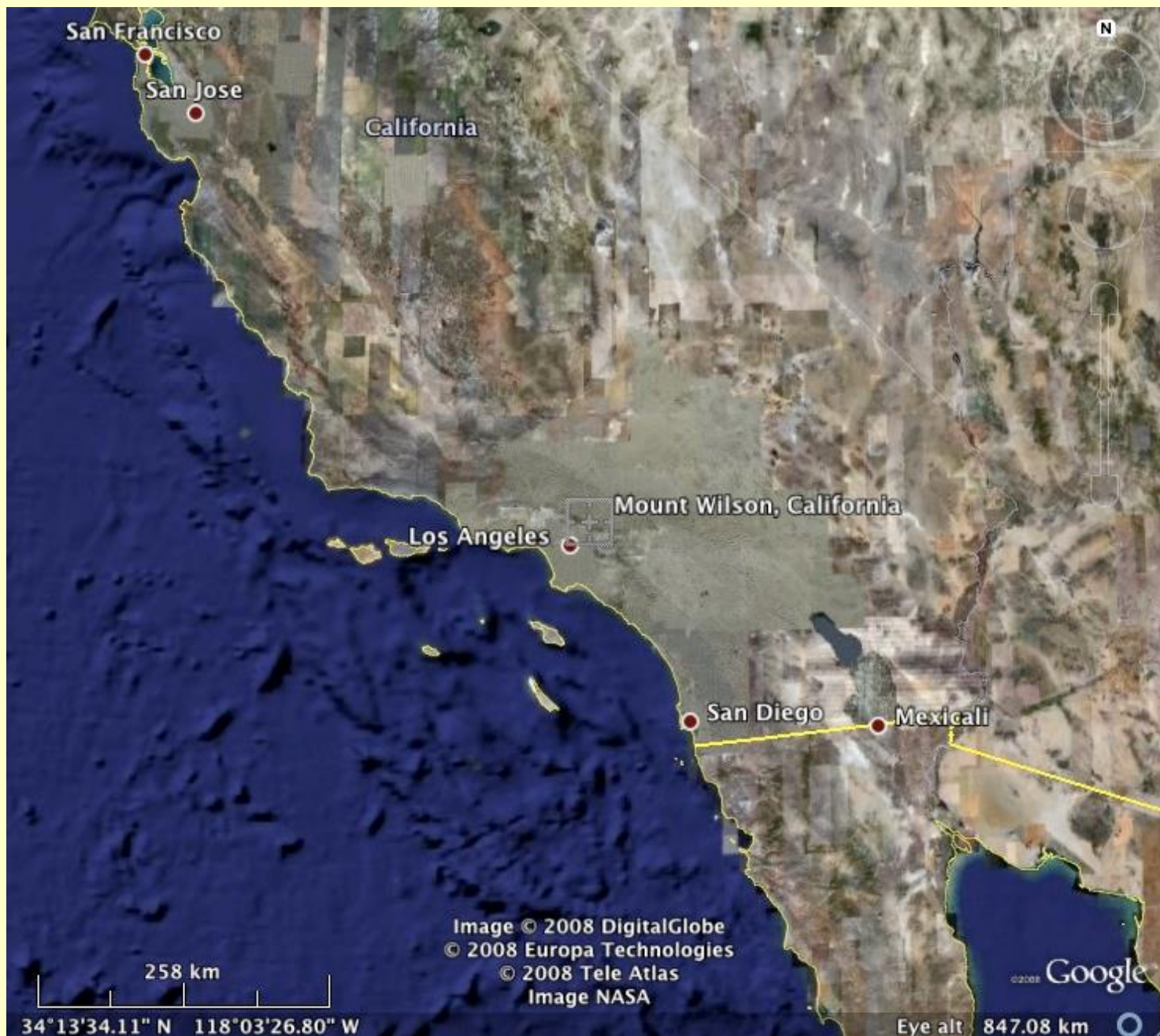


Artistic view (Muzerolle et al. 2009)

- PAE (Preliminary Acceptance Europe) from 20 Jun 2017 to 12 Sep: green light for the transport to Paranal
- Departure from Nice on 4&11 Oct 2017
- Arrival at Paranal: end of October
- 1st light around Feb. 2018
- Commissioning >Feb/Mar 2018



The CHARA Collaboration



First science publication.... 5 years later!

FIRST RESULTS FROM THE CHARA ARRAY. I. AN INTERFEROMETRIC AND SPECTROSCOPIC STUDY OF THE FAST ROTATOR α LEONIS (REGULUS)

H. A. McALISTER, T. A. TEN BRUMMELAAR, D. R. GIES,¹ W. HUANG,¹ W. G. BAGNUOLO, JR.,
M. A. SHURE, J. STURMANN, L. STURMANN, N. H. TURNER, S. F. TAYLOR,
D. H. BERGER, E. K. BAINES, E. GRUNDSTROM,¹ AND C. OGDEN

Center for High Angular Resolution Astronomy, Georgia State University, P.O. Box 3969, Atlanta, GA 30302-3969;
hal@chara.gsu.edu, theo@chara-array.org, gies@chara.gsu.edu, huang@chara.gsu.edu,
bagnuolo@chara.gsu.edu, mashure@yahoo.com, judit@chara-array.org,
sturmann@chara-array.org, nils@chara-array.org, taylor@chara.gsu.edu,
berger@chara-array.org, baines@chara.gsu.edu,
erika@chara.gsu.edu, ogden@chara.gsu.edu

S. T. RIDGWAY

Kitt Peak National Observatory, National Optical Astronomy Observatory, P.O. Box 26732,
Tucson, AZ 85726-6732; sridgway@noao.edu

AND

G. VAN BELLE

Michelson Science Center, California Institute of Technology, 770 South Wilson Avenue,
MS 100-22, Pasadena, CA 91125; gerard@ipac.caltech.edu

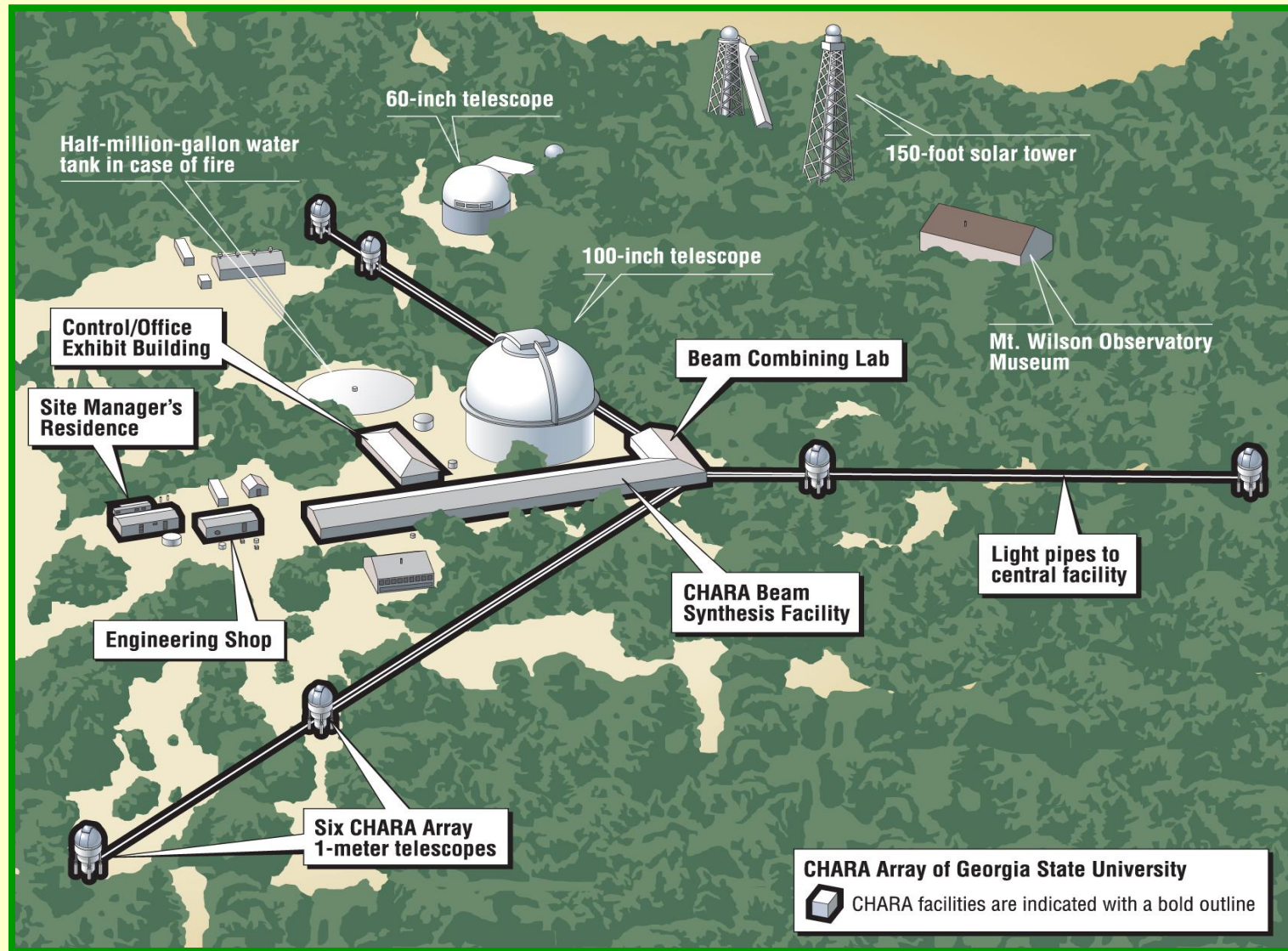
Received 2004 November 15; accepted 2005 January 10

ABSTRACT

We report on *K*-band interferometric observations of the bright, rapidly rotating star Regulus (type B7 V) made with the CHARA Array on Mount Wilson, California. Through a combination of interferometric and spectroscopic measurements, we have determined for Regulus the equatorial and polar diameters and temperatures, the rotational velocity and period, the inclination and position angle of the spin axis, and the gravity darkening coefficient. These first results from the CHARA Array provide the first interferometric measurement of gravity darkening in a rapidly rotating star and represent the first detection of gravity darkening in a star that is not a member of an eclipsing binary system.

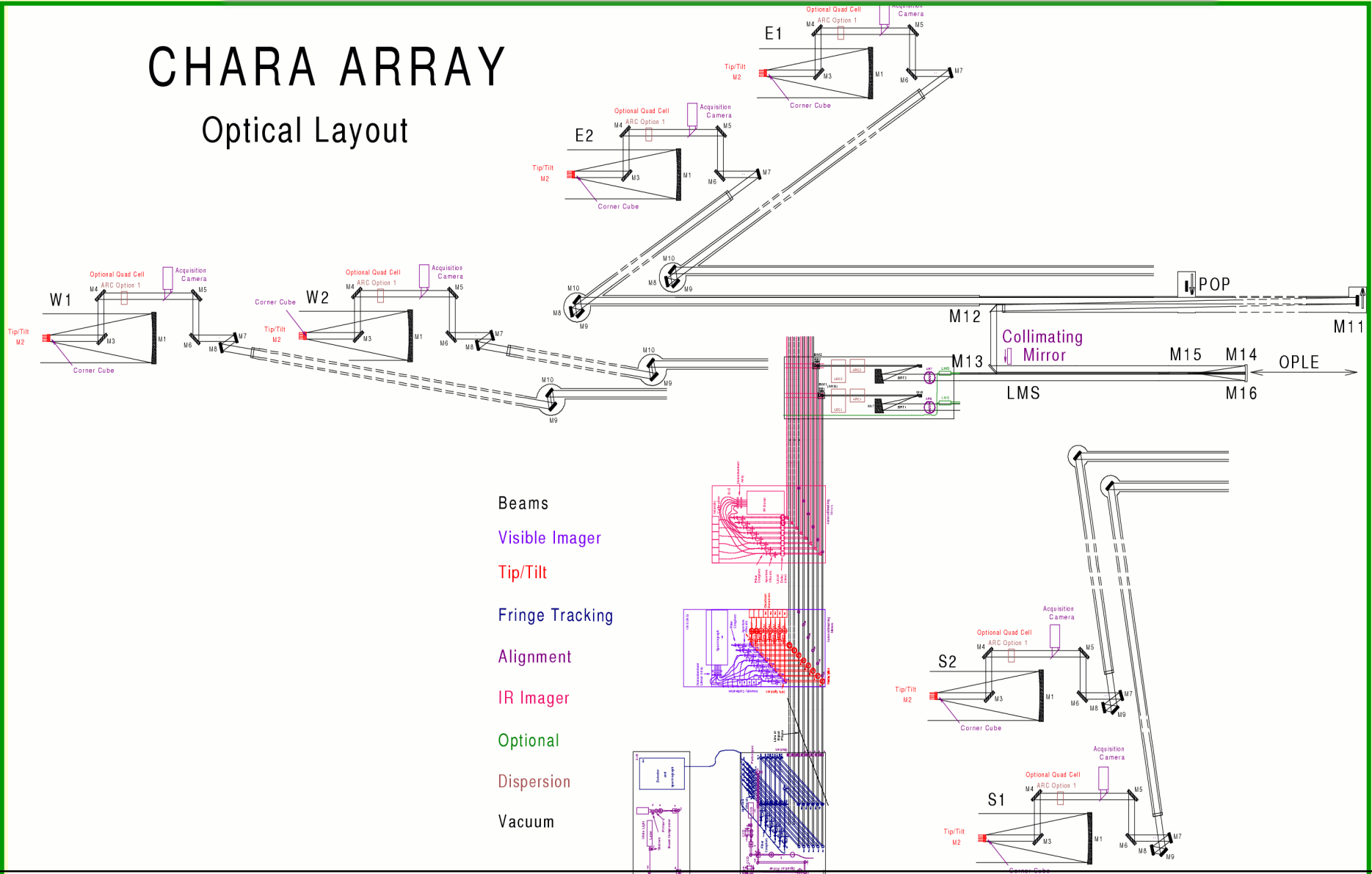
Subject headings: infrared: stars — stars: fundamental parameters — stars: individual (α Leonis, Regulus) — stars: rotation — techniques: interferometric

Layout of the CHARA Array

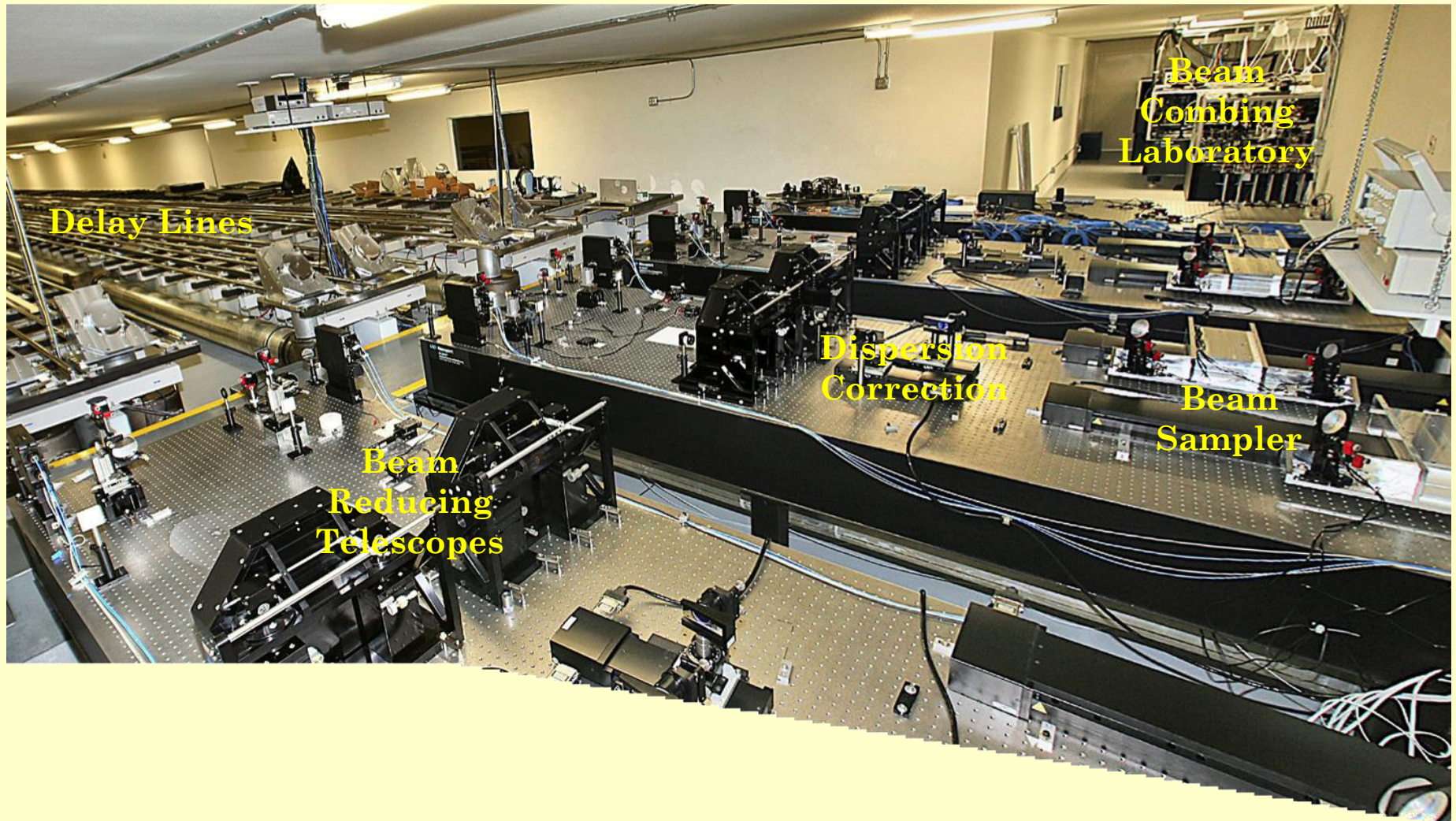


Overall Optical Layout

CHARA ARRAY Optical Layout



Optics Laboratory



Delay Lines

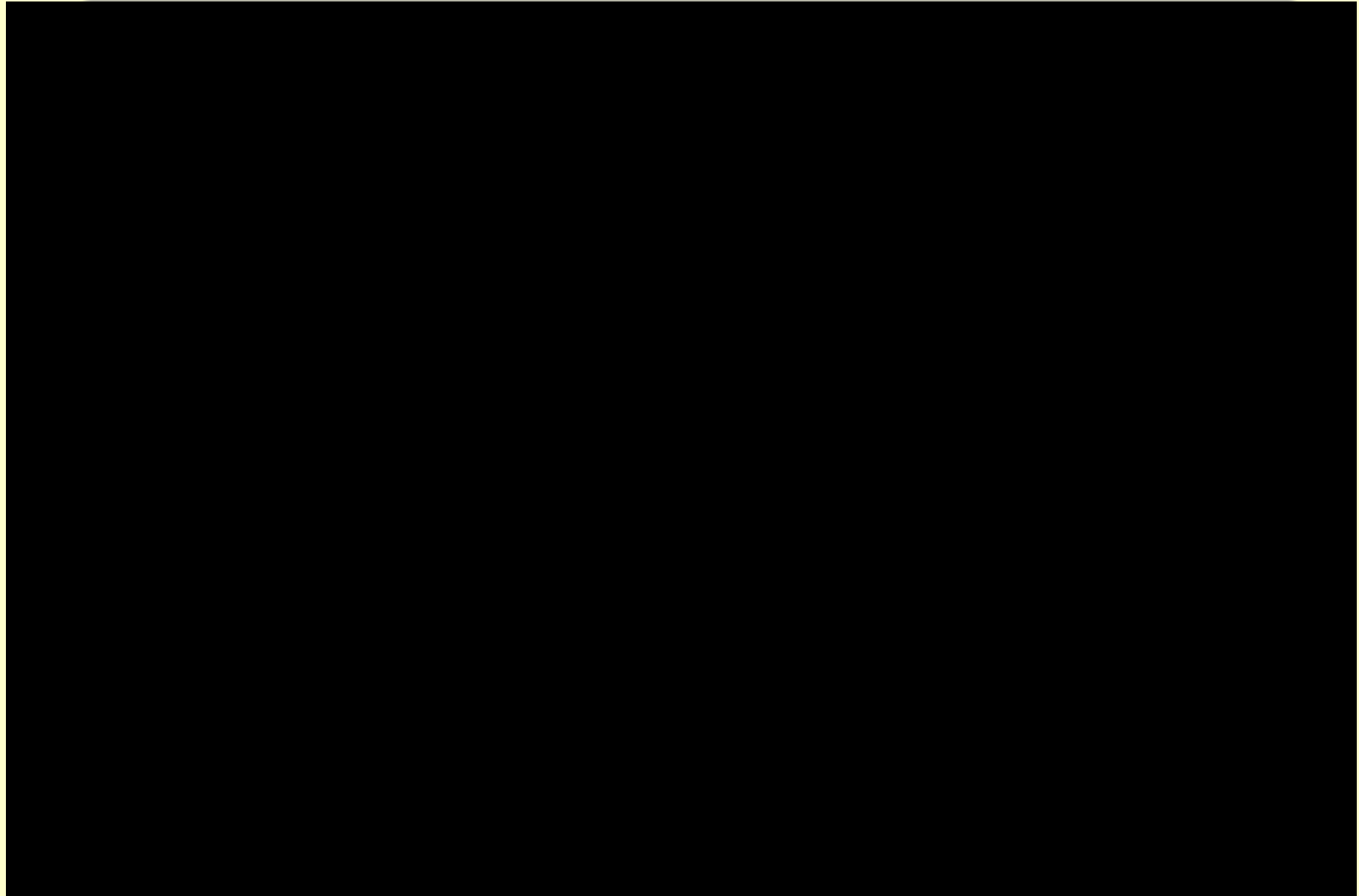
Beam
Combing
Laboratory

Dispersion
Correction

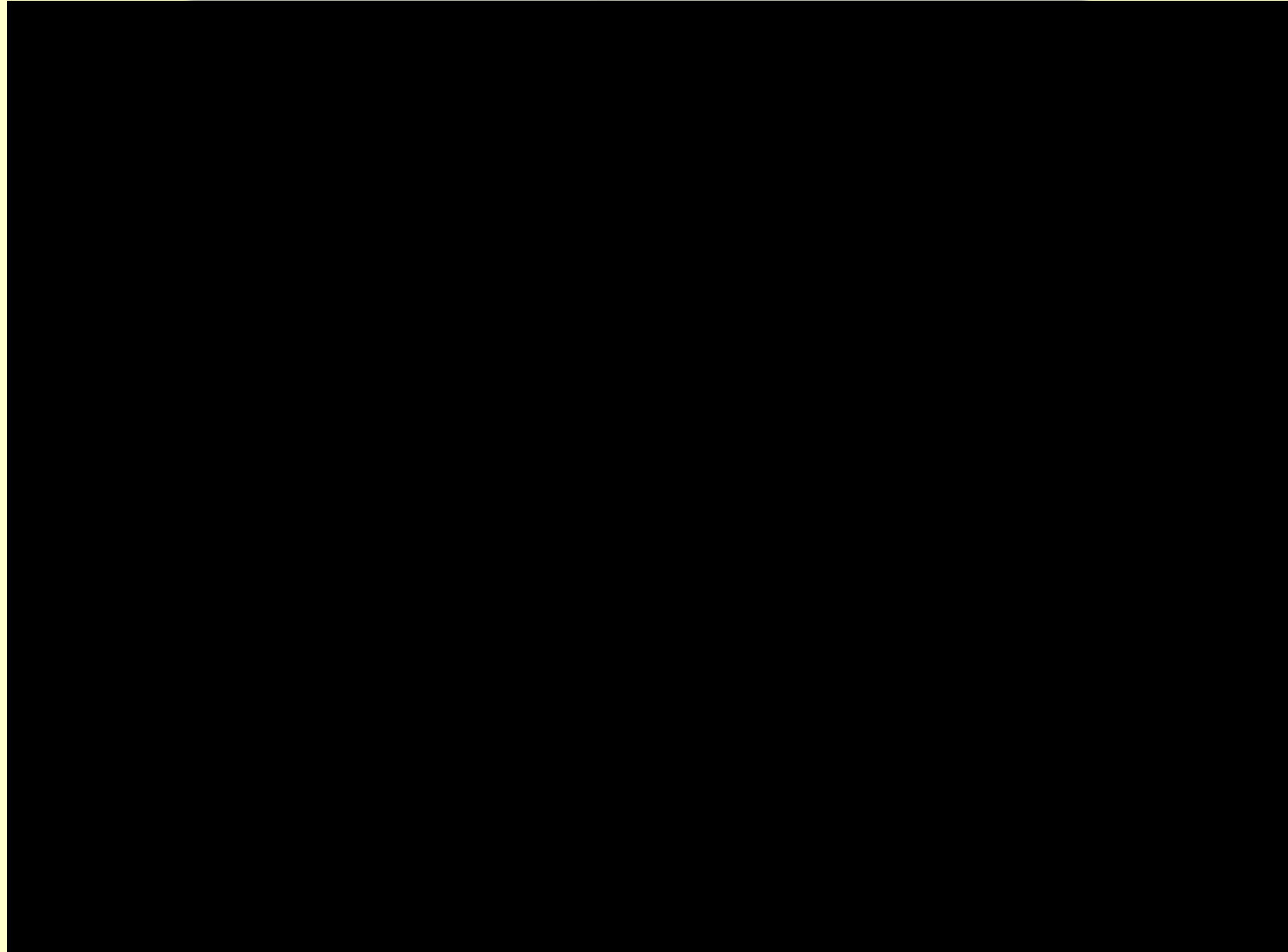
Beam
Sampler

Beam
Reducing
Telescopes

The 30 second CHARA tour.



Delay Lines

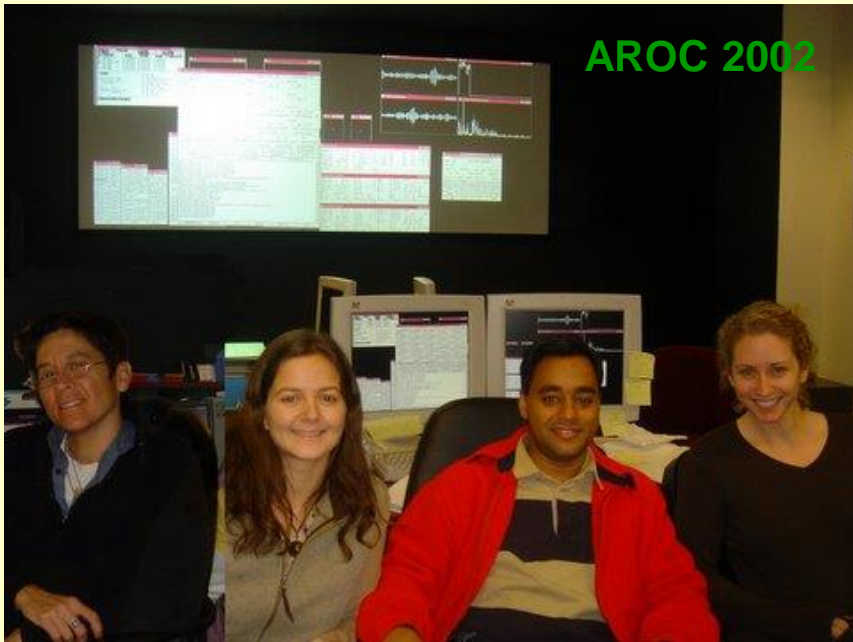


“Beam Combiners are us”

- CHARA CLASSIC – 2 way open air J, H & K
- CHARA CLIMB – 2x3 way open air J, H & K
- FLUOR – 2 way fiber based K band
- MIRC – 6 way fiber based imager J, H & K
- VEGA – 4 way open air V,R,I R=30000
- PAVO – 3 way aperture plane V,R,I
- CHAMP – 6 beam fringe tracker J, H & K
- More to come... (CIMB++, MIRCx, MYSTIC, FRIEND++.....)



ROCMI 2006

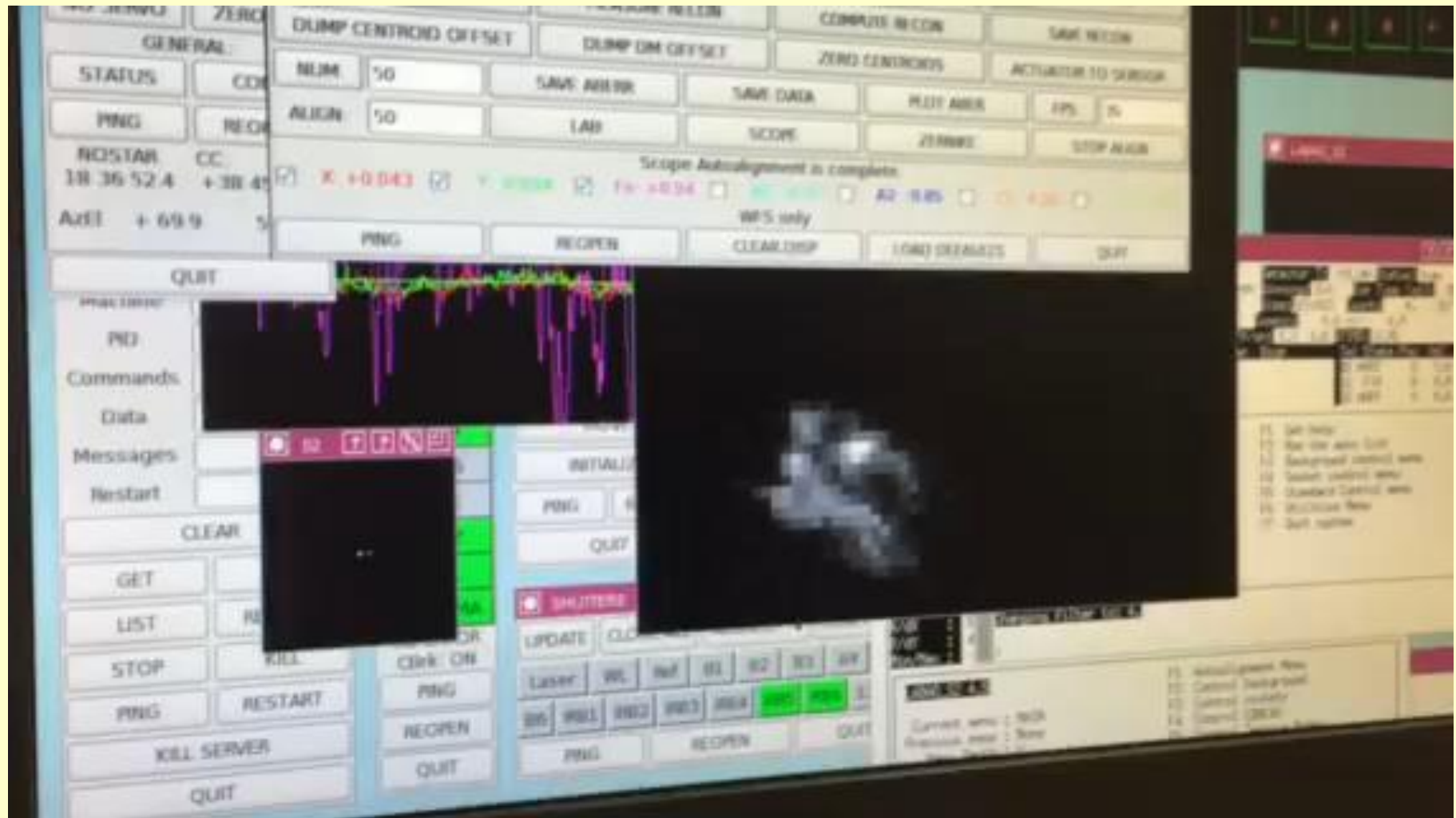


The CHARA Adaptive Optics Program

- The CHARA Adaptive Optics Program is broken into 2 Phases.
- This is purely an artifact of funding realities.
- **Phase I (NSF/ATI)**, which includes Wave Front Sensors for each telescope and non-common-path AO systems for the laboratory, was funded in 2010 and is now nearing completion.
- **Phase II (NSF/MRI)**, which includes deformable mirrors for each telescope, began in mid-2015.

The program is fully funded.

CHARA-AO Program First On Sky Test



The CHARA Array Adaptive Optics Program

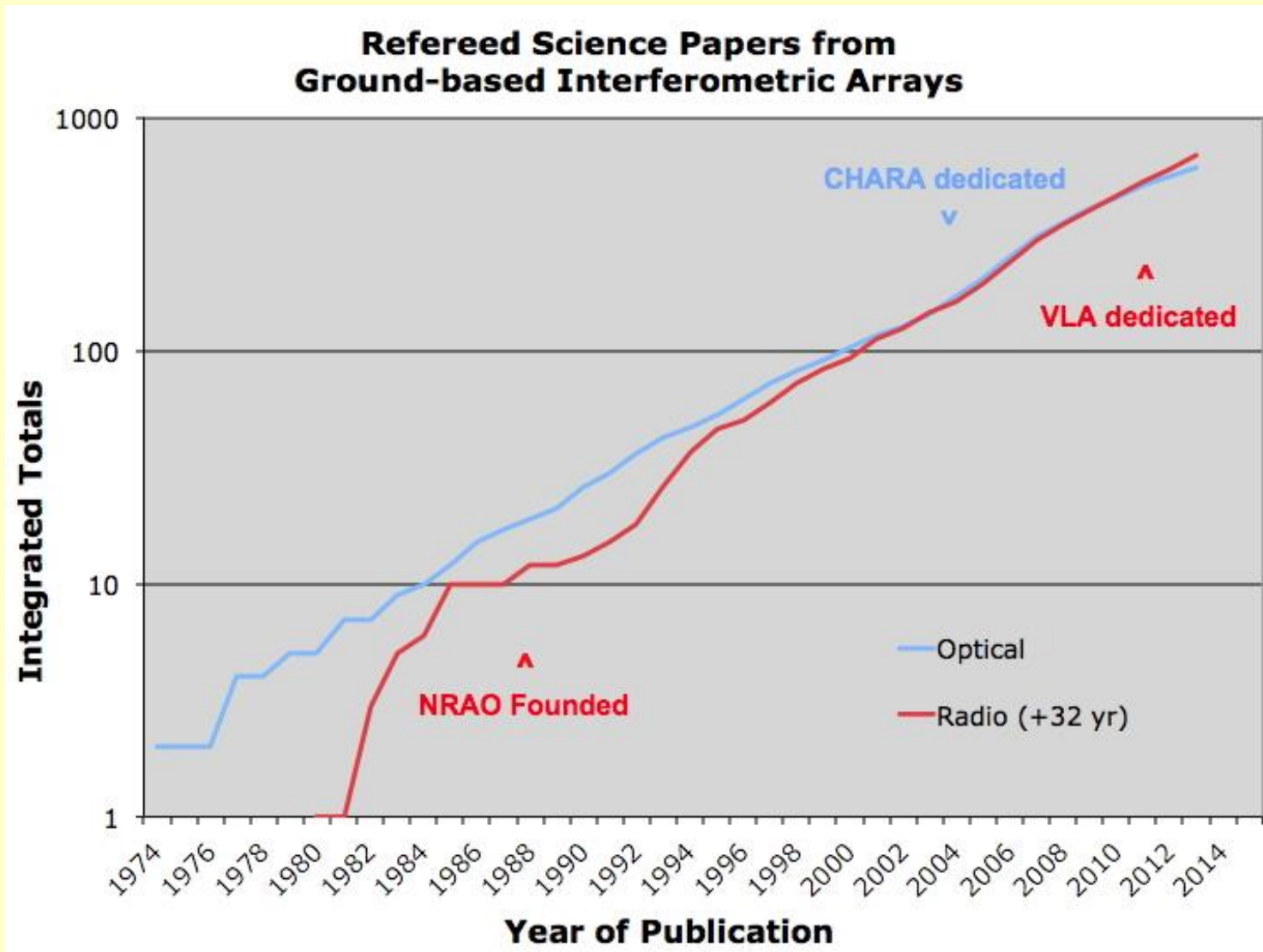
The screenshot displays the CHARA Array Adaptive Optics control software. Key components include:

- Top Left:** A menu with options like 'ALL', 'ALIGN', and 'CONFIGURE'. Below it is a table with columns 'WL' and 'Ref', listing various beam paths (B2, B3, B5, B6, IRB2, IRB3, IRB5, IRB6, W1WFS, ETWFS, W2WFS, EZWFS, REOPEN, QUIT).
- Top Center:** A control panel for 'LABAD_S2_V2.0' with buttons for 'COG', 'FULL AP', 'ON EDGE', 'MIDDLE', 'UP', 'DOWN', 'LEFT', 'RIGHT', 'CONTRACT', 'EXPAND', 'MEAN', 'SAVE ABERR', 'SAVE DATA', 'PLOT', 'LAB', 'M7', 'SCOPE', 'BEACON FOC', 'TOGGLE REF', 'AUTO M7', 'AUTO SCOPE', and 'STOP ALIGN'.
- Top Right:** A plot window titled 'LABAD_S2' showing a multi-colored wavefront error plot.
- Center:** A large window displaying a grid of beam profiles, each enclosed in a green square. The grid is arranged in a roughly triangular pattern.
- Bottom Center:** A control panel for 'S2 SECONDARY' with fields for 'Absolute', 'Relative', and 'Focus' in microns, and 'Tilt' in arcsec. It also includes 'X', 'Y', and 'Z' coordinates in microns and a 'SERVO OFF' button.
- Bottom Right:** Another window showing a grid of beam profiles, similar to the central window but with a different arrangement.
- Bottom Left:** A terminal window showing command-line output, including 'Cara sent=10', 'Timer Get Ics Status', and 'Send=GET STATUS-1'.
- Bottom Center:** Another terminal window showing error messages: 'ailed to get pixel names.', 'ailed to get beam types.', 'ailed to get config from 0', 'ailed to get reference from 0', and 'ailed to get active scopes 0'.

Enabling Milliarcsecond Astrophysics: Open access for the CHARA Array

- The NSF/MSIP program is a response to the previous decadal report that stated that the NSF needs to direct more funding to mid-scale programs, including new instruments, access to existing instruments, and access to existing data archives.
- Our proposal has been funded for \$4M over 5 years to provide 50-75 nights per year of open access to the CHARA Array through the NOAO TAC process.

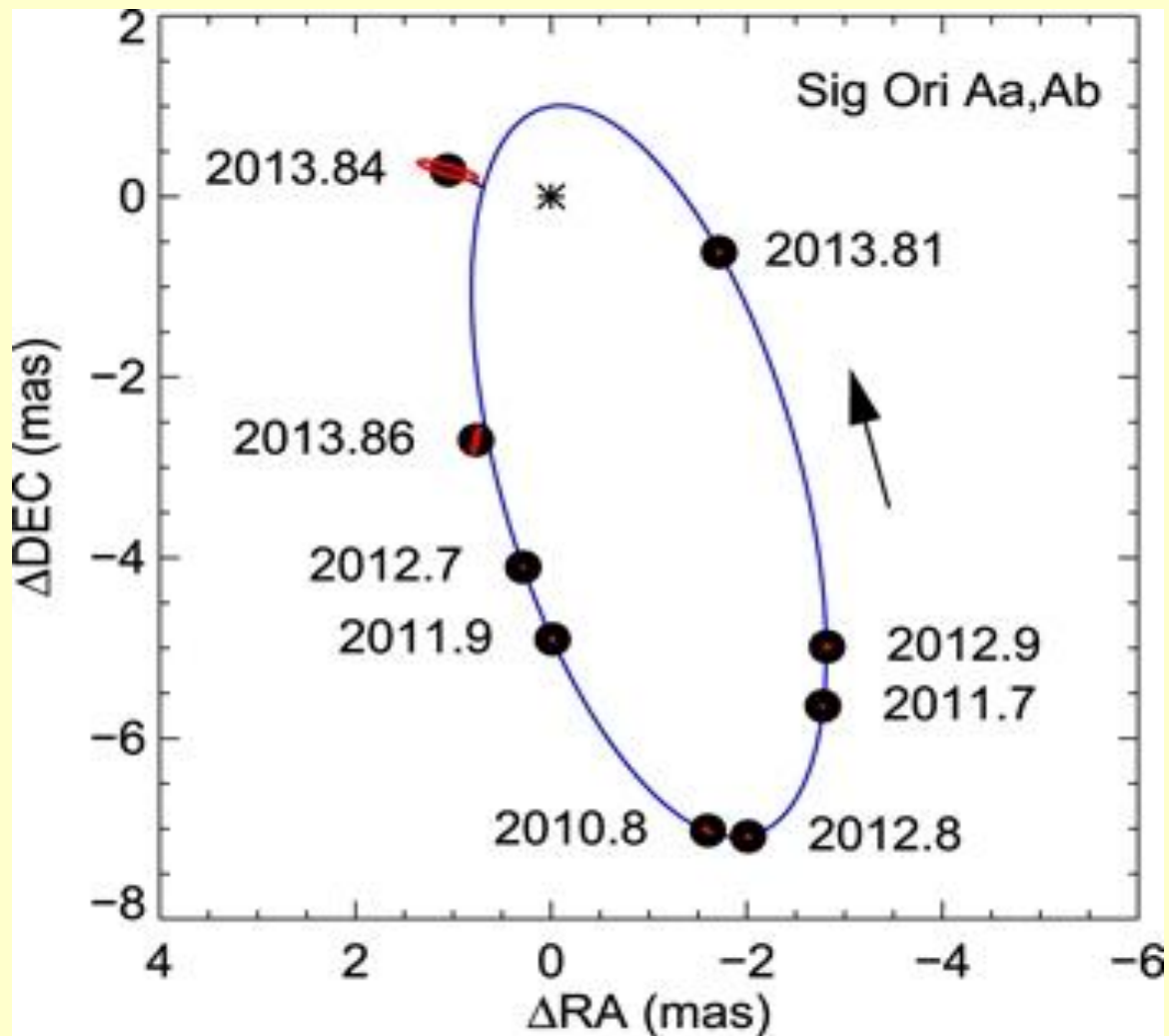
Proposal focus A – “Optical Interferometry is not as obscure or as difficult as many believe.”



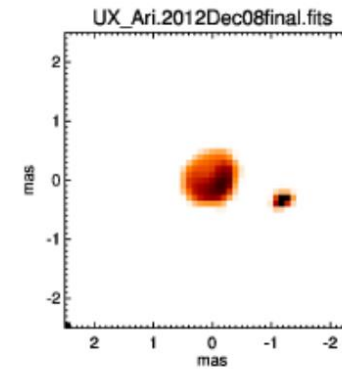
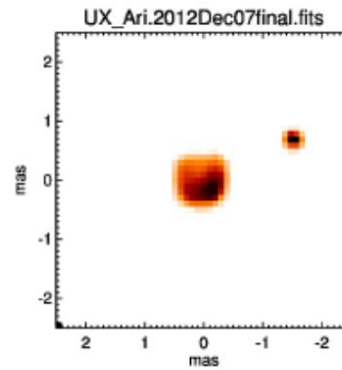
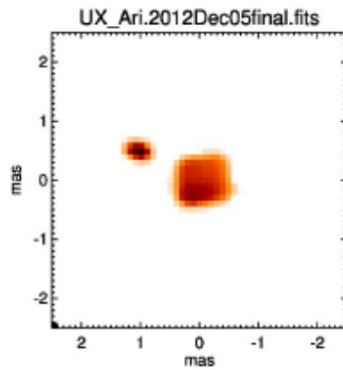
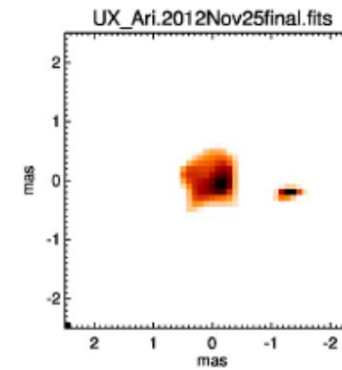
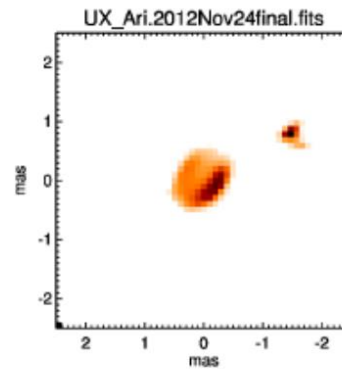
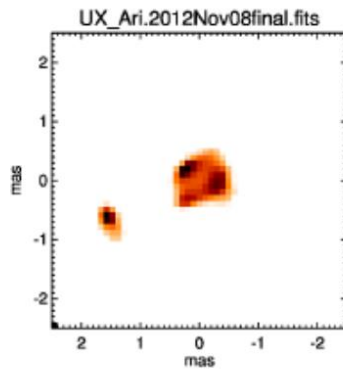
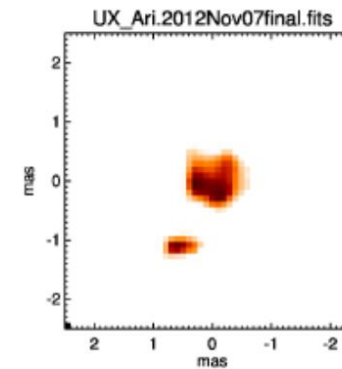
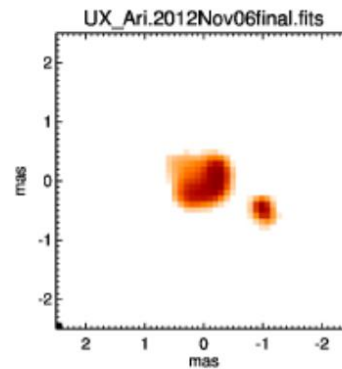
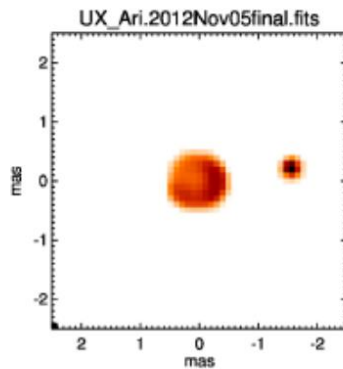
Stellar Diameters – Our bread and butter science

- The fundamental properties of stars are not really very well known, and certainly poorly measured until quite recently.
- Basic parameters like size, temperature and luminosity can now be directly measured for a large range of stellar types.
- Imaging stellar surfaces is now routine.

Orbit of *sigma Ori* (Schaefer et al.)

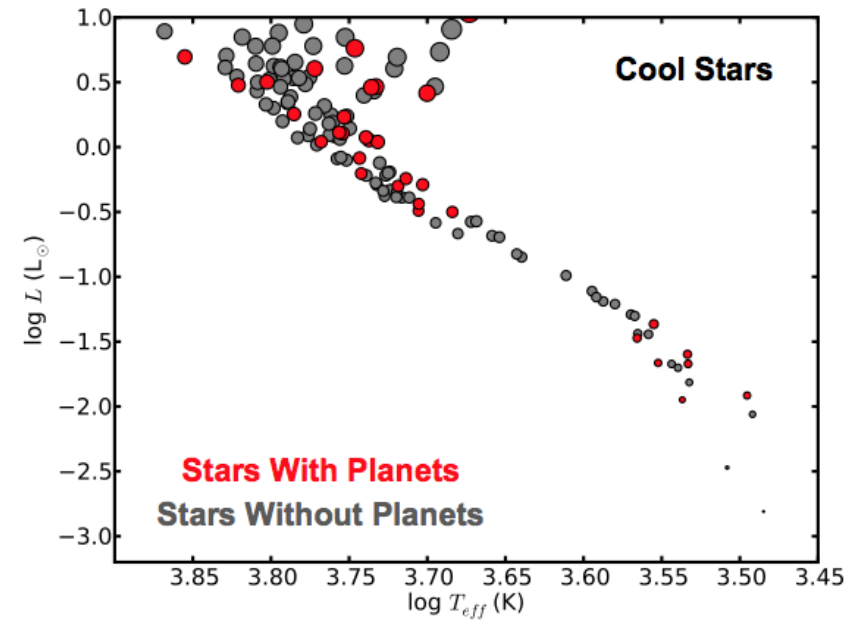
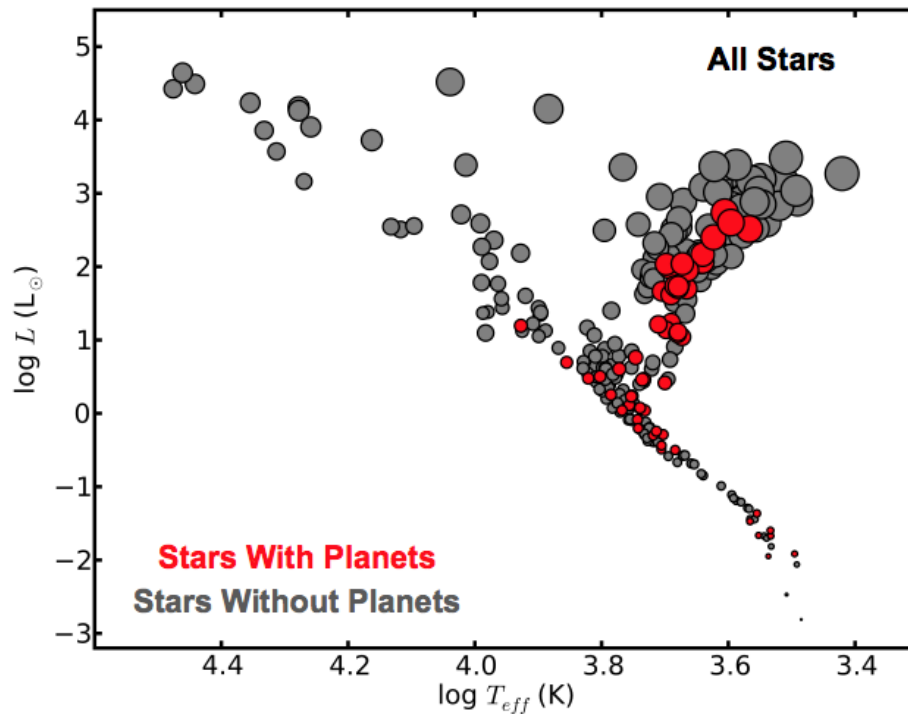


The Orbit of UX Arietis – Hummel et. al.



An Interferometric HR Diagram

Compliments of Tabetha Boyajian and Kaspar von Braun

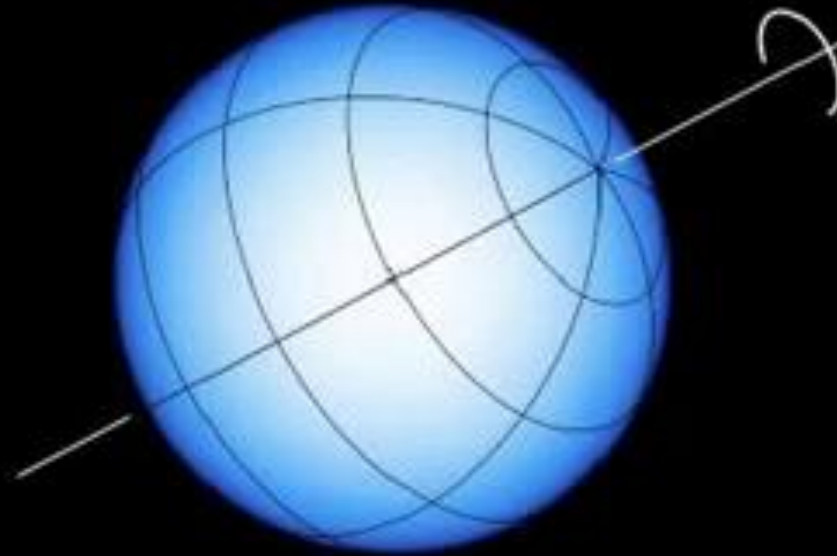


Log T_{eff} (K)

Measurements of the flux from the stars from the HARPS arrays.
 These data from 2009

Rotating Stars Are Oblate:

Model of a fast-spinning star



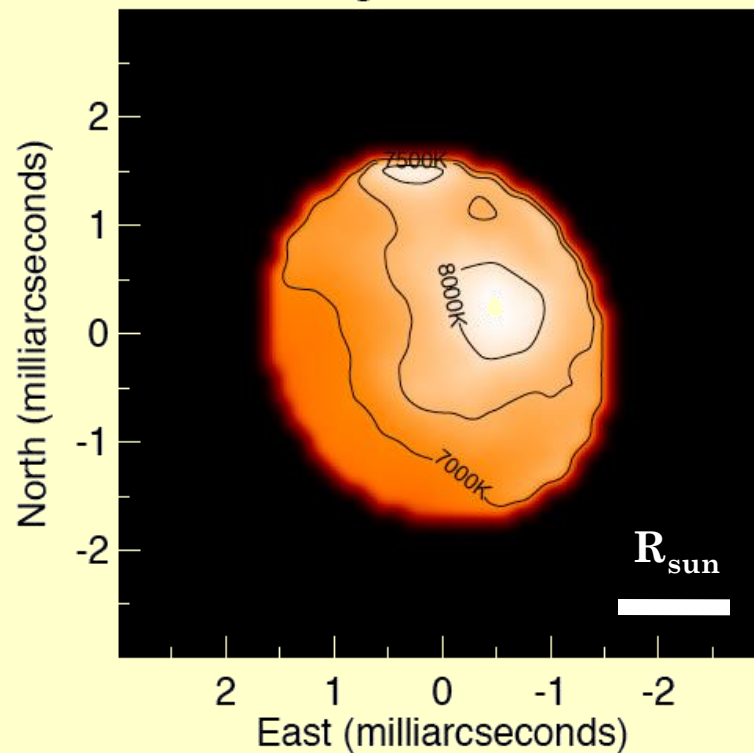
0.1 revolutions/day

First image of a main-sequence star

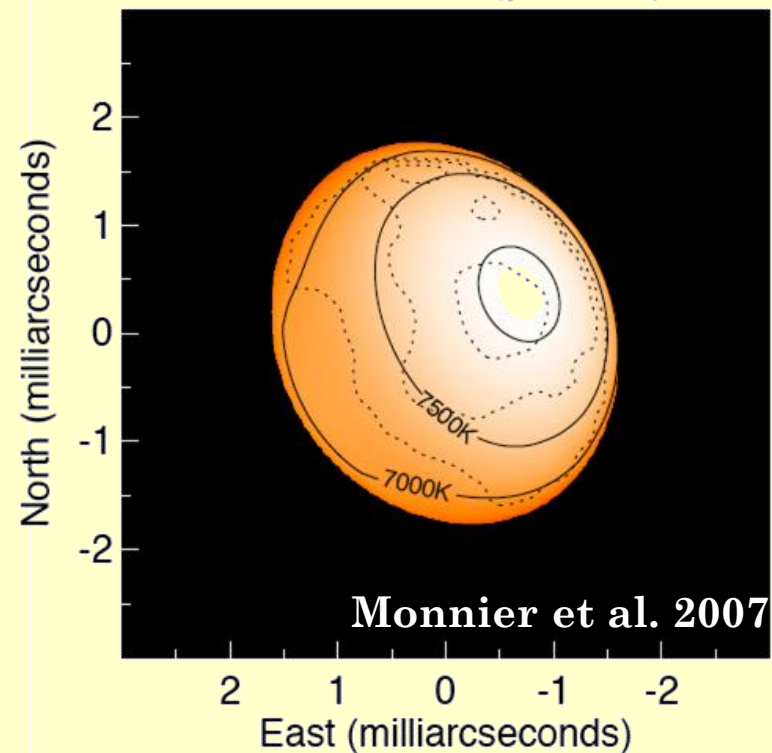
(besides the Sun...)

- Altair (a Aql, $V=0.7$)
 - Nearby hot star ($d=5.1\text{pc}$, SType A7V, $T=7850\text{K}$)
 - Rapidly rotating ($v \sin i = 240\text{ km/s}$, $\sim 90\%$ breakup)

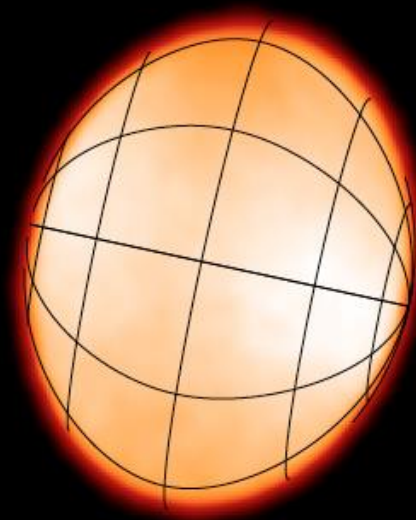
Altair Image Reconstruction



Altair Model ($\beta=0.19$)

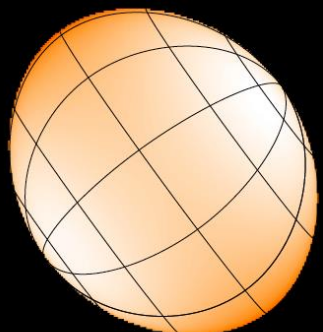


MIRC Observations of Rapid Rotators



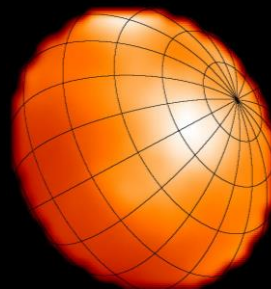
Regulus

Che et al. 2011



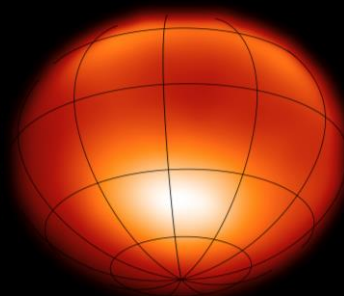
Rasalhague

Zhao et al. 2009



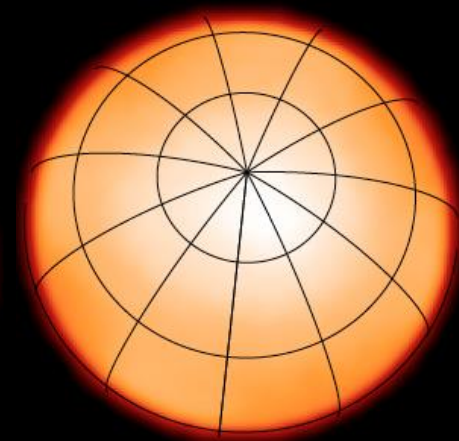
Altair

Monnier et al. 2007



Alderamin

Zhao et al. 2009



Bet Cas

Che et al. 2011

from recent review by Ming Zhao

2 R_{sun}

Imaging spots is hard because the dynamic range is large.

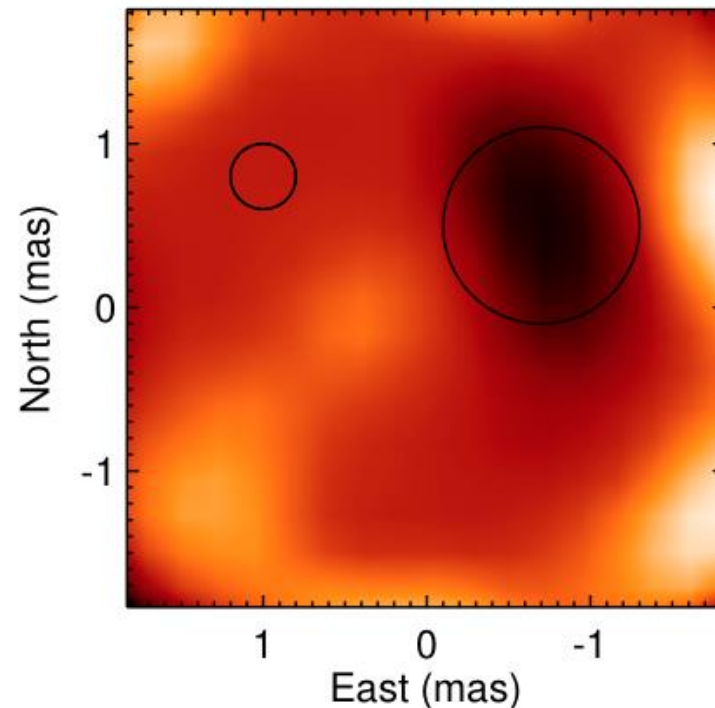


Figure 10.
diameters ϵ

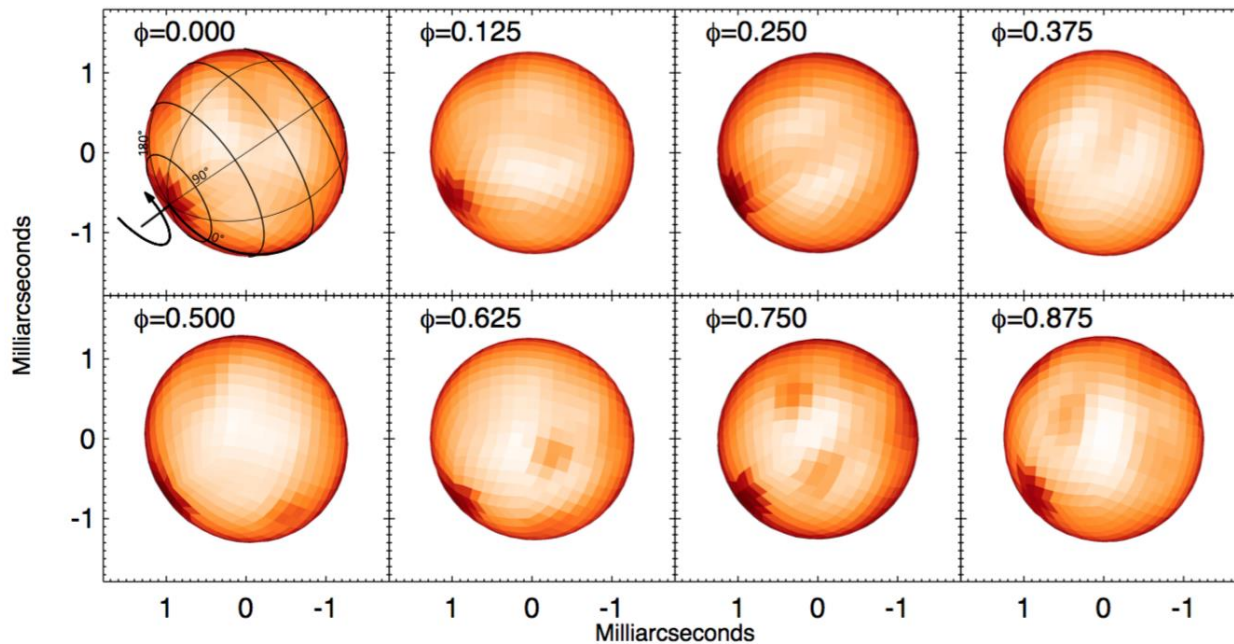
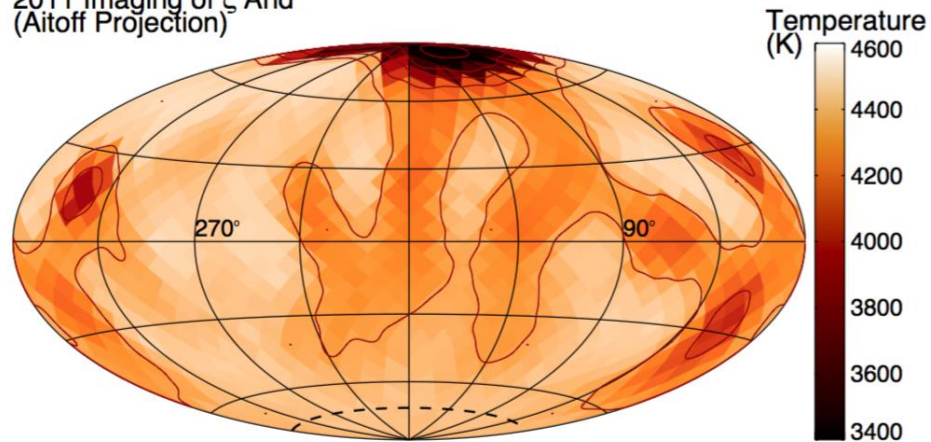
FIG. 2.— Shown is a closeup of the SQUEEZE reconstruction for the Sep 2th, 2011 data near an apparent starspot. The black circle on the right shows the aperture used to extract starspot properties from reconstructed image. The black circle on the left shows the aperture over the “quiet” photosphere. The “quiet” photosphere is defined as a part of the stellar surface devoid of flux gradients. The size of the aperture is identical to the minimum achievable angular resolution.

angular

Parks et al. 2015

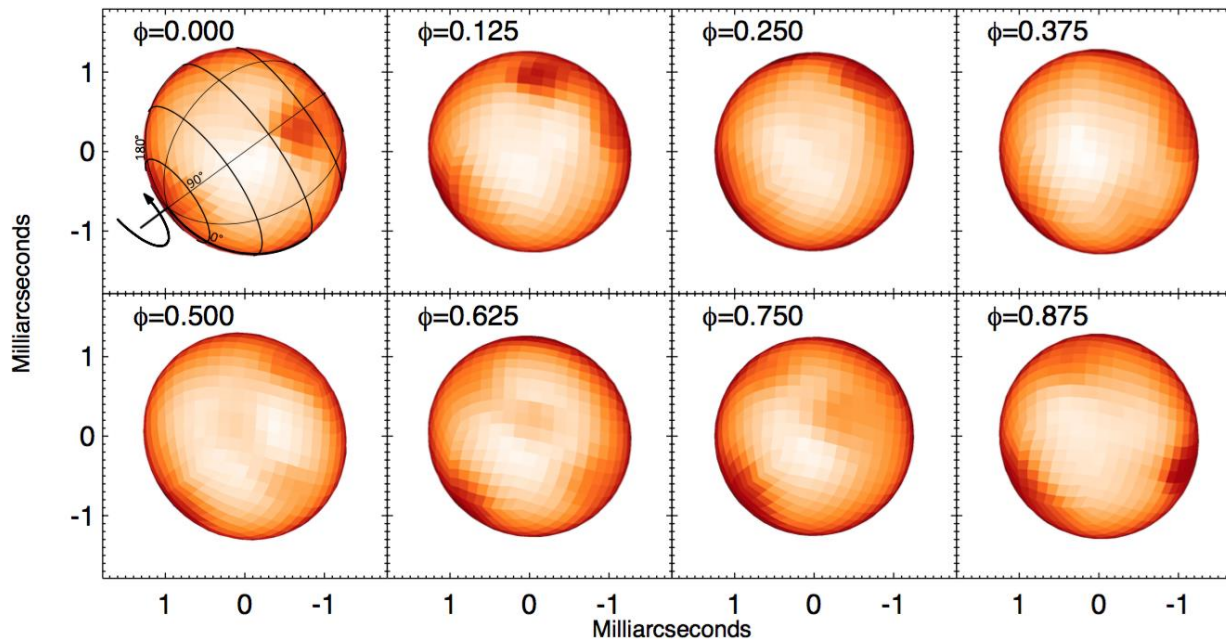
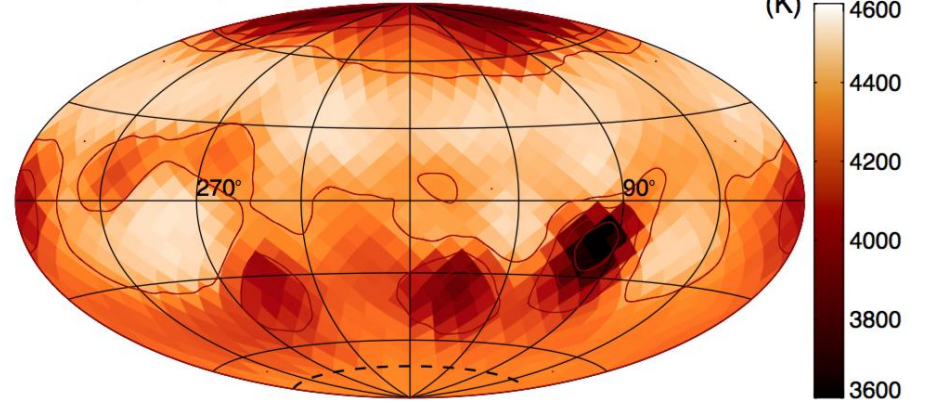
Spotted K giant ζ Andromeda (Roettenbacher et al. 2015)

2011 Imaging of ζ And
(Aitoff Projection)



Spotted K giant ζ Andromeda (Roettenbacher et al. 2015)

2013 Imaging of ζ And
(Aitoff Projection)



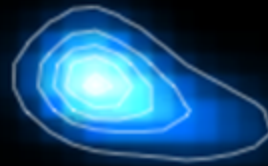
β Lyrae – First Imagery: 4-frame movie

Zhao et al. Science 2007.

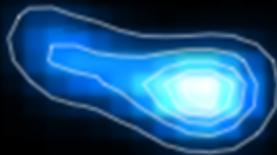
5 Jul 2007



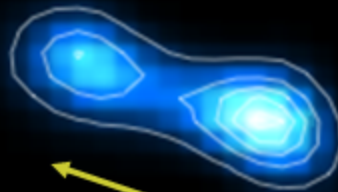
7 Jul 2007



9 Jul 2007

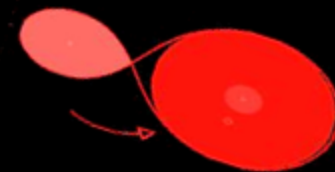


12 Jul 2007



1 mas \sim 0.3 AU

Four images are consistent with model and show hints of mass exchange.

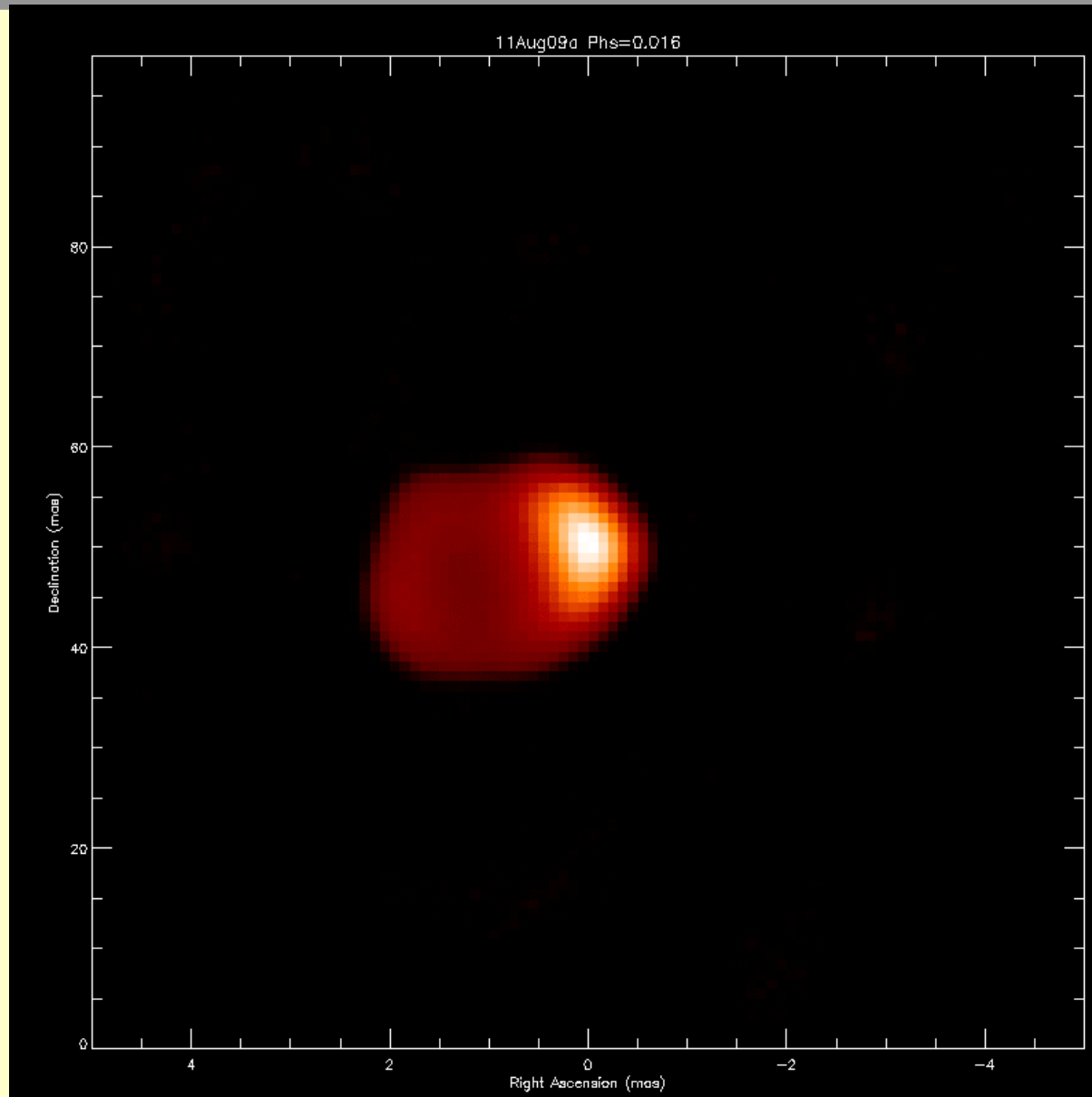


Model of
Linnell *et al.*
1988

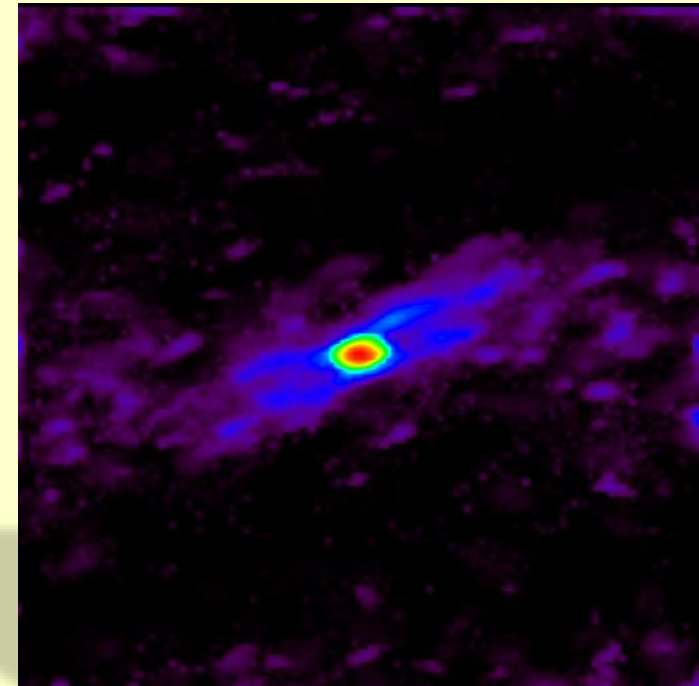
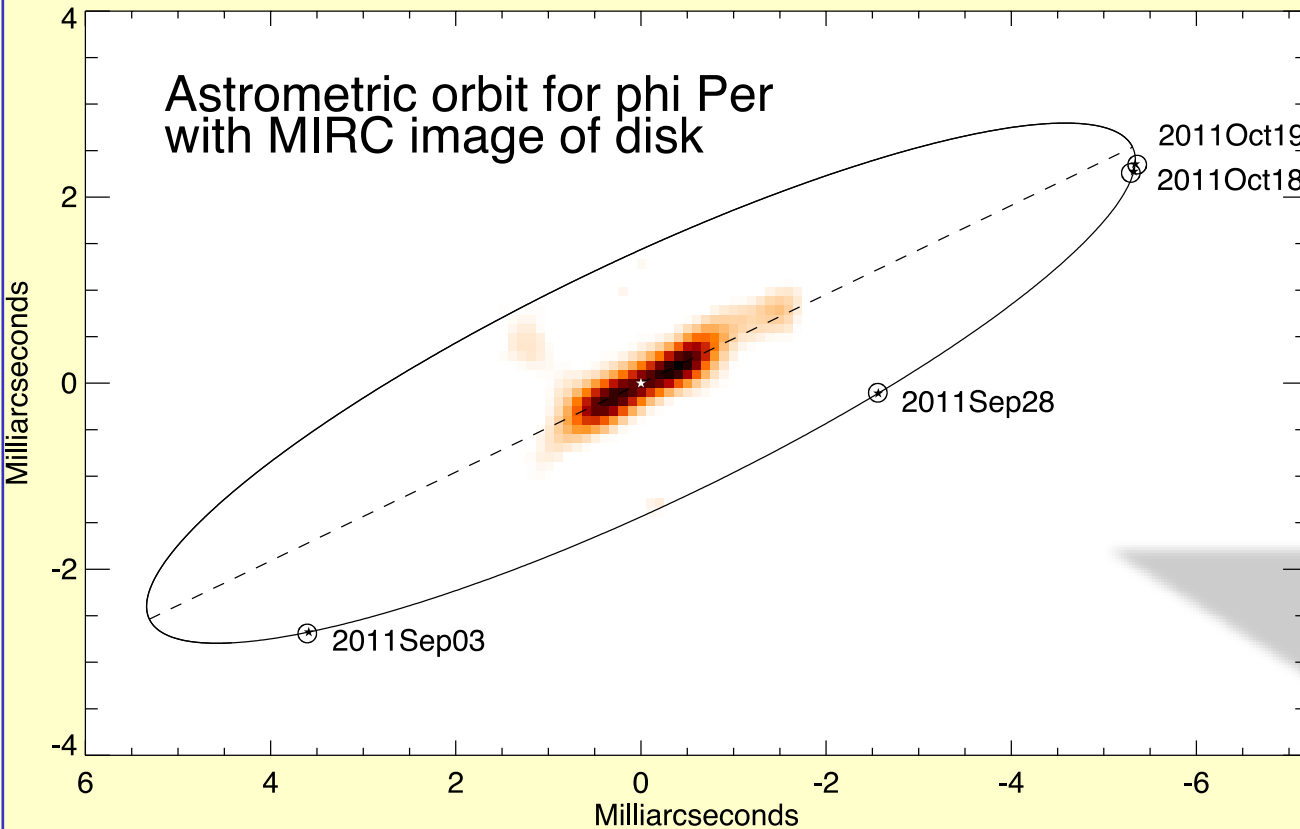
β Lyrae – The Movie



Algol the Movie: Baron et al 2011.

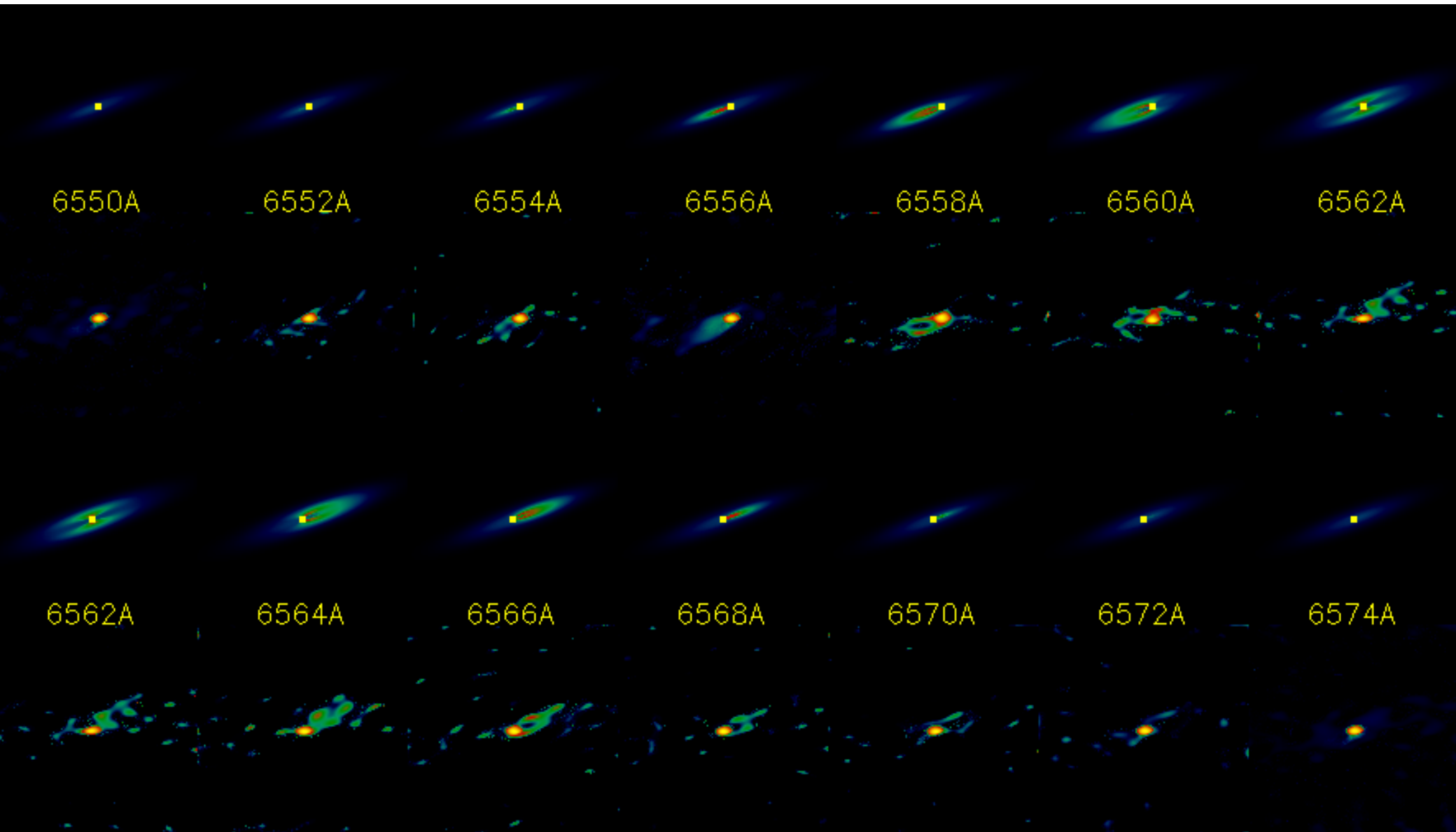


Imaging a Be Star disk and the orbit its faint companion

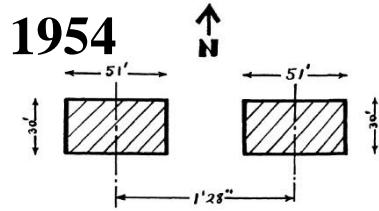


VEGA 4T

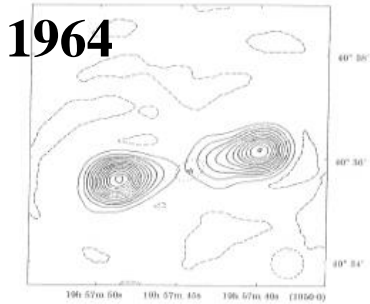
And even more ... spectral imaging



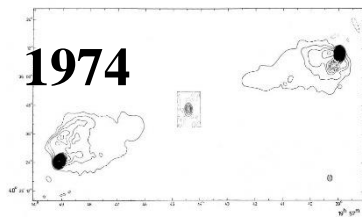
La radio source Cygnus-A au cours du



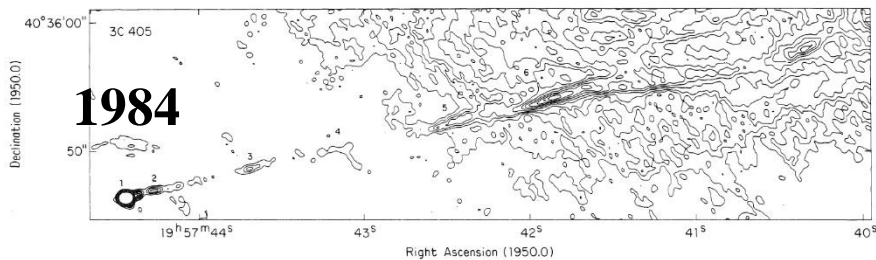
Jennesson et al., 1954



Ryle et al., 1964



Hargrave and Ryle 1974



Perley et al., 1984

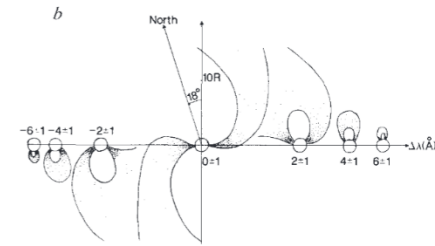
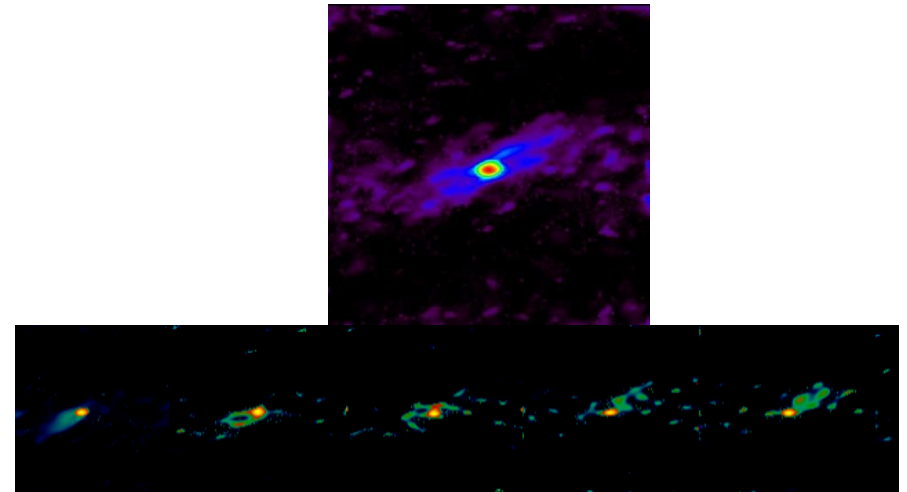


FIG. 2 The rotating hydrogen disk of γ -Cas, according to the model of

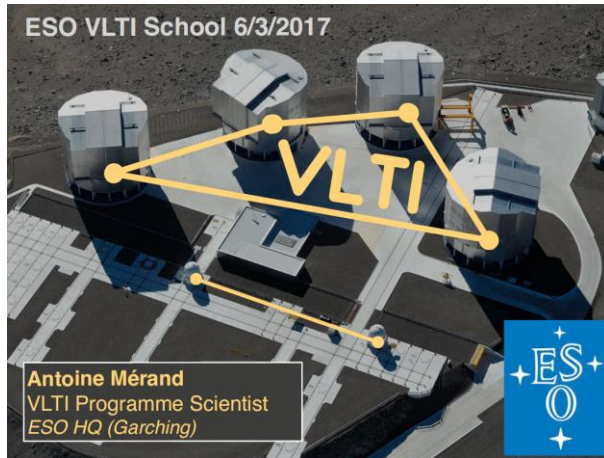
γ Cas, GI2T 1989



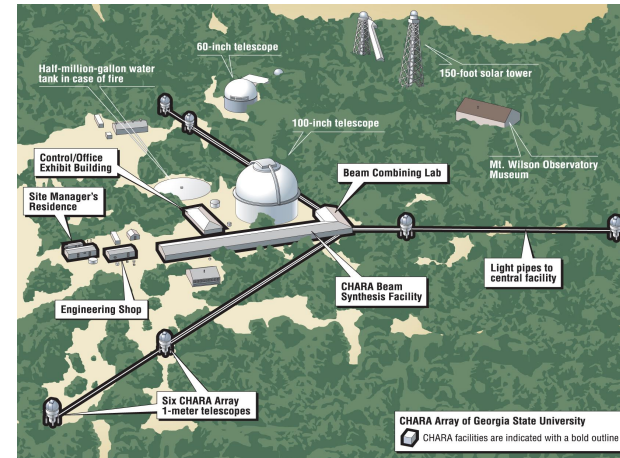
ϕ Per, VEGA 2015

Today the reality ... and tomorrow?

ESO/VLTI



CHARA



NPOI



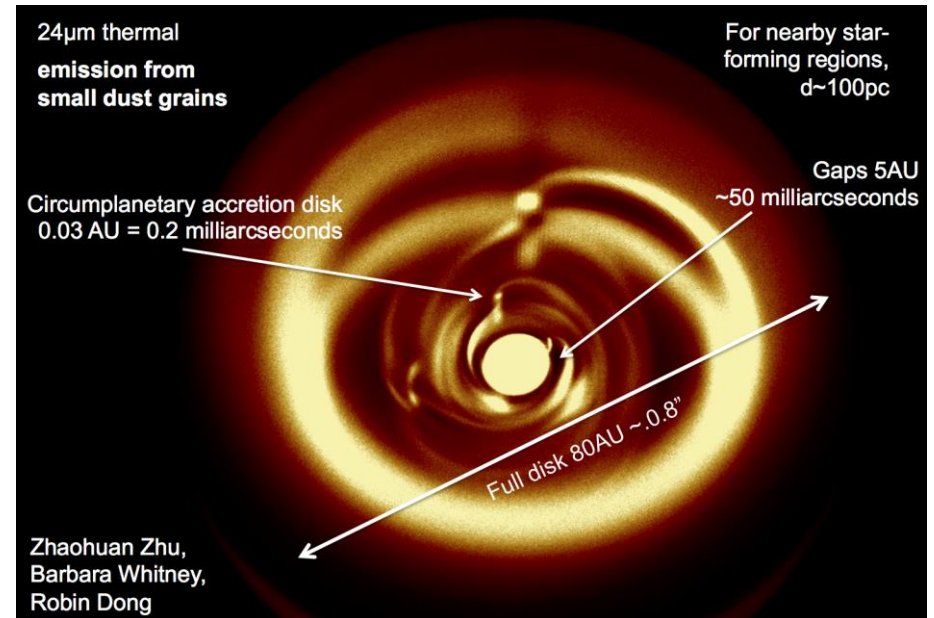
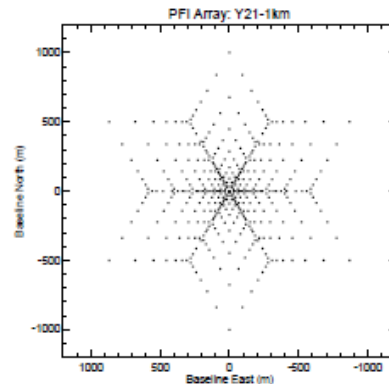
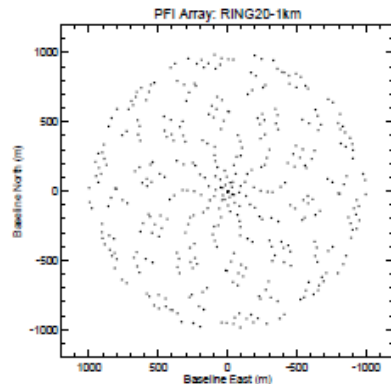
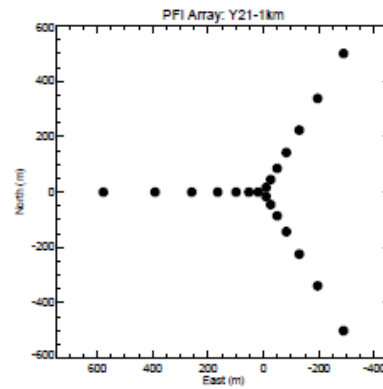
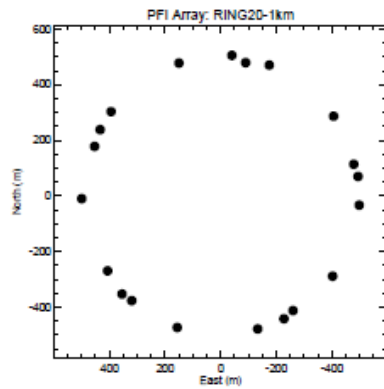
MROI



Planet Finder Imager studies ?

Table 1. Four Example PFI Arrays are explored in this report.

Shorthand Name	Array Shape	Number of Telescopes	Maximum Baseline (m)	Minimum Baseline (m)	Max Spanning Baseline (m)
RING20-1km	Ring array	20	1000	42	300
RING20-5km	Ring array	20	5000	209	1500
Y21-1km	Y array	21	1000	33	187
Y21-5km	Y array	21	5000	165	935



Probably necessary to change our approach?

The optical interferometers are really complex machines

The extension of the current concepts to ~optical ALMA is not obvious

What are the other possibilities:

Intensity interferometers?

Space?

A more direct ‘direct imaging interferometer’: Optical Arecibo?

An optical version of Arecibo or of the new FAST radiotelescope?



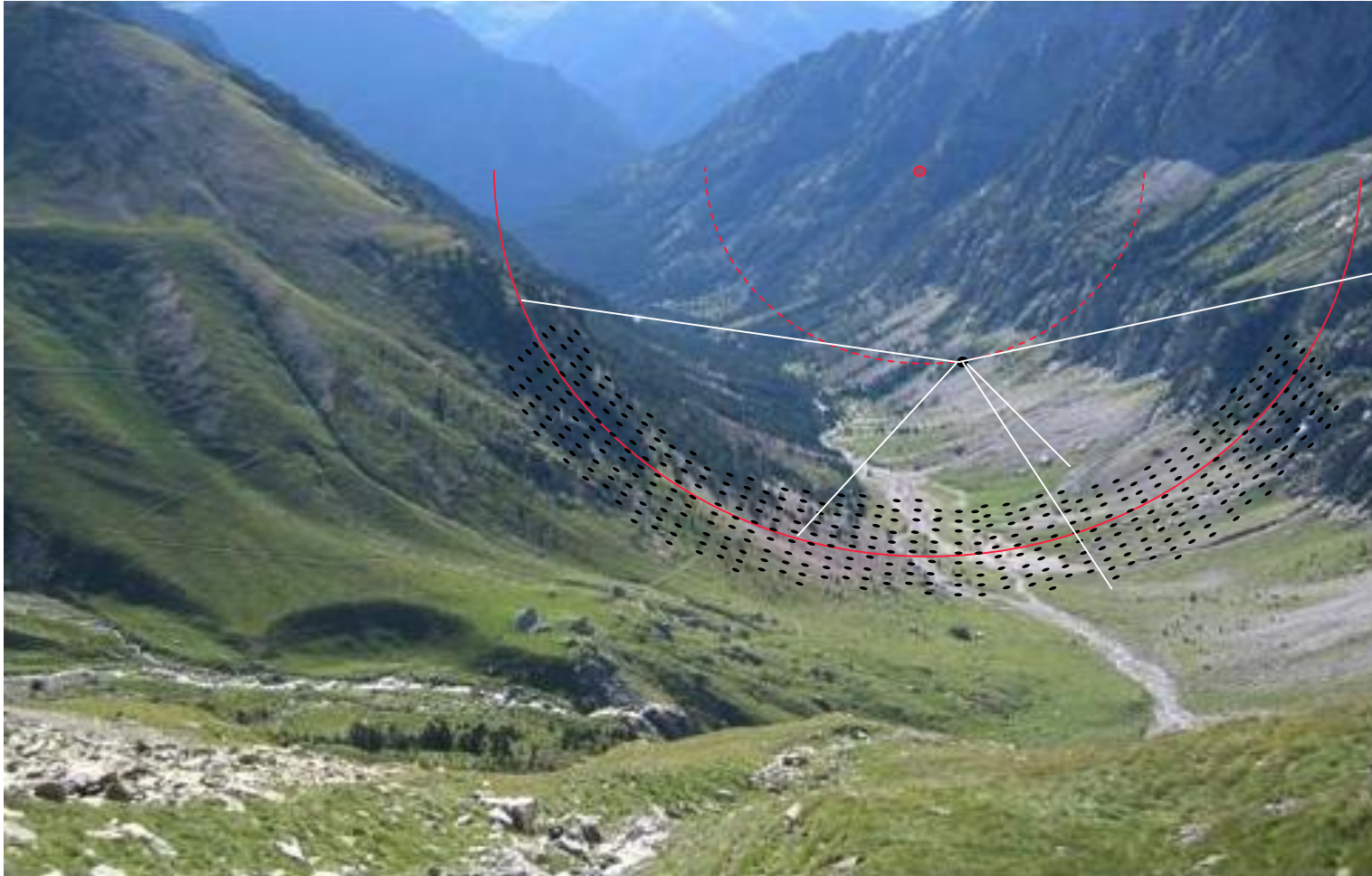
- No delay lines needed
- But moving focal optics



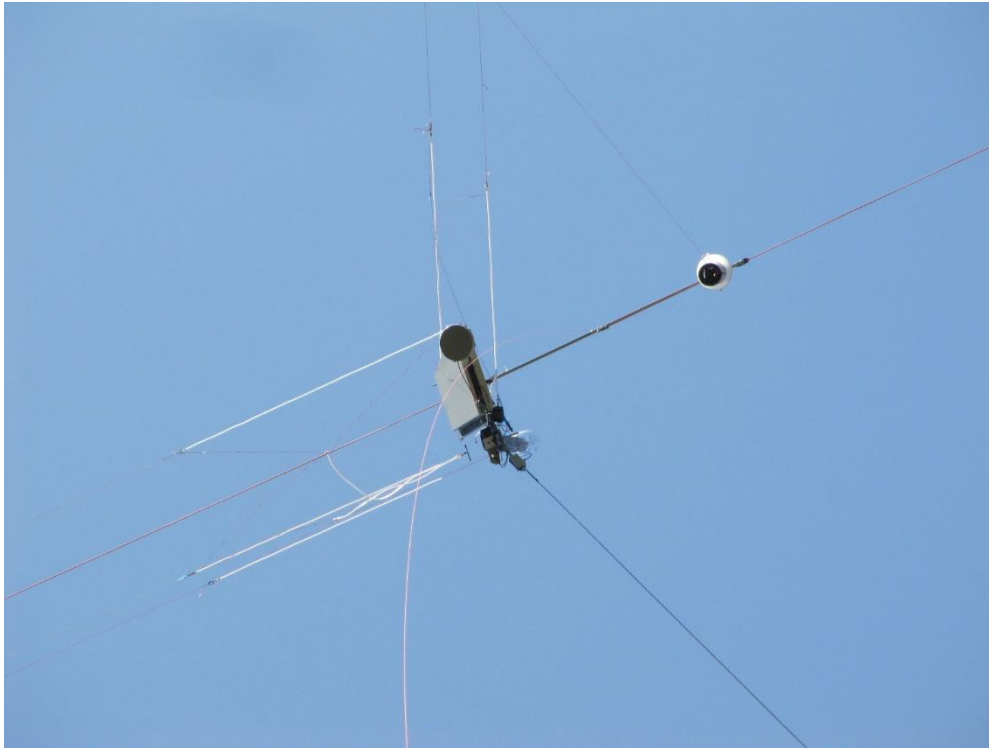
Cables for shape adjustment,
activable for a sliding
paraboloidal deformation



Construction of a 57m hypertelescope in the southern Alps, France



Preliminary results



focal gondola, 101m high, computer-driven

- 2015: Vega image obtained at coudé from one sub-aperture
- 2017: Full validation of the tracking and orientation, new optical bench with embarked cameras. More tests to come...